Velocity Prediction Program Development for Hydrofoil-Assisted Sailing Monohulls

BORBA LABI Gaetan

Master Thesis

presented in partial fulfillment
of the requirements for the double degree:
“Advanced Master in Naval Architecture” conferred by University of Liege
"Master of Sciences in Applied Mechanics, specialization in Hydrodynamics, Energetics and Propulsion” conferred by Ecole Centrale de Nantes

developed at the University of Rostock
in the framework of the

“EMSHIP”
Erasmus Mundus Master Course
in “Integrated Advanced Ship Design”

Ref. 159652-1-2009-1-BE-ERA MUNDUS-EMMC

Supervisor:	Prof. Nikolai Kornev, University of Rostock
Internship tutor:	Senior Lecturer Jean-Baptiste Souppez, Solent University
Reviewer:	Prof. Dario Boote, University of Genoa

Rostock, February 2019

ABSTRACT

In the last decade the popularity of hydrofoil-assisted monohulled yachts has increased, especially for high performance racing crafts, as the ones used in the Vendée Globe. In the academic environment some research has been done to follow the industry evolution to better understand the behaviour of such vessels, yielding to the need of developing a tool able to predict the performance of such boats. For this reason, the present document aims to propose a simplified model that forecasts the velocity of hydrofoil-assisted monohulled yachts through the development of velocity prediction program (VPP).

Due to the complexity of describing the behaviour of a complete sailing yacht, the developed tool uses empirical and analytical equations only, being a useful solution for a preliminary design stage. The aerodynamic model is based in the Offshore Racing Congress (ORC) documentation, the hydrodynamic model uses the Delft Systematic Yacht Hull Series (DSYHS) method, and the foil model is based in the Glauert's biplane theory, corrected and adapted for hydrofoil with towing tank tests. The combination of the three models allowed the development of a VPP that balances forces and moments in three degrees of freedom: surge, sway and roll.

The VPP includes three different hydro foils designs: Dali Moustache, developed for the IMOCA 60 class by VPLP and used in the 2016-17 Vendée Globe regatta; Chistera, also developed by VPLP but now for the new Beneteau Figaro 3; Dynamic Stability System, patented by Hugh Burkewood Welbourn and largely used in several different vessels for racing and cruising.

Finally, the present thesis: compares the performance of different foils, pointing its advantages and drawbacks; discuss possible optimizations for the foils design and the precautions that should be taken; presents the limitations of the used models, which yields to the VPP limitations and suggests future works that should be done to better predict the performance of such yachts.

Keywords: velocity prediction program, sailing yacht, hydrofoil, fluid dynamics, preliminary design.

ACKNOWLEDGEMENTS

Initially I would like to thank my family, especially my parents, for the brilliant education and opportunities they provided me.

Then, I want to thank my supervisor at Solent University, Jean-Baptiste Souppez, who helped me on every step of this research, exchanging information, providing knowledge and opening the doors of the institution, which I also want to thank for allowing me to use their facilities, as computers, laboratories and library.

It is also important to thank Juliette Dewavrin, a former EMship student that started the research in foiling yacht at Solent University in 2017 and whom model was used in this present work.

I also want to thank Florian Gohier and Jacob Pawel, also visiting students at Solent University, and Jack Cunningham-Burley from Solent University, who shared moments with me at the towing tank, helping with the model, its preparation, installations, test and data analysis.

Finally, I want to thank my Supervisor, Prof. Nikolai Kornev from University of Rostock, and the Thesis reviewer Prof. Dario Boote from University of Genoa.

CONTENTS

BORBA LABI Gaetan 1
ACKNOWLEDGEMENTS 5
CONTENTS 7
DECLARATION OF AUTHOSHIP 13
NOMENCLATURE – SYMBOLS EXPLANATIONS 15
1. INTRODUCTION 18
2. STATE OF THE ART - HYDROFOILS 19
2.1. Hydrofoils history 19
2.2. Underpinning Theory 20
2.3. Hydrofoils classification 22
2.3.1. “Dali-Moustache” foil 24
2.3.2. “Chistera” foil 25
2.3.3. Dynamic Stability System (DSS) 26
2.3.4. Previous work 27
3. VELOCITY PREDICTION PROGRAM 27
3.1. VPP history 28
3.2. Conventional VPP 29
3.3. Dynamic VPP 30
4. AERODYNAMIC MODEL 31
4.1. Sailing Background 32
4.2. Offshore Racing Congress VPP 33
4.3. Main sail 34
4.4. Jib or Genoa 37
4.5. Spinnaker 39
4.5.1. Symmetric Spinnaker tacked on a pole 39
4.5.2. Asymmetric Spinnaker tacked on a Centre Line 40
4.5.3. Asymmetric Spinnaker on Pole 40
4.6. Sails plan definition 41
4.6.1. Main sail with Jib sail 41
4.6.2. Main sail with Spinnaker 43
4.7. Windages force 43
4.7.1. Mast 43

4.7.2. Rig 43
4.7.3. Hull 44
4.7.4. Crew 44
4.8. Forces resolution 45
4.9. Experimental Aerodynamic validation 46
5. HYDRODYNAMIC MODEL 49
5.1. Delft Systematic Yacht Hull Series 50
5.2. Canoe Upright Resistance at Calm Water 51
5.3. Change in Resistance Due to Heel 53
5.4. Appendages Resistance 54
5.5. Side Force Production 55
5.6. Experimental Hydrodynamic Validation 56
6. FOILS MODEL 59
6.1. Dynamic Stability System (DSS) 60
6.1.1 Experimental Correction 61
6.2. Dali Moustache (DM) 64
6.2.1. Experimental correction 66
6.3. Figaro Foil (FF) 68
6.3.1. Experimental correction 70
7. VELOCITY PREDICTION PROGRAM STRUCTURE 72
7.1. Rolling Moment Loop 74
7.2. Surge Loop 75
7.3. Sway Loop 75
7.4. VPP Validation 75
8. VPP RESULTS WITH FOILS 79
8.1. Foils Optimization 81
9. CONCLUSION 88
9.1. VPP 88
9.2. Results 89
9.3. Optimization 90
9.4. Future Works 90
10. REFERENCES 93
APPENDIX A1: YACHT PARAMETERS FOR AERODYNAMIC FORMULATION 95
APPENDIX A2: TOWING TANK FACILITY AND MODEL MANUFACTURE 96

TABLE OF FIGURES

Figure 1- Hydroptère sailing trimaran (L'Hydroptère bat le record de vitesse à la voile, 2013) 19
Figure 2 - Pressure distribution around foil moving from the right to the left side of the page (Barkley, 2016) 20
Figure 3 - Forces decomposition in a foil (J. -B. Souppez, 2017) 21
Figure 4 - 3D wing and the tip vortex effect (Barkley, 2016) 22
Figure 5 - Comparation between surface piercing foils and fully submerged foils (Matthew Sheahan, 2015) 23
Figure 6 - IMOCA 60 project developed by VPLP using the "Dali-Moustache" foil (*Designing the IMOCA 60*, 2016) 24
Figure 7 - Beneteau Figaro 3 project developed by VPLP using "Chistera" foil (*Figaro Beneteau 3*, no date) 26
Figure 8 - Infiniti 56C project using DSS (*DSS Dynamic Stability System*, no date) 27
Figure 9 - Sailing triangle, presenting concepts of true wind and apparent wind (J. -B. Souppez, 2017) 32
Figure 10 - Sail's mains dimensions considering the yacht's front is in the righthand side of the page (author's drawing) 33
Figure 11 - Main sail dimensions according to IMS (author's drawing) 35
Figure 12 - Jib sail dimensions according to IMS (author's drawing) 38
Figure 13 - Model comparation with experimental results and numerical solutions for *Fujin* yacht with two different jib sails 49
Figure 14 - Model validation comparing with Delft results 59
Figure 15 - Hull with DSS foil (author's drawing) 61
Figure 16 - DSS foil comparation between tank results, model calculation and model correction 64
Figure 17 - Hull with Dali Moustache foil (author's drawing) 65
Figure 18 - DM foil comparation between tank results, model calculation and model correction 68
Figure 19 - Hull with Figaro foil (author's drawing) 69
Figure 20 - Figaro foil comparation between tank results, model calculation and model correction 71
Figure 21 - VPP validation, comparing results with two commercial software 78

Figure 22 - VPP results comparing the three different foils and the hull with no foil at different wind conditions sailing up and down wind 81
Figure 23 - Aspect ratio optimization 82
Figure 24- Angle of attack optimization 82
Figure 25 – α 1 optimization 83
Figure 26 - VPP results comparing the three different foils optimized and the hull with no foil at different wind conditions sailing up and down wind 85
Figure 27 - Polar plot for the 4 different configuratons: no foil, DSS, DM and FF 87
Figure 28 - Polar plot comparing the boat speed before and after the foils were optimized 88

TABLE OF TABLES

Table 1 - Main sail force coefficients (ORC, 2017) 36
Table 2 - Jib force coefficients (ORC, 2017) 38
Table 3 - Symmetric Spinnaker force coefficients (ORC, 2017) 40
Table 4 - Asymmetric Spinnaker tacked on Centre Line force coefficients (ORC, 2017) 40
Table 5 - Asymmetric Spinnaker on pole force coefficients (ORC, 2017) 41
Table 6 - Drag coefficient multiplier (ORC, 2017) 42
Table 7 - Fujin principal dimensions (Masuyama *et al.*, 2009) 46
Table 8 - Sails detailed measurements (Masuyama *et al.*, 2009) 47
Table 9 - Range of hull parameters tested in the DSYHS (Keuning and Sonnenberg, 1998) 51
Table 10 - Coefficients for polynomial equation for upright residuary resistance of bare hull (Katgert and Keuning, 2008) 53
Table 11 - Coefficients for polynomial equation of canoe wetted surface under heel (Keuning and Sonnenberg, 1998) 53
Table 12 - Coefficients for polynomial equation of change in resistance of bare hull heeled 20^{o} (Keuning and Sonnenberg, 1998) 54
Table 13 - Coefficients for polynomial residuary resistance equation on the keel (Keuning and Sonnenberg, 1998) 55
Table 14 - Coefficient of polynomial equation for the variation of resistance in appendages due to heel (Keuning and Sonnenberg, 1998) 55
Table 15 - Coefficients for polynomial equation to determine the side force (Keuning and Sonnenberg, 1998) 55
Table 16 - Coefficients to estimate the effective span (Keuning and Sonnenberg, 1998) 56
Table 17 - Sysser 62 dimensions and parameters 57

Table 18 – Towing tank mode dimensions 62
Table 19 - Efficiency correction coefficient for DSS 64
Table 20 - Dali Moustache foil main dimensions for tank test at model scale 66
Table 21- Efficiency correction coefficient for DM 68
Table 22 - Figaro foil main dimensions for tank test at model scale 70
Table 23 - Efficiency correction coefficient for Figaro 71
Table 24 - VPP test yacht main dimensions 77
Table 25 - *Gz* values as a function of heel angle 77
Table 26 - Foils main dimensions at full scale 79
Table 27 - Foils dimensions after optimization 84

DECLARATION OF AUTHOSHIP

Declaration of Authorship

I, Gaetan Borba Labi*, declare that this thesis and the work presented in it are my own and have been generated by me as the results of my own original research.*

"Velocity Prediction Program Development for Hydrofoil-Assisted Monohulled Yachts"

Where I have consulted the published work of others, this always clearly attributed.

Where I have quoted from work of others, the source is always given. With the exception of such quotations, this thesis is entirely my own work.

I have acknowledged all main sources of help.

Where the thesis is based on work done by myself jointly with others, I have made clear exactly what was done by others and what I have contributed myself.

This thesis contains no material that has been submitted previously, in whole or in part, for the award of any other academic degree or diploma.

I cede copyright of the thesis in favour of the University of Rostock

Date: *Signature*

NOMENCLATURE – SYMBOLS EXPLANATIONS

A	Area [m²]	DVPP	Dynamic Velocity Prediction Program
AMS	Hull maximum section area [m²]	E	Main foot [m]
AR	Aspect ratio	eff	Efficiency coefficient
Arm_{crew}	Crew weight right moment arm [m]	EHM	Mast height from deck [m]
AWA	Apparent Wind Angle [°]	Fa	Aft hull's free board [m]
AWS	Apparent Wind Speed [m/s]	FF	Figaro foil
B	Yacht Beam [m]	Ff	Front hull's free board [m]
BAS	Boom above sheer line [m]	Fh	Perpendicular to keel force [N]
BEM	Boundary Element Method	FHA	Heeling aerodynamic force [N]
Bwl	Hull beam at water line [m]	Fn	Froude number
c	Chord [m]	FRA	Forward aerodynamic force [N]
Cd	Drag coefficient	g	Gravity acceleration [m/s²]
CEH	Centre of Effort [m]	Gz	Hydrostatic righting moment arm [m]
Cf	Friction coefficient	h	Foil distance from free surface [m]
CFD	Computer Fluid Dynamic	h_0	Distance of foil from free surface at its root [m]
CH	Aerodynamic heeling coefficient	HB	Main sail headboard [m]
Cl	Lift coefficient	HBI	Vertical distance between rig base and water level [m]
Cm	Midship area coefficient	HMA	Heeling aerodynamic moment [N.m]
CR	Aerodynamic thrust coefficient	I	Rigging height from deck [m]
D	Drag [N]	IG	Height of Jib's hoist [m]
DM	Dali Moustache	IMS	International Measurement System
DOF	Degrees Of Freedom	J	Mast to bow distance [m]
DSKS	Delft Systematic Keel Series	JGL	¼ Jib luff horizontal length from sail's foot [m]
DSS	Dynamic Stability System	JGM	½ Jib luff horizontal length from sail's foot [m]
DSYHS	Delft Systematic Yacht Hull Series	JGT	7/8 Jib luff horizontal length from sail's foot [m]

JGU	¾ Jib luff horizontal length from sail's foot [m]	RM4	Hydrodynamic vertical centre of pressure [m]
JH	Top Jib horizontal length [m]	RMA	Righting Moment Arm [m]
JL	Jib Luff [m]	RMV	Dynamic righting moment [N.m]
k	Form factor	Rn	Reynolds number
L	Lift [N]	Rrh	Upright yacht residuary resistance [N]
LCB_{fpp}	Longitudinal centre of Buoyancy from the forward perpendicular [m]	Rrk	Keel residuary resistance [N]
LCF_{fpp}	Longitudinal centre of Flotation from the forward perpendicular [m]	Rt	Total resistance [N]
LPG	Jib perpendicular length from its luff at clew [m]	Rv	Appendage viscus resistance [N]
L_v	Yacht length [m]	S	Foil area [m²]
Lwl	Hull length over water line [m]	Sc	Hull wetted area at rest [m²]
MGL	¼ main span horizontal length from sail's foot [m]	SF	Spinnaker foot length [m]
MGM	½ main span horizontal length from sail's foot [m]	SL	Vertical length on Spinnaker centre [m]
MGT	7/8 main span horizontal length from sail's foot [m]	SLE	Spinnaker leech [m]
MGU	¾ main span horizontal length from sail's foot [m]	SLU	Spinnaker luff [m]
MW	Mast wigth [m]	SMG	Middle Spinnaker horizontal length [m]
ORC	Offshore Racing Congress	t	Thickness [m]
P	Main sail span [m]	T	Yacht draft [m]
PPP	Performance Prediction Program	Tc	Canoe draft [m]
RANS	Reynolds-Averaged Navier-Stokes	Te	Effective span [m]
Rf	Appendage frictional resistance [N]	TPS	Horizontal distance from spinnaker centre line to mast [m]
Rfh	Upright yacht viscous resistance [N]	TR	Keel tip and root chord ration
$Rfh\varphi$	Heeled yacht viscous resistance [N]	TWA	True wind angle [°]
RGz	Hydrostatic righting moment [N.m]	TWS	True wind speed [m/s]
Ri	Induced resistance [N]	V	Vessel speed [m/s]
RM	Righting moment [N.m]	VPP	Velocity Prediction Program

Wcrew	Crew weight [kg]	ν	Kinematic viscous [m²/s]
WS	Foil wetted area [m²]	ρ	Density [kg/m³]
zc	Height above the main base of the centroid of each trapezoid	φ	Yacht heel angle [°]
Zcbk	Keel vertical position of centre of buoyancy [m]	ΔRrhφ	Change in residuary resistance due to heel [N]
Zce	Height of centre of effort [m]	ΔRrkφ	Keel change in residuary resistance due to heel [N]
α	Foil angle with horizontal when yacht upright [°]	∇	Yacht volumetric displacement [m³]
β	yacht leeway angle [°]	∇c	Canoe volumetric displacement [m³]
β0	Apparent wind angle correction [°]	∇k	Keel volumetric displacement [m³]

1. INTRODUCTION

Due to the recent increase in popularity of hydrofoil-assisted monohulled yachts, the necessity of developing such vessels with efficient tool is obvious. Many commercial software, using different methods, are able to describe the behaviour of sailing yachts, but it is noticeable the lack of methods able to predict the velocity of sailing boats carrying such hydrofoils. For this reason, the main goal of this thesis is to develop a Velocity Prediction Program (VPP) for hydrofoil-assisted monohulled yachts, targeting the preliminary design stage.

Because of the high complexity of the problem, which includes a dynamic aerodynamic and hydrodynamic understanding of an entire craft and its interaction, the goal of this particular project is to develop a VPP based on empirical and analytical equations, yielding to a program that has a low computational cost. The hydrodynamic model is based on the Delft Systematic Yacht Hull Series (DSYHS) (Keuning and Sonnenberg, 1998), and the aerodynamic model on the Offshore Racing Congress (ORC) (ORC, 2017). The hydrofoil model is based on the Glauert's biplane theory applied for hydrofoil near the free surface (Daskovsky, 2000). Experimental tests in the towing tank of Solent University are used to adapt and fit Glauert's theory to the particular application of hydrofoil-assisted monohulled yachts.

The three types of foils included in the research are: Dali moustache, developed by VPLP and used in the last Vendée Globe (2016-17) in the IMOCA 60 class; Chistera foil, also created by VPLP and used in the new Beneteau Figaro 3; and the Dynamic Stability System (DSS) patented by Hugh Burkewood Welbourn.

Once the VPP runs and is validated, the results obtained from it allows a better understanding of these new boats assisted with hydrofoils. It is possible to compare the benefits in righting moment with the drawbacks in drag, and visualise the gain or loss in side force, allowing the designer to choose the best hydrofoil and its dimensions for a certain application.

2. STATE OF THE ART - HYDROFOILS

2.1. Hydrofoils history

The usage of hydrofoils for naval application is not recent, according to Matthew Sheahan (Matthew Sheahan, 2015) the first patent for such technology was released in 1869, in France, by Emmanuel Denis Fargot, while the first hydrofoil boat was actually built some time later, in 1906 by Enrico Forlanini, which reached the impressive speed of 36.9 knots. But it was in the United Stated of America that the first sailing boat with hydrofoils was produced, in 1938 by R. Gilruth and Bill Carl.

On the late 60's, according to Dewavrin (Dewavrin, 2018), the hydrofoils got popular in sailing multihull vessels, as Icaru's catamaran in 1969 and Eric's Tabarly trimaran seven years later. At the same period, in 1970, David Keiper sailed the first hydrofoil cruiser in an offshore cross in the South Pacific.

In 1980 Eric Tabarly pushed the foil technology to its limits, setting a new record on the transatlantic cross between Europe and the American continent. 10 years later Dan and Greg Ketterman with Russell Long reached the world record of the fastest sailing boat of all times, crossing the barrier of the 30 knots. In 1997 the French foil sailing vessel Techniques Avancées reached a new speed record over 42 knots. In 2009 another French vessel, Hydroptère, was the first sailing boat to cross the speed of 50 knots, and 3 years later the Sailrocket II sailed at the impressive speed of 65.45 knots, the actual world's record (Dewavrin, 2018)

Figure 1- Hydroptère sailing trimaran (L'Hydroptère bat le record de vitesse à la voile, 2013)

In some very traditional sailing races the hydrofoil technology is also being applied, as the Vendée Globe and the America's Cup, which are using different concepts of monohulls for different applications, once the first one is an offshore race and the second an inshore regatta. Regarding pleasure yacht, the foiling technology is also finding some space, for example with the Infiniti yachts, which are using Dynamic Stability Systems (DSS) in their new super yachts. Dinghies are not far behind, the Olympic class Nacra 17 has foils, as the very popular monohull moths.

2.2. Underpinning Theory

Hydrofoils are wings, similar to the ones in airplanes, but instead of being submerged in a gas fluid, it works inside a liquid fluid. Its profile may be symmetric or asymmetric, and its main goal is to produce lift without generating too much drag, or resistance to advance. It is possible because its shape and angle of attack, when moving inside a fluid, generates a pressure field on its top that has an average pressure lower than the one in its bottom part, this pressure difference generates the so-called lift. The following figure shows the pressure profile around a standard foil moving from the right to the left side of the page.

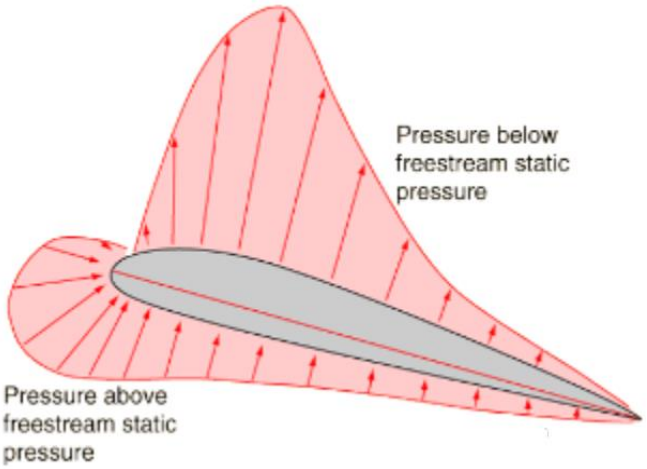

Figure 2 - Pressure distribution around foil moving from the right to the left side of the page (Barkley, 2016)

Such pressure distribution generates a force on the profile that may be decomposed in two parts, one vertical called lift, and another horizontal called drag, as presented in Figure 3.

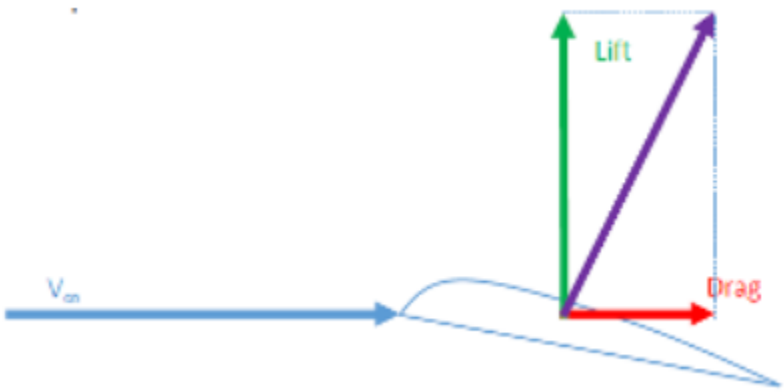

Figure 3 - Forces decomposition in a foil (J. -B. Souppez, 2017)

The drag and lift forces are proportional to the foil square speed, its surface area, angle of attack, fluid density and of course its geometry. Knowing it, it is interesting to find an ideal shape, with important lift and low drag. It is also important to mention that the water is a thousand times denser than the air, so for a similar foil in similar conditions, the force generated by the foil is a thousand times higher inside water if compared to an air submerged foil.

Unfortunately, a 3D foil has an increase in drag and drop in lift due to the effect of tip vortex, presented in the Figure 4. This effect increases the drag and decreases the lift due to downwash. To overcome such drawback, winglets are popular solutions, which consist in a small perpendicular foil extension in its end, similar to what is done in the Dali Moustache hydrofoil, which is presented in more details later in this document.

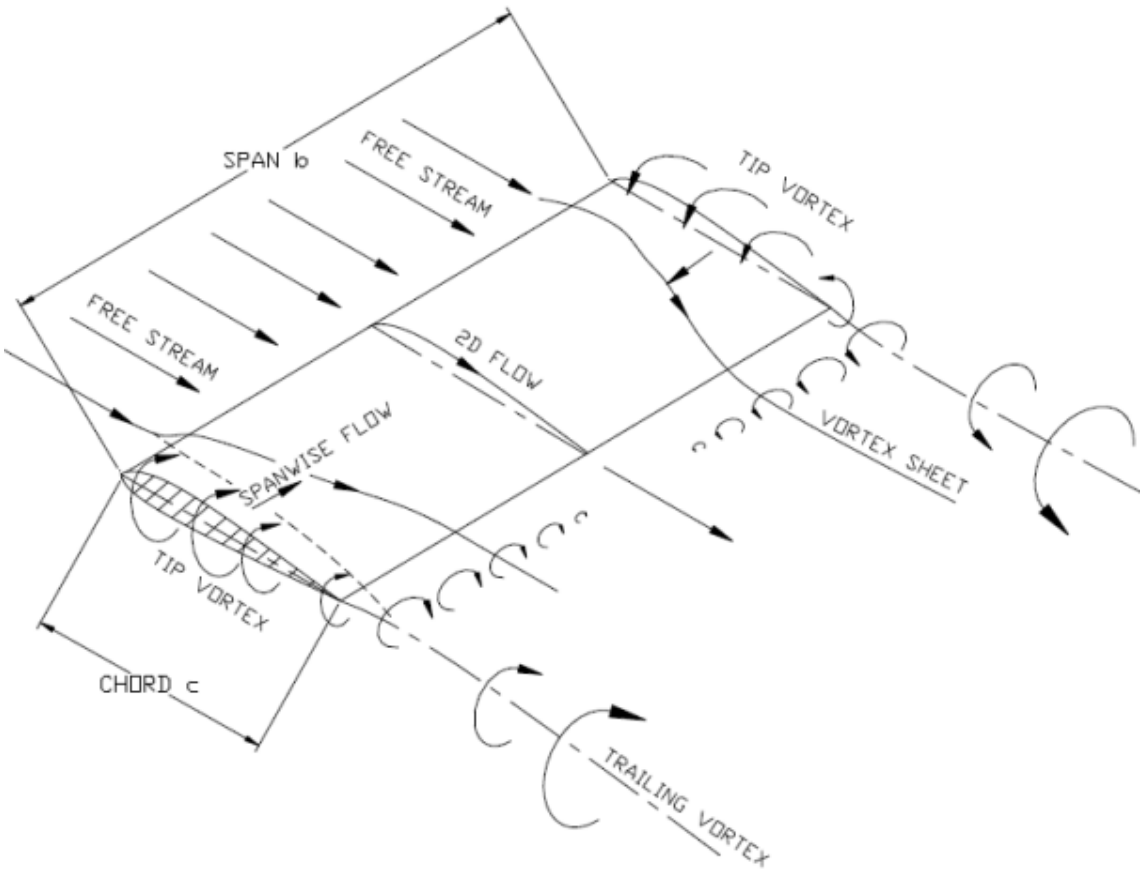

Figure 4 - 3D wing and the tip vortex effect (Barkley, 2016)

The main advantages of using hydrofoils in sailing yachts are linked to its important increase in the vessel's lift force, removing part of the craft from the water, reducing considerably its resistance to advance. It may also bring benefits regarding the boat's stability, inducing a higher righting moment, and improving sea keeping properties, as the incoming waves may be partially or completely avoided by the main hull if it is high enough from the free surface on top of the hydrofoils.

2.3. Hydrofoils classification

According to Sheahan (Matthew Sheahan, 2015), there is two main types of hydrofoils, the surface piercing foils (also called V shape foil), and the fully submerged foils. Figure 5 shows the main difference of such families of foils.

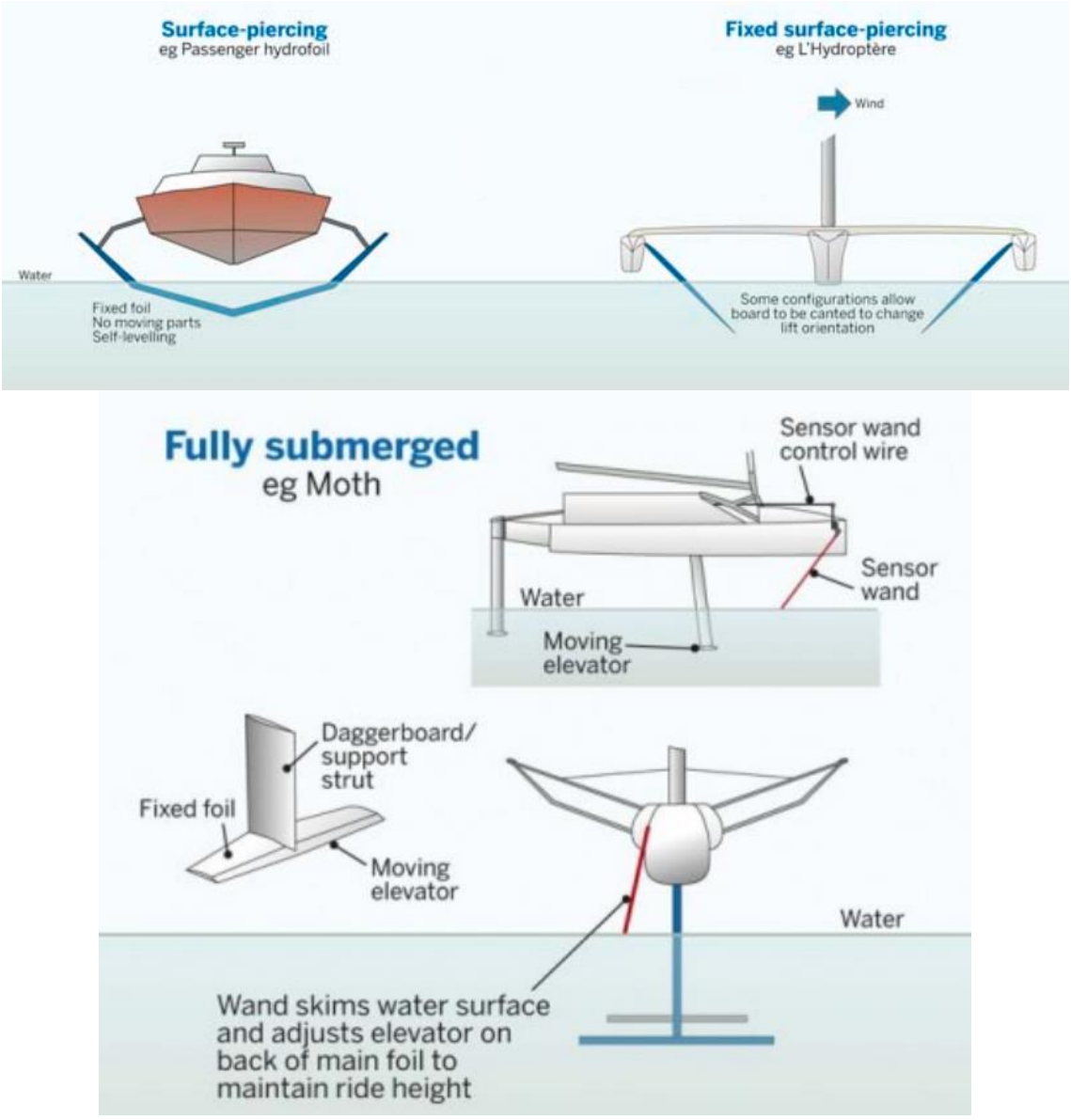

Figure 5 - Comparation between surface piercing foils and fully submerged foils (Matthew Sheahan, 2015)

According to Pierrier (Perrier, 2017), the main difference in both systems consist in the way the lifting force is corrected. For surface piercing foils, whenever the boat heels or gets too far from the water, the submerged foil area changes, impacting directly in the lifting force. For fully submerged foils, as Figure 5 already suggests, it is necessary to have a moving elevator to balance the lifting force, this active system may require extra power generation to move the foil's flap, what increases the system's complexity.

Regarding hydrofoil-assisted monohulled yachts, its foils have mainly passive systems, it means, surface piercing foils. Dewavrin (Dewavrin, 2018) divides this foil's family in three different groups: "Dali-Moustache" foil (DM), "Chistera" foil and Dynamic Stability System (DSS).

2.3.1. "Dali-Moustache" foil

The "Dali-Moustache" foil, in memory to the famous artist Salvador Dali, has a shape that remembers his iconic moustache. This type of foil was used in the Vendée Globe (2016-17), increasing the yachts performance and making this race even more impressive, revolutionizing the concept of the IMOCA 60 class. The foils in this VPLP project has a V shape, being located in both sides of the vessel, working as dagger boards that may be retracted, as presented in the following figure. Understand that dagger boards are retractable keels that generate hydrodynamic side force in order to balance aerodynamic loads.

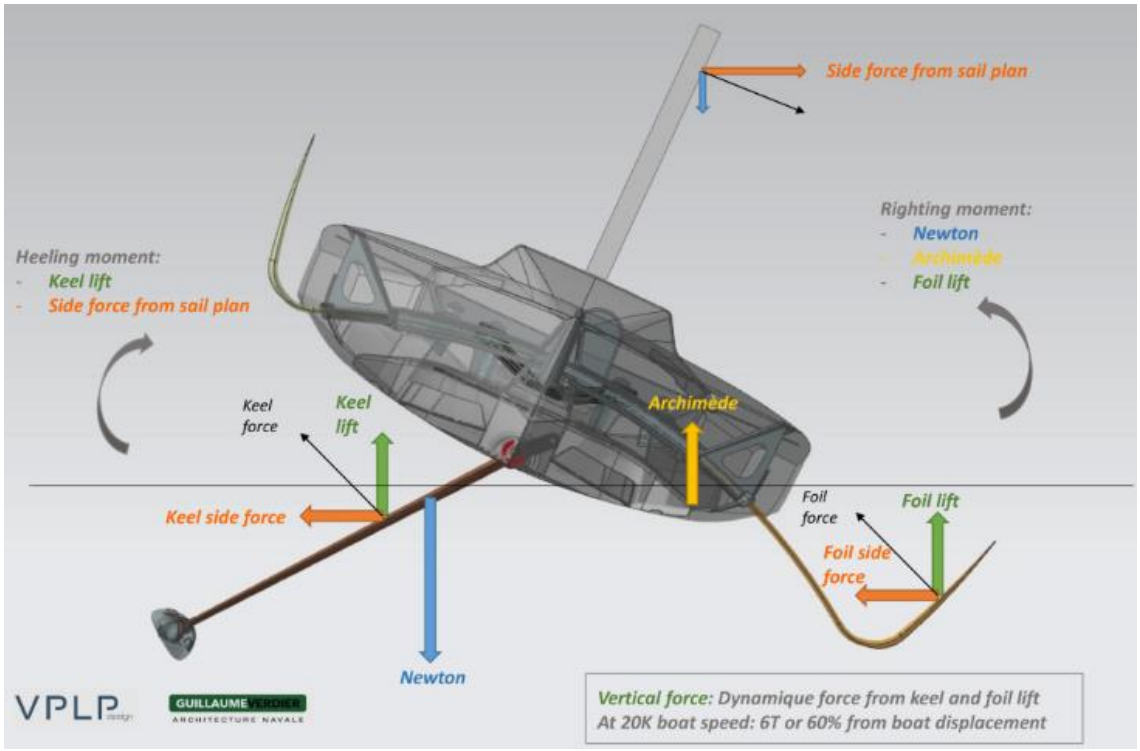

Figure 6 - IMOCA 60 project developed by VPLP using the "Dali-Moustache" foil (*Designing the IMOCA 60*, 2016)

The foil works as a dagger board, moving perpendicularly to the hull side, being used in the out position in the leeward side only. The lift force in the hydrofoil increases the vessel righting moment and side force, as decreases the craft's displacement, once it lifts the boat vertically, therefore decreasing the hull wetted area and as consequence decreasing the resistance. Another possible positive consequence of elevating the vessel is related to its seakeeping properties, once the craft's responses in heave and pitch may decrease in amplitude for similar incoming waves.

The dagger board foil is divided in two main parts, a so-called foil in its extremity, and a shaft that links it to the main hull, each part having a quite perpendicular angle between each other. It is interesting to notice that the keel moves as a controlled pendulum, such system is called

as canting keel, which is able to significantly improve the vessel's righting moment and also generates lift to remove the yacht from the water.

Aygor (Aygor, 2017) performed an experimental analysis in towing talk of the IMOCA 60 with the "Dali Moustache" configuration. Some of his main observations affirm that for low hell angles the drag force is too important compared to the vertical lift, compromising the efficiency of such system. On the other hand, despite free surface effects, the V shape of the foil avoids tip vortex generation, what is interesting and may have important benefits for the yacht's performance.

2.3.2. "Chistera" foil

"Chistera" foils are quite similar to "Dali Moustache" foil, but this new configuration, also developed by the same naval architecture office VPLP, is upside down if compared with the previous. The first yacht that presented such system is the new Figaro 3, from Beneteau ship yard, a 35 feet vessel made for crew and single-handed races inshore and offshore.

Some of the main benefits of this new concept is the decrease of the foil drag in light wind, so in case of small heel angles the foil lightly touches the water with one free surface piercing only. For stronger breezes, the vessel should have a more important heel, increasing the foil wetted surface, generating lifting forces that improve the vessel's performance by providing righting moment and side force, while decreasing the craft's displacement.

The "Chistera" foil, also known as asymmetric tip foil, is a retract device that allows the keel design to be considerably skinnier, once the last appendage is not alone responsible for avoiding leeway drift and balancing the aerodynamic loads generated by the sails. Comparing the new Figaro 3 with hydrofoils to its precedent models Figaro 1 and Figaro 2, skippers and naval architects expect an increase in yachts speed up to 15% due to the new technology (*Figaro Beneteau 3*, no date).

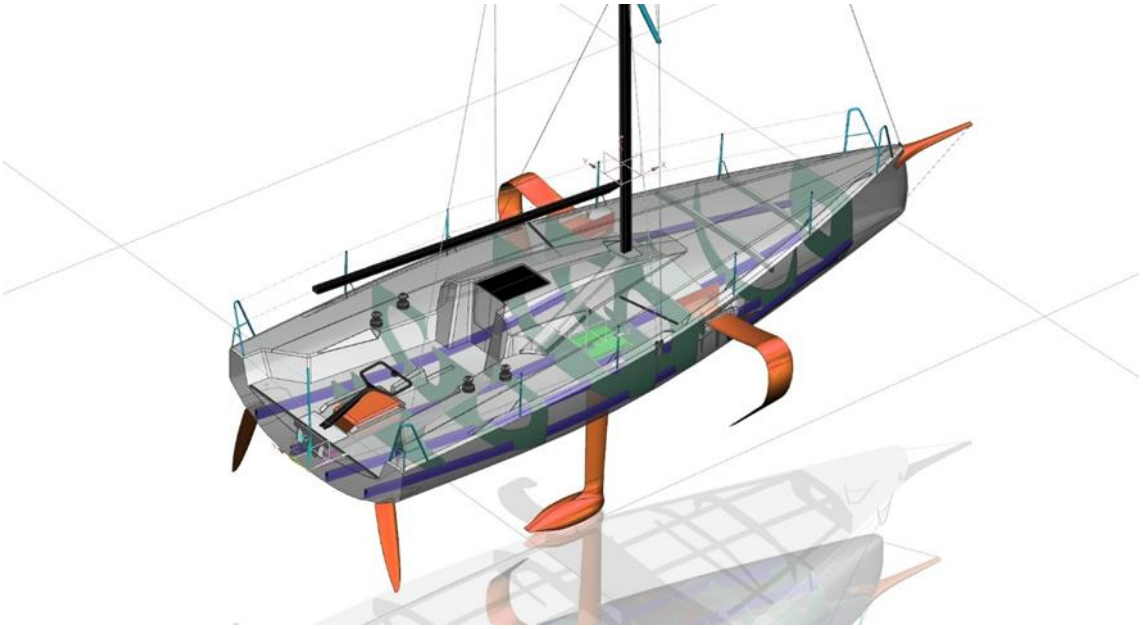

Figure 7 - Beneteau Figaro 3 project developed by VPLP using "Chistera" foil (*Figaro Beneteau 3*, no date)

2.3.3. Dynamic Stability System (DSS)

In 2010 Hugh Burkewood Welbourn created the patent for Dynamic Stability Systems (DSS) (Welbourn, 2010). In essence, this foil system consists in a single horizontal retract board in the leeward side of the yacht, generating vertical force and righting moment, with a side force component as a consequence. This less complex and expensive devise (if compared with the two precedent hydrofoils) decreases the heeling angle, the water borne surface area, while increases crew comfort, vessel speed and stability, being suitable for racing and cruising yachts.

Welbourn (Welbourn, 2010) patent restricts the dimensions of the foil, especially regarding its aspect ratio, angle of attack, span and location in the yacht's hull. In his document there is several solutions in how to install and implement such system, allowing the reader to identify the best way to use these foils in any project.

The ship yard Infiniti Performance Yachts has recently developed both racing and cruising yachts with DSS foils in vessels that may be 36 feet long up to 56 feet. In one of their projects, the cruising boat Infiniti 56C, presented in the following figure, the DSS foil is used with a canting keel, providing comfort to the crew even in strong wind conditions.

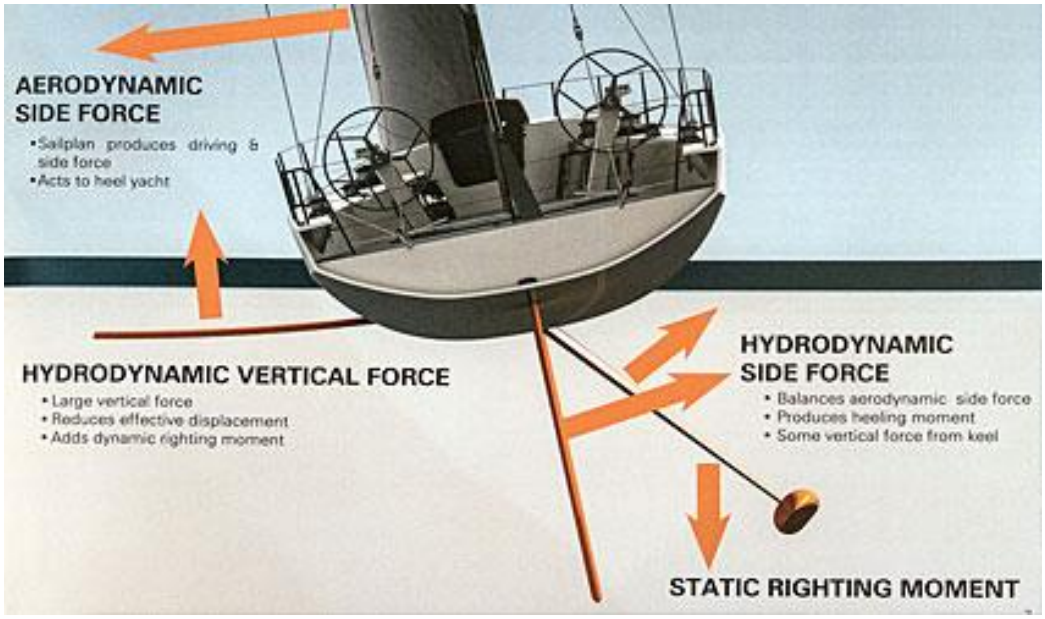

Figure 8 - Infiniti 56C project using DSS (*DSS Dynamic Stability System*, no date)

2.3.4. Previous work

The present work is a continuation of the studies developed by Dewavrin (Dewavrin, 2018) and Gohier (Gohier, 2018), who used the same model and the same foils as the ones used in this research. The previous authors listed the benefits and drawback of the three foils (Dali Moustache, Chistera and DSS), noticing a significant increase in drag, what is negative for the vessel's performance, but also an increase in righting moment, what conduces to smaller heel angle and more crew comfort.

As a continuation in the same line of research, it is important to balance the foil's drawbacks and benefits in order to be really capable to understand in which situations and circumstances it is interesting to have hydrofoils. To do so, a performance prediction is necessary, which is done through the balance of aero and hydro dynamic forces and moments, which basically consist in the development of a Velocity Prediction Program (VPP).

3. VELOCITY PREDICTION PROGRAM

Nowadays VPPs are the main tools used to predict the performance of sailing yachts by designers or researches. These programs may be divided in two main groups as Bohm (Bohm, 2014) suggests: conventional or dynamic VPPs, in which the first kind is more common, seeking a solution for steady state scenarios only. Basically, VPP divides the problem in three solutions, aerodynamic and hydrodynamic at a first step, and after solving each one

separately, solves the equilibrium between them and try to find an optimum boat speed for each wind condition (intensity and direction). Conventional monohull VPPs may differ in complexity regarding the number of degrees of freedom (DOF) it considers. The simplest solution has 2-DOF, ship resistance and heeling moment, while 4-DOF solutions includes side force and yawing moment. Bohm (Bohm, 2014) explains that vertical sail forces and resulting pitching moment are usually neglected for monohulls.

3.1. VPP history

According to Bohm (Bohm, 2014), it was around 1900 that the interest in VPPs became important around the world, with the emergence of yacht sports and regattas. The precursor in the study of crafts hydrodynamics was William Froude, studying merchant and war ships mainly. In 1901 George L. Watson perform the first studies regarding sailing boats, testing eleven models in towing tank for the America's cup. Ken Davidson did important improvements in the field in 1936, determining the resistance considering the influence of sail forces on dynamic trim and sinkage (Bohm, 2014).

In the 1930's, Ken Davidson performed full scale measurements of boat speed and heel angle, such conditions were simulated in towing tank to measure ship resistance and side force. Combining full scale and model results it was possible to determine the sail forces.

In 1974 at TU Delft, in the Netherlands, the Delft Systematic Yacht Hull Series (DSYHS) was created, performing several towing tank tests with different models, being able to generate a method that empirically estimates the wave resistance of a yacht as a function of its form parameters. The same institution has also created the Delft Systematic Keel Series (DSKS) to calculate the influence of appendages. For preliminary design, the DSYHS is probably the most efficient method to predict the hydrodynamic loads of a sailing vessel, it is quite reliable, simple and easy to apply, despite its drawback that limits its application to a certain range of vessel's speed and dimensions (Keuning and Sonnenberg, 1998).

In 1978 J. E. Kerwin presented a method developed at the Massachusetts Institute of Technology (MIT) as part of the Ocean Race Handicapping Project, which goal was to predict the sailing performance of yachts for different sail states and wind conditions. For that, the hydrodynamic forces were estimated with towing tank results, while the aerodynamic loads relied on coefficients dependent of apparent wind angles. With such data base, several interactions are performed to calculate the maximum boat speed, based on the equilibrium of forces. It was Kerwin that introduced the concept of flat and reef for the optimization of

aerodynamic forces. Varying these two parameters it is possible to change the size and lifting capability of sails (Bohm, 2014).

C.A. Marchai in the 1970's did important improvements in the understanding of aerodynamic loads in sailing yachts by experimental tests in wind tunnels. For the 1995 America's Cup the most accurate method known so far was created, the Twisted-Flow wind tunnel, which changes vertically the flow direction and intensity to better simulate the wind seen by a real sailing yacht.

In the 1980's sailing yacht dynamometers were developed and installed in full scale vessels to measure the loads on rigs and the shape of sail, such data combined with towing tank results allowed the separation between hydrodynamic and aerodynamic loads.

With the popularity of computers increasing, the use of Computer Fluid Dynamic (CFD) programs has emerged in the yacht industry. According to Souppez (Souppez, Arredondo-Galeana and Viola, 2019), in 1968 Milgram first used an inviscid code, based on the Vortex Lattice Method, to study up wind sails. The numerical model of downwind sails was just possible later in the 1980's with the introduction of turbulent methods as the Reynolds-Averaged Navier-Stokes (RANS), coupled with structural software able to predict the sails deformation.

For the 1983 America's cup the Australian team used Boundary Elements Method (BEM) to study the appendages hydrodynamics, but with the increase of computer's power, the entire hull started to be modelled and other fluid dynamic methods started to be used, including fluid viscosity and turbulence. Nowadays, viscous CFD solvers are used to describe the resistance of the entire boat and allowing the optimization of yachts numerically.

The evolution in the studies of hydrodynamic and aerodynamic allowed the development of more sophisticated VPPs, yielding to programs able to predict with high accuracy the behaviour of complex yachts. The consequence of the increment in precision conduces to an augmentation in cost, demanding for the VPP developer the ability to understand the different methods and balance different demands to make the right choice.

3.2. Conventional VPP

According to Bohm (Bohm, 2014), conventional VPPs rely in pre-calculated database of aerodynamic and hydrodynamic characteristics of the yacht. With such information, the balance of forces may be done to find an equilibrium condition, and an optimizer may be used to trim the sail (reef and flat) to find the maximum velocity of the yacht.

The database may be generated or with experimental tests, towing tank and wind tunnel, or numerically (BEM, RANS), or with empirical series (as DSYHS). The selection of each model, depending on its complexity and accuracy, plays an important role in the results the VPP may generate, and of course, in the cost of its development and application, regarding time consuming and computational cost.

In general, such VPPs are able to generate polar plots of optimal boat speed as a function of true wind speed and angle. One of the most used and known conventional VPPs is the IMS VPP, developed to be used by the Offshore Racing Congress (ORC) using the International Measurement System (IMS) to make the handicap calculation of different yachts that may participate to the same races and regattas. In the market there is some other commercial programs, as MaxSurf VPP and WinVPP, which do not include hydrofoils, but are used in the present work for validation.

3.3. Dynamic VPP

Still considering Bohm (Bohm, 2014), the Dynamic VPP (or DVPP), is also known as Performance Prediction Program (PPP), and this one differs from the conventional VPP because it solves the yacht's equation of motion in a time series. This kind of VPP may have two different approaches: the first one is based on coefficients extended to manoeuvring extracted from measured data; the second directly calculates all time dependent hydrodynamic and aerodynamic data.

The first approach has the main goal to simulate the velocity losses due to tacking and gybing, in order to optimize these manoeuvres. This type of VPP is quite recent, with important publications being done after 1995 and relying on experimental data. The second approach attempts to enhance the accuracy of the performance prediction by performing time interactions at which the fluid dynamics are directly calculated (Bohm, 2014). With modern computers, in the last 20 years, many studies have been done using different numerical methods to describe the fluids dynamics, from potential flow to viscous flow, coupling fluid dynamics with material resistance (Fluid Structure Interaction), discretising the fluid domain by panel methods or finite volumes.

In this present work, the goal is to understand the benefits of hydrofoils and develop a tool for preliminary design. For this reason, a Dynamic VPP is not necessary due to its complexity, driving this project to a conventional VPP solution, with analytical and empirical aero and hydro dynamic models to describe the yachts behaviour.

4. AERODYNAMIC MODEL

It is important for any VPP to have a solid aerodynamic model to describe the sail's forces and moments to balance with the hydrodynamic loads. This model should consider the boat speed, heel angle, wind conditions and sail characteristics, as area, planform, shape and the interaction between sails.

Bohm (Bohm, 2014) defines sail planform as "*a set of ratios which is fixed for a given set of sails, e.g. sail area, girth dimension, etc*." and sail shape as "*an additional set to represent changes of the flying shape due to the action of the trimmers*". The reader should understand the trimmers as the boat sailors that set the sail for the given wind conditions.

Still according to Bohm (Bohm, 2014) there is two main approaches to describe the aerodynamic loads in a sailing yacht. The first one uses an explicit sail shape or trim, where the VPP must have access to all possible sail setups and corresponding force coefficients, which consist in a test matrix where the VPP is able to find the optimal sail shape for a given wind condition and boat state. The advantage of such approach is that the force coefficient of each individual sail can be precisely described and depowering due to its trim. On the other hand, sail shapes cannot be related to trim setting. In general lines, this explicit method is used in CFD applications for very competitive sailing teams, being a detailed design model, not suitable for the context of this text.

The second approach has an implicit description of sails trim, where only one optimal sail trim has to be found and any consequence of it in the sail shape is accounted by a penalty. This simplification that basically consists in not linking the aerodynamics of sails to their actual shape, is simpler and suitable for preliminary design VPPs. Such approach is also called as Kerwin model.

Graf and Bohm (Graf and Böhm, 2005), as Bohm (Bohm, 2014), used the implicit description of sails trim, applying the Kerwin model and its improvements, done by authors like Hazen. This model trims the sails with two parameters, flat and reef. The first one decreases the sails lift coefficient, while the second changes the sail's area, therefore both have impact in the sail force in lift and drag.

The Kerwin model is largely used nowadays in different VPPs, as the very famous one used by the Offshore Racing Congress (ORC, 2017), called as IMS VPP, which solves the aerodynamic problem in two dimensions only, but it is extremely accurate and includes

sources of drag from the hull, spars, rigging and crew. This model is the one that will work as a base for the development of the present work.

4.1. Sailing Background

Before presenting the aerodynamic model itself, it is important to put the reader apart of some basic sailing background to make the continuation of the text clearer. Initially, it is important to understand that true wind is the actual wind that the natural forces generate, it is the one forecasted by weather channels or that someone fells when standing at the beach. The velocity of this wind, and the angle that its direction makes with the movement of the vessel are the so-called true wind speed (TWS) and true wind angle (TWA).

When a body is moving across the true wind, there is a relative velocity between them, which is called apparent wind. The wind speed the yacht “sees”, or someone onboard fells, is the apparent wind speed (AWS), and the angle this wind direction has with the yacht movement is the apparent wind angle. The following figure represent these concepts.

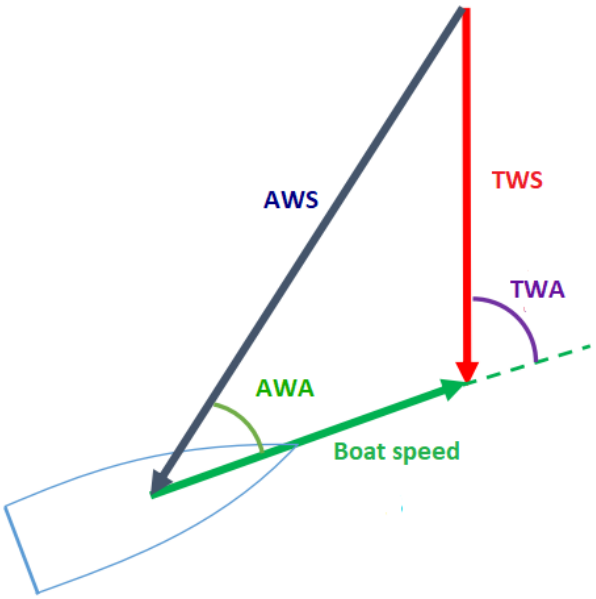

Figure 9 - Sailing triangle, presenting concepts of true wind and apparent wind (J. -B. Souppez, 2017)

Some other terms that should be presented are the sails mains dimensions: foot, bottom part length; leech, back part length; luff, front part length; tack, front edge; clew, back edge; head, top edge. The following figure represents the location of such parameters.

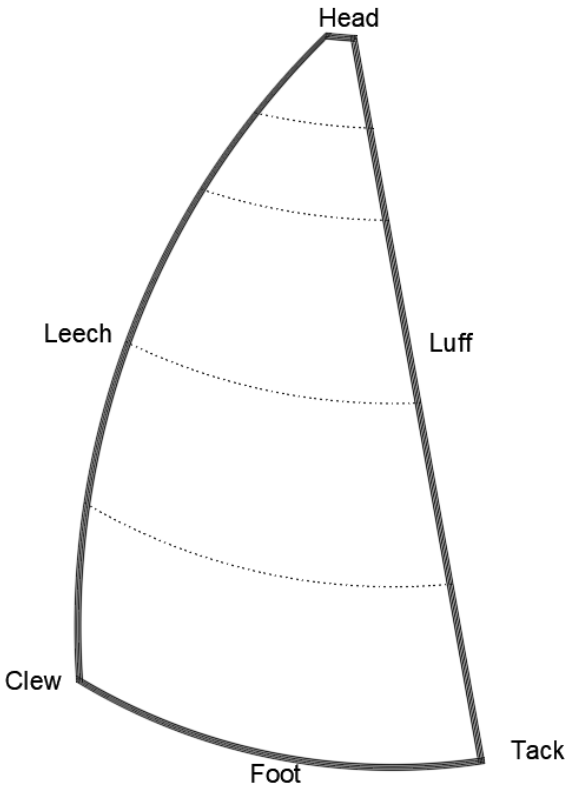

Figure 10 - Sail's mains dimensions considering the yacht's front is in the righthand side of the page (author's drawing)

To conclude this introduction, it is important to introduce the concept of sail reef and flat. The first consists in decreasing the sail area by lowering it down and rolling or folding part of it, in mostly of yachts it is done in windy conditions. Flat refers to changes in the sail shape by tensioning parts of it with lines in order to reduce the sail camber, decreasing the lift and drag the sail generates, being also used in strong breezes.

4.2. Offshore Racing Congress VPP

The ORC VPP has as its main application the calculation of the racing yachts handicaps, which is not the goal of this project. From ORC documentation (ORC, 2017) the aerodynamic model is extracted and presented in the flowing pages. The sails input data is based in the International Measurement System (IMS) (ORC, 2001).

The method estimates a lift and drag coefficient for each sail individually, depending on the mast and rig configuration, as a function of the apparent wind. These parameters are then combined into a set of sails plan that describes the entire sails load. Two other concepts are included to simulate the sailors sail trim, to decrease the heeling moment, this process is called depowering. These two parameters are flat and reef: the first one decreases the lift and

drag coefficient, varying from its maximum value 1 (which represents no flat) until 0.62; the second decreases the sails size, initially by reefing the head sail until its minimum foot length, and then decreasing the main sail area.

The lift force direction is perpendicular to the apparent wind direction, while the drag is parallel. The last one includes: windage drag (hull, spars, rigging and crew), parasitic drag (sail's skin friction and pressure drag from flow separation), and induced drag (three-dimensional effect from the loss of flow circulation from the head and foot of the sails.

For every sail and windage a vertical centre of effort is calculated in order to estimate the correspondent lever arm that heels the vessel for a giving aerodynamic force.

4.3. Main sail

Initially, it is important to be able to estimate the main sail's area with some measures defined by IMS.

$$Area_{main} = \frac{MGL + E}{2} * MGLH + \frac{MGL + MGM}{2} * (MGMH - MGLH) + \frac{MGM + MGU}{2} * (MGUH - MGMH) + \frac{MGU + MGT}{2} * (MGTH - MGUH) + \frac{MGT + HB}{2} * (P - MGTH) \quad (1)$$

Where:

- *P*: Main sail span [m]
- *E*: Main foot [m]
- *HB*: Main sail headboard [m]
- *MGL*: ¼ main span horizontal length from sail's foot [m]
- *MGM*: ½ main span horizontal length from sail's foot [m]
- *MGU*: ¾ main span horizontal length from sail's foot [m]
- *MGT*: 7/8 main span horizontal length from sail's foot [m]

$$MGLH = \frac{MGMH}{2} + \frac{MGL - \frac{E + MGM}{2}}{MGMH} * (E - MGM) \quad (2)$$

$$MGMH = \frac{P}{2} + \frac{MGM - \frac{E}{2}}{P} * E \quad (3)$$

$$MGUH = \frac{MGMH + P}{2} + \frac{MGU - \frac{MGM}{2}}{P - MGMH} * MGM \quad (4)$$

$$MGTH = \frac{MGUH + P}{2} + \frac{MGT - MGU/2}{P - MGUH} * MGU \tag{5}$$

The following figure represents the dimensions just listed:

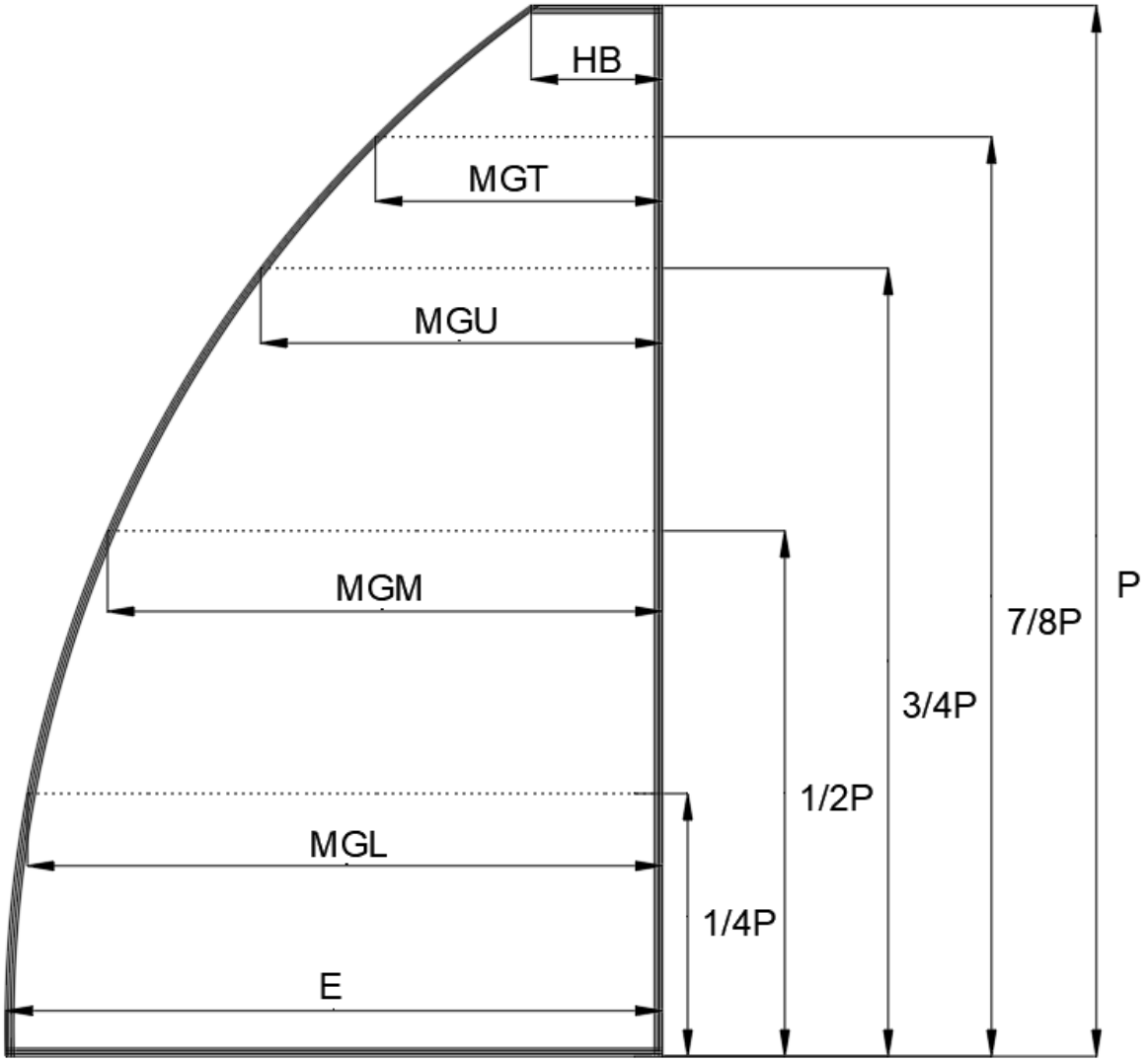

Figure 11 - Main sail dimensions according to IMS (author's drawing)

To define the main sail planform shape, a parameter called *roach* is calculated:

$$ROACH = \frac{\frac{UPPER3/4}{0.375 * P * MGL} - 1}{0.844} \tag{6}$$

Where:

$$\frac{UPPER3}{4} = \frac{P}{8} * (MGL + 2 * MGM + 1.5 * MGU + MGT + 0.5 * HB) \tag{7}$$

Then drag and lift coefficients may be estimated as a function of β_0, which is a correction of the apparent wind angle seen by the sails for a given heel angle:

$$\beta_0 = AWA - \varphi_{up} \tag{8}$$

Where *AWA* is the apparent wind angle, and ϕ_{up} is:

$$\varphi_{up} = 10 * (\frac{\varphi}{30})^2 \tag{9}$$

And φ is the vessel's heel angle in degrees. With the following table it is possible to interpolate the values of Cd_{low}, Cl_{low}, Cd_{high} and Cl_{high}, which represent the range of drag and lift coefficient for a given wind condition.

β_0	0	7	9	12	28	60	90	120	150	180
Cd_{low}	0.04310	0.02586	0.02328	0.02328	0.03259	0.11302	0.38250	0.96888	1.31578	1.34483
Cl_{low}	0.00000	0.86207	1.05172	1.16379	1.34698	1.35345	1.26724	0.93103	0.38793	-0.11207
Cd_{high}	0.03448	0.01724	0.01466	0.01466	0.02586	0.11302	0.38250	0.96888	1.31578	1.34483
Cl_{high}	0.00000	0.94828	1.13793	1.25000	1.42681	1.38319	1.26724	0.93103	0.38793	-0.11207

Table 1 - Main sail force coefficients (ORC, 2017)

With the values of *Cd* and *Cl*, it is possible to calculate the medium value of each coefficient:

$$C_{medium} = C_{low} * \left(1 - \frac{f_{coef}}{2}\right) + C_{high} * \frac{f_{coef}}{2} \tag{10}$$

Where:

$$f_{coef} = \sqrt{sin\left[\frac{\pi}{0.6} * min\left(0.3; max\left(0; \frac{1}{Fractionality} - 1\right)\right)\right]} \tag{11}$$

And,

$$Fractionality = I/(P + BAS) \tag{12}$$

Where:

- *BAS*: Boom distance above sheer line (refer to APPENDIX A1)
- *I*: Rigging height from deck (refer to APPENDIX A1)

Finally, the main sail area may be reduced by reefing it, which practically represents a reduction in sail area:

$$Area_{main} = Area_{main} * reef \tag{13}$$

Where reef is a coefficient that varies between 0.5 and 1.

There is also the shadow effect, that includes the loss of main sail area due to the presence of the mast, that deviates the wind, so the final main area is calculated with the equation:

$$Area_{main} = Area_{main} - \frac{3}{2} * P * MW \tag{14}$$

Where *MW* is the mast width in meters (refer to APPENDIX A1).

The height of the centre of effort of the main sail (*CEH*), which is important to estimate the heeling moment, is calculated as:

$$CEH_{main} = \frac{\sum_i A_i * zc_i}{\sum_i A_i} + 0.024 * P \quad (15)$$

Where:

- A_i: Area of each trapezoid that composes the main sail (refer to Figure 9)
- zc_i: Height above the *P* base of the centroid of each trapezoid

4.4. Jib or Genoa

For the head sail, which may be a Jib or a Genoa, the process is similar to the one done for the main sail. Initially, the area is calculated:

$$Area_{jib} = 0.1125 * JL * (1.445 * LPG + 2 * JGL + 2 * JGM + 1.5 * JGU + JGT + 0.5 * JH) \quad (16)$$

Where:

- *JL*: Jib luff [m]
- *LPG*: Jib perpendicular length from its luff at clew [m]
- *JGL*: ¼ Jib luff horizontal length from sail's foot [m]
- *JGM*: ½ Jib luff horizontal length from sail's foot [m]
- *JGU*: ¾ Jib luff horizontal length from sail's foot [m]
- *JGT*: 7/8 Jib luff horizontal length from sail's foot [m]
- *JH*: Top Jib horizontal length [m]

The following figure provides a visual understanding of the Jib's dimensions.

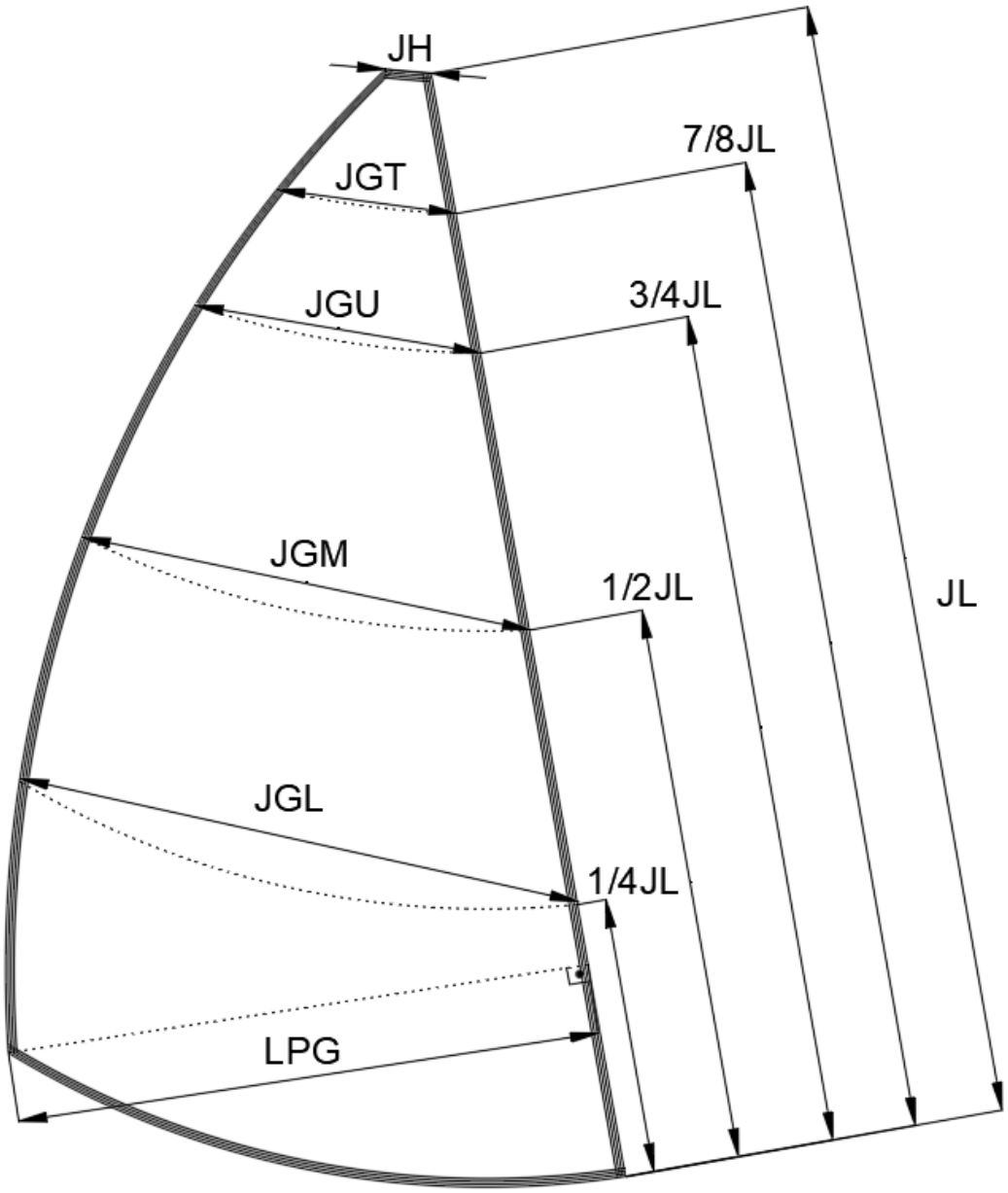

Figure 12 - Jib sail dimensions according to IMS (author's drawing)

Then, the high and low value of the lift and drag coefficient are estimated as a function of β_0 using the following table.

β_0	7	15	20	27	50	60	100	150	180
Cd_{high}	0.050	0.032	0.031	0.037	0.250	0.350	0.730	0.950	0.900
Cl_{high}	0.000	1.100	1.475	1.500	1.450	1.250	0.400	0.000	-0.100
Cd_{low}	0.050	0.032	0.031	0.037	0.250	0.350	0.730	0.950	0.900
Cl_{low}	0.000	1.000	1.375	1.450	1.450	1.250	0.400	0.000	-0.100

Table 2 - Jib force coefficients (ORC, 2017)

And the medium lift and drag coefficients may be calculated as:

$$C_{medium} = C_{low} * f_{coef} + C_{high} * (1 - f_{coef}) \quad (17)$$

Finally, the centre of effort may be estimated with the following equation, very similar to the main sail calculation:

$$CEH_{jib} = \frac{\sum_i A_i * zc_i}{\sum_i A_i} \quad (18)$$

4.5. Spinnaker

There are 3 different Spinnaker configurations, what yields to 3 different formulations, presented separately.

4.5.1. Symmetric Spinnaker tacked on a pole

The Spinnaker area is the maximum value between the Spinnaker area and the Spinnaker default area times the *power function*. To calculate these areas, the following equation is used:

$$Area_{spinnaker} = \frac{SL * (SF + 4 * SMG)}{6} \quad (19)$$

Where:

- *SL*: Vertical length on Spinnaker at its centre [m]
- *SF*: Spinnaker foot length [m]
- *SMG*: Middle Spinnaker horizontal length [m]

The default area is calculated with the exact same equation, but using default values of *SL*, *SF* and *SMG*, which are calculated as:

$$SL_{default} = 0.95 * \sqrt{ISP^2 + J^2} \quad (20)$$

$$SF_{default} = 1.8 * \max(SPL, J) \quad (21)$$

$$SMG_{default} = 0.75 * SF_{default} \quad (22)$$

Where *ISP* is the Spinnaker hoist height and *SPL* is the pole length (refer to APPENDIX A1). The *power* function is calculated with the following formulation:

$$power = \min(0.92 + |fsp|^{1.5}, 1.2) \quad (23)$$

Where,

$$fsp = \min\left(1 - \frac{1.488 * SPL}{A_{spinnaker} \Big/ ISP * AWA_{fact}} - 0.17{,}0\right) \tag{24}$$

$$AWA_{fact} = 0.5196 * AWA^{0.1274} \tag{25}$$

If *AWA* is lower or equal to 28º, AWA_{fact} is 0.794.

To estimate the drag and lift coefficient of the symmetric Spinnaker, the following table is used as a function of the apparent wind angle (*AWA*).

AWA	28	41	50	60	67	75	100	115	130	150	170	180
Cd	0.1915	0.2815	0.3550	0.4392	0.4896	0.5328	0.6192	0.6588	0.6732	0.6732	0.6732	0.6732
Cl	-0.0248	0.6944	0.9068	1.0440	1.0800	1.0800	0.9576	0.8136	0.6120	0.3240	0.1080	0.0000

Table 3 - Symmetric Spinnaker force coefficients (ORC, 2017)

The height of the centre of effort is calculated as:

$$CEH_{spinnaker} = 0.517 * ISP \tag{26}$$

4.5.2. Asymmetric Spinnaker tacked on a Centre Line

For the asymmetric Spinnaker the area and height of effort calculation is very similar to the symmetric, changing just the values of *SL*, $SF_{default}$ and *SPL*.

$$SL = \frac{SLU + SLE}{2} \tag{27}$$

$$SF_{default} = \max(1.8 * SPL, 1.8 * J, 1.6 * TPS) \tag{28}$$

$$SPL = 0.9 * TPS \tag{29}$$

Where *SLU* is the Spinnaker luff length, *SLE* is its leech length and *TPS* is the horizontal distance from its Centre Line and the mast.

The lift and drag coefficients are calculated with the following table:

AWA	28	41	50	60	67	75	100	115	130	150	170	180
Cd	0.16215	0.25184	0.32502	0.40897	0.45920	0.50225	0.57400	0.59552	0.50225	0.38027	0.30852	0.287
Cl	0.01830	0.73500	0.94666	1.08342	1.10494	1.09059	0.94709	0.75337	0.32287	0.03587	0.00000	0.000

Table 4 - Asymmetric Spinnaker tacked on Centre Line force coefficients (ORC, 2017)

4.5.3. Asymmetric Spinnaker on Pole

The only difference between this configuration and the previous is the usage of *SPL* as the length of the pole, and a different table to interpolate the force coefficients.

AWA	28	41	50	60	67	75	100	115	130	150	170	180
Cd	0.16215	0.25184	0.32502	0.40897	0.4592	0.50225	0.59839	0.65292	0.67086	0.67086	0.67086	0.67086
Cl	0.01830	0.73500	0.94666	1.08342	1.10494	1.09059	0.95427	0.81077	0.60987	0.32287	0.10762	0.00000

Table 5 - Asymmetric Spinnaker on pole force coefficients (ORC, 2017)

4.6. Sails plan definition

There is two possible sails plan, the first is more suitable for upwind sailing, which consists in the combination of the Main sail and Jib sail; and the second one for downwind sailing, combining the Main sail with the Spinnaker.

4.6.1. Main sail with Jib sail

Initially, a reference area is calculated, being the sum of both the Main and the Jib sails area.
The Height of the centre of effort *Zce* is calculated as:

$$Zce = \frac{\sum CEH_i * \sqrt{Cl_i^2 + Cd_i^2} * bk_i * Area_i}{Area_{ref} * \sqrt{Cl_i^2 + Cd_i^2}} \tag{30}$$

Where *i* represents or the Main sail or the Jib, and *bk* is a blanketing function, which for the Main sail is equal to 1, and for the Jib sail is equal to 1 for apparent wind angle lower than 135^o and 0 for higher values of apparent wind angle.
When the Jib is reefed, *Zce* must be decreased because of the effect of foot reduction, so it must be subtracted by *ΔCEH*:

$$\Delta CEH = (1 - ftj) * 0.05 * IG \tag{31}$$

Where:

$$ftj = 2 * reef_{jib} - 1 \tag{32}$$

And *IG* is the height of the Jib's hoist (refer to APPENDIX A1).
The flat also has an effect on the position of the centre of effort:

$$Zce = Zce_{flat=1} * [1 - 0.203 * (1 - flat) - 0.451 * (1 - flat) * (1 - fractionality)] \tag{33}$$

The drag coefficient is calculated with the following equation:

$$Cd = Cdmax * \left(flat * f_{cdmult} * f_{cdj} + \left(1 - f_{cdj}\right)\right) + CE * Clmax^2 * flat^2 * f_{cdmult} \tag{34}$$

Where:

$$Cdmax = Cd_{main} * \frac{Area_{main}}{Area_{ref}} + Cd_{jib} * bk_{jib} * \frac{Area_{jib}}{Area_{ref}} \quad (35)$$

$$Clmax = Cl_{main} * \frac{Area_{main}}{Aref} + Cl_{job} * bk_{jib} * \frac{A_{jib}}{Aref} \quad (36)$$

$$f_{cdj} = \frac{bk_{jib} * Cd_{jib} * Area_{jib}}{Cdmax * Area_{ref}} \quad (37)$$

$$CE = KPP + \frac{Area_{ref}}{\pi * heff^2} \quad (38)$$

$$KPP = \frac{KPP_{main} * Cl_{main}^2 * Area_{main} + KPP_{jib} * Cl_{jib}^2 * bk_{jib} * Area_{jib}}{Area_{ref} * Clmax^2} \quad (39)$$

$$KPP_{main} = 0.016 \quad (40)$$

$$KPP_{jib} = 0.017 \quad (41)$$

$$heff = cheff * (P + BAS + HBI) \quad (42)$$

$$cheff = eff_{span} * (0.8 + 0.2 * be) \quad (43)$$

$$be = \begin{cases} 1, if\ AWA \leq 30^o \\ 0.5 * (1 - 1.5 * x + 0.5 * x^3, if\ 30^o < AWA < 90^o \\ 0, if\ AWA \geq 90^o \end{cases} \quad (44)$$

$$eff_{span} = 1.1 + 0.08 * (ROACH - 0.2) + 0.5 * (0.68 + 0.31 * fractionality + 0.075 * overlap - 1.1) \quad (45)$$

$$overlap = \frac{LPG}{J} \quad (46)$$

$$x = \frac{AWA - 60}{30} \quad (47)$$

And *HBI* is the vertical distance between the rig base and the water level (refer to APPENDIX A1), and f_{cdmult} is a function of the flat and is interpolated from the following table.

flat	0 .6	0.65	0.70	0.75	0.80	0.85	0.90	0.95	1.00
f_{cdmult}	1.055	1.048	1.035	1.020	1.008	1.002	1.000	1.004	1.06

Table 6 - Drag coefficient multiplier (ORC, 2017)

Finally, the lift coefficient is calculated with the equation:

$$Cl = Clmax * flat \quad (48)$$

4.6.2. Main sail with Spinnaker

The reference area is also the sum of both the area of the Main sail and the Spinnaker.

The *Zce* is calculated the same way as previously, using *bk* for the Spinnaker equal to 1. Because there is no Jib sail, the *ΔCEH* is not considered, but the effect of flat has the same impact and is included in the same way as before.

The values of lift and drag coefficient are calculated in a simpler way:

$$Cl = Clmax * flat \tag{49}$$

$$Cd = Cdmax * flat \tag{50}$$

4.7. Windages force

The windages area includes everything on board besides the sails, that are exposed to the wind: mast, rig, hull and crew. All these components generate drag (D) only, which is calculated as:

$$D_{windage} = \frac{1}{2} * AWS^2 * \rho_{air} * \sum_i Cd_i * Area_i \tag{51}$$

Where *i* correspond for the windage elements, *AWS* for the Apparent Wind Speed and ρ_{air} for the air density in kg/m³.

4.7.1. Mast

The mast area is equal to its width (*MW*) times its height from the deck (*EHM*). The height of the centre of effort (*Zce*) is calculated with the following equation:

$$Zce_{mast} = HBI + \frac{EHM}{2} \tag{52}$$

The mast drag coefficient depends on the Apparent Wind Angle:

$$Cd_{mast} = \begin{cases} AWA * \frac{Cd_{mast\,90} - Cd_{mast\,0}}{90} + Cd_{mast\,0}, if\ AWA \leq 90^o \\ (AWA - 90) * \frac{Cd_{mast\,0} - Cd_{mast\,90}}{90} + Cd_{mast\,90}, if\ AWA > 90^o \end{cases} \tag{53}$$

Where Cd_{mast90} is equal to 0.6, and Cd_{mast0} is 0.4.

4.7.2. Rig

The rig itself is divided in two parts, the round one (which concerns wires) and the non-round. The area of both is calculated by multiplying the rig height (*I*) and its approximated diameter (*dRig*), which is calculated as:

$$dRig = 2 * \sqrt{\frac{4 * wRig/I}{\rho_{rig}/\pi}} \tag{54}$$

Where *wRig* is the rig's weight, and ρ_{rig} is its material density in kg/m³.

The height of the aerodynamic centre of effort is:

$$Zce_{rig} = HBI + \frac{I}{2} \tag{55}$$

And the drag coefficient is 1.2 for the round part of the rig, and 0.45 for the non-round.

4.7.3. Hull

The exposed hull area that generates drag depends on the apparent wind angle:

$$Area_{hull} = \begin{cases} AWA * \frac{Area_{hull90} - Area_{hull0}}{90} + Area_{hull0}, if\ AWA \leq 90^o \\ (AWA - 90) * \frac{Area_{hull0} - Area_{hull90}}{90} + Area_{hull90}, if\ AWA > 90^o \end{cases} \tag{56}$$

Where,

$$Area_{hull\,0} = FBAV * B \tag{57}$$

$$Area_{hull\,90} = FBAV * L_v \tag{58}$$

Where L_v is the yacht's length, and *B* is its beam, and *FBAV* is calculated as:

$$FBAV = 0.625 * Ff + 0.375 * Fa \tag{59}$$

Where Ff is the front hull's free board, and Fa is its aft free board (refer to APPENDIX A1).

The centre of effort height is:

$$Zce_{hull} = 0.66 * (FBAV + B * \sin(\varphi)) \tag{60}$$

The hull drag coefficient is equal to 0.68.

4.7.4. Crew

The crew's height of the centre of effort is calculated as:

$$Zce_{crew} = HBI + \frac{1}{2} + \frac{B}{2} * \sin(\varphi) \tag{61}$$

The crew's area exposed to the wind is calculated similarly as done previously for the hull:

$$Area_{crew} = \begin{cases} AWA * \frac{Area_{crew90} - Area_{crew0}}{90} + Area_{crew0}, if\ AWA \leq 90^o \\ (AWA - 90) * \frac{Area_{crew0} - Area_{crew90}}{90} + Area_{crew90}, if\ AWA > 90^o \end{cases} \tag{62}$$

Where $Area_{crew0}$ is 0.25 and $Area_{crew90}$ is equal to 0.5 times the number of crew members onboard. The crew's drag coefficient *Cd* is constant and equal to 0.9.

4.8. Forces resolution

Finally, the aerodynamic forces and momentum may be solved. The thrust force in the vessels *x* direction is equal the difference between the lift generated by the sails plan and the drag generated by it and the windages:

$$FRA = FRA_{b4\ windages} - FRA_{windages} \tag{63}$$

Where $FRA_{b4\ windages}$ is the thrust force before windages are included:

$$FRA_{b4\ windages} = CR * \frac{1}{2} * \rho_{air} * AWS^2 * Area_{ref} \tag{64}$$

Where $Area_{ref}$ is the sum of sails area, and *CR* is calculated as:

$$CR = Cl * \sin(AWA) - Cd * \cos(AWA) \tag{65}$$

The windages drag force is calculated with the following equation:

$$FRA_{windages} = D_{windage} * \cos(AWA) \tag{66}$$

The aerodynamic heeling force is equal to the sum of the sails plan and windages side force:

$$FHA = FHA_{b4\ windages} + FHA_{windages} \tag{67}$$

Where the heeling force before the windages is calculated as:

$$FHA_{b4\ windages} = CH * \frac{1}{2} * \rho_{air} * AWS^2 * Area_{ref} \tag{68}$$

The heeling force coefficient is calculated with the following equation:

$$CH = Cl * \cos(AWA) + Cd * \sin(AWA) \tag{69}$$

The windages heeling force is very similar to its drag force, equation (66), but instead of using the *cos*, it uses *sin*.

The heeling moment is calculated as the sum of the heeling moment generated by the sails plan and windages:

$$HMA = HMA_{b4\ windages} + HMA_{windages} \tag{70}$$

Where:

$$HMA_{b4\ windages} = FHA_{b4\ windages} * (HBI + Zce * reef) \tag{71}$$

$$HMA_{windage} = \frac{1}{2} * AWS^2 * \rho_{air} * \sum_i Cd_i * Area_i * Zce_i \quad (72)$$

4.9. Experimental Aerodynamic validation

To validate the aerodynamic model here presented and verify the numerical implementation, the paper published by Masuyama (Masuyama *et al.*, 2009) was used as a reference. In this document the authors present experimental results extracted from a full scale *Fujin* yacht, which was equipped with load cells and CCD cameras to dynamically measure the crafts motion, sails shape and loads. The sails shape was then used in two different numerical methods for validation and comparation, the methods are: Vortex Lattice Method (VLM) and Reynolds-Averaged Navier-Stokes (RANS).

Two different sails set are compared in this document, the first one is composed by the main sail and a 75% jib sail, and the second is similar but with a 130% jib sail. All sails are measured according the IMS rules, which is very convenient because it agrees with the ORC model used. According with the authors, the numerical solutions and the experimental data are in good agreement for the drag (*Cd*), lift (*Cl*), thrust (*CR*) and side force (*CH*) coefficients as for the height of the centre of effort (*Zce*).

The two following tables presents the vessel's main dimension and the sails measurements in detail.

HULL		Rig	
Length over all [m]	10.35	Rigging height from deck [m]	11.00
Length of water line [m]	8.80	Base of foretriangle [m]	3.61
Maximum breadth [m]	3.37	Main span [m]	12.55
Breadth of water line [m]	2.64	Main foot [m]	4.51
Displacement [ton]	3.86		

Table 7 - Fujin principal dimensions (Masuyama *et al.*, 2009)

	Main sail	130% Jib sail	75% Jib sail
Peak height [m]	13.82	10.70	9.90
Luff length [m]	12.50	11.45	10.60
Foot length [m]	4.44	4.89	3.16
Sail area [m²]	33.20	26.10	13.70
Height [%]	Chord length [m]		
0	4.44	4.89	0.00
10	4.13	4.44	2.90
20	3.85	3.94	2.45
40	3.23	2.94	1.70
60	2.43	1.97	1.06
80	1.39	0.98	0.53
100	0.15	0.10	0.10

Table 8 - Sails detailed measurements (Masuyama *et al.*, 2009)

The following figures present the validation results for both jib sails (75% and 130%), comparing the experimental results for sails in port and starboard sides, RANS calculation, VLM calculation and the present model, for *Cd*, *Cl*, *CR*, *CH* and *Zce*.

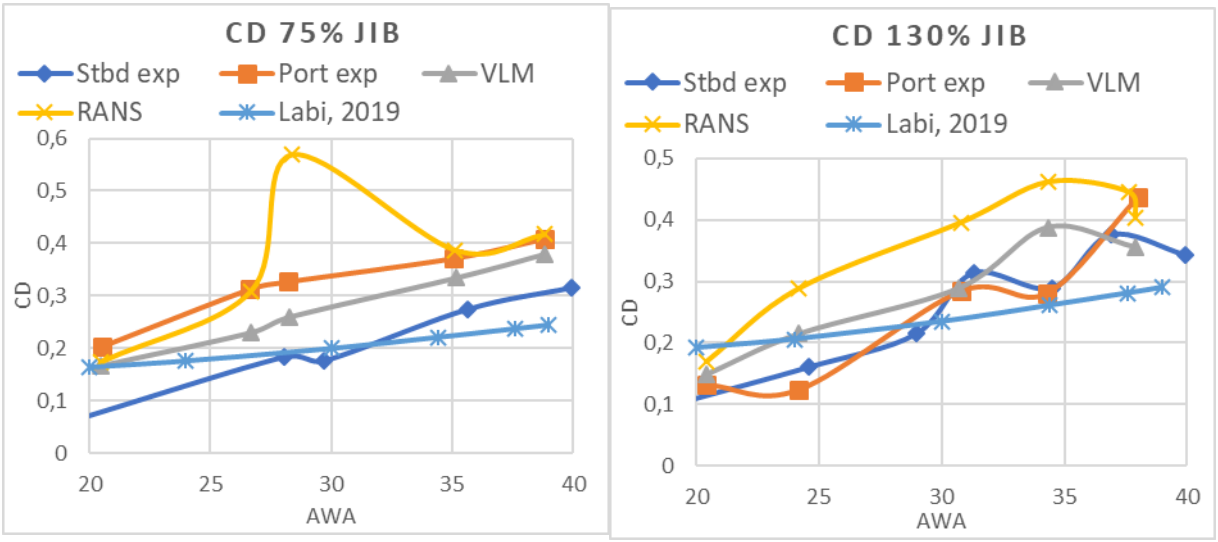

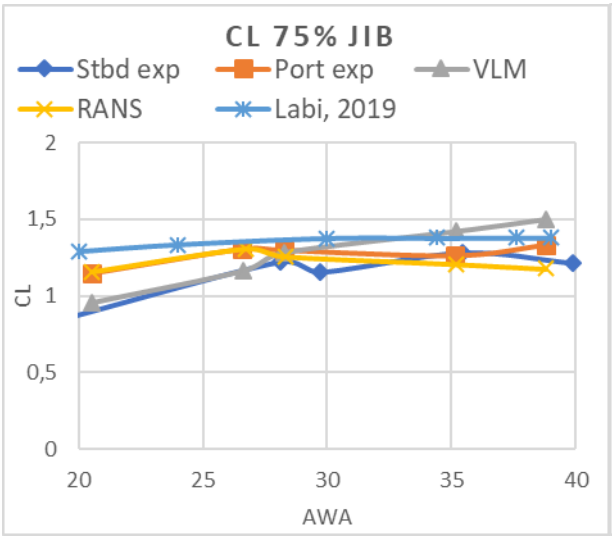
CL 75% JIB
Stbd exp
Port exp
VLM
RANS
Labi, 2019
CL
AWA

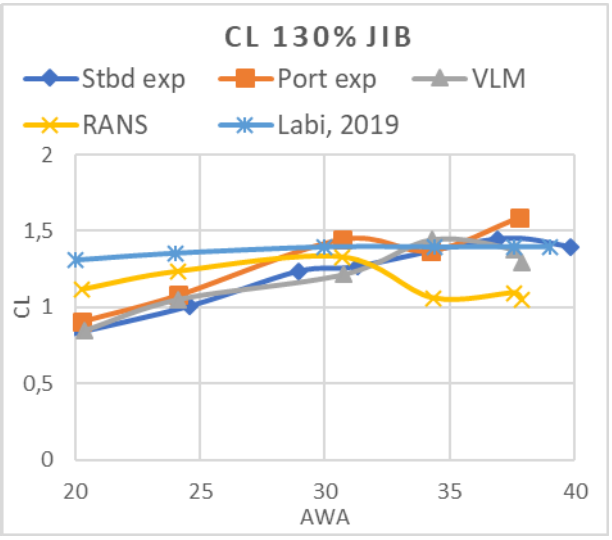
CL 130% JIB
Stbd exp
Port exp
VLM
RANS
Labi, 2019
CL
AWA

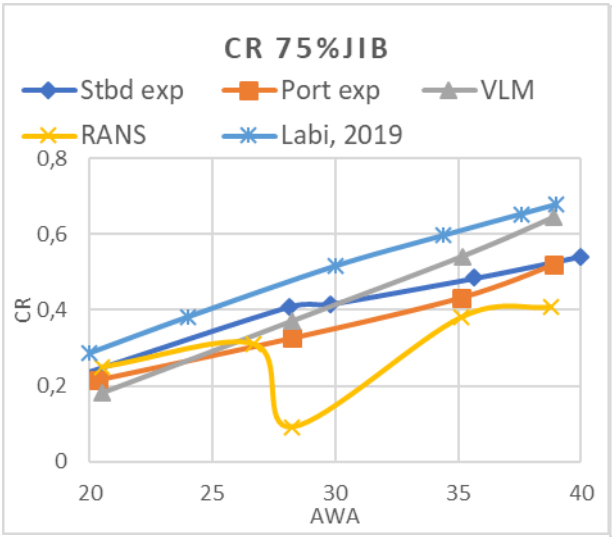
CR 75%JIB
Stbd exp
Port exp
VLM
RANS
Labi, 2019
CR
AWA

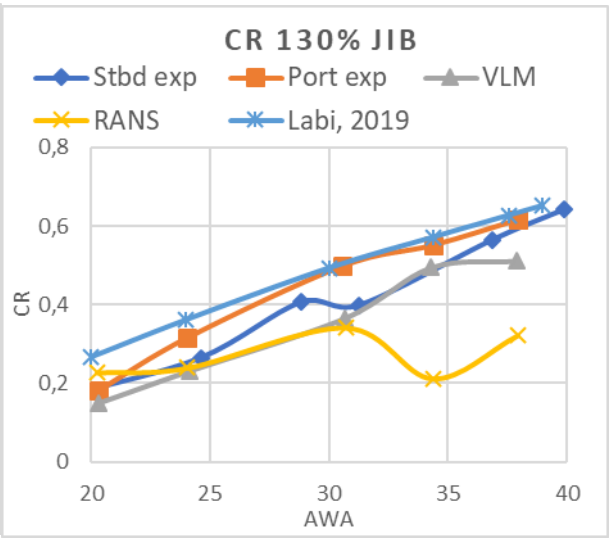
CR 130% JIB
Stbd exp
Port exp
VLM
RANS
Labi, 2019
CR
AWA

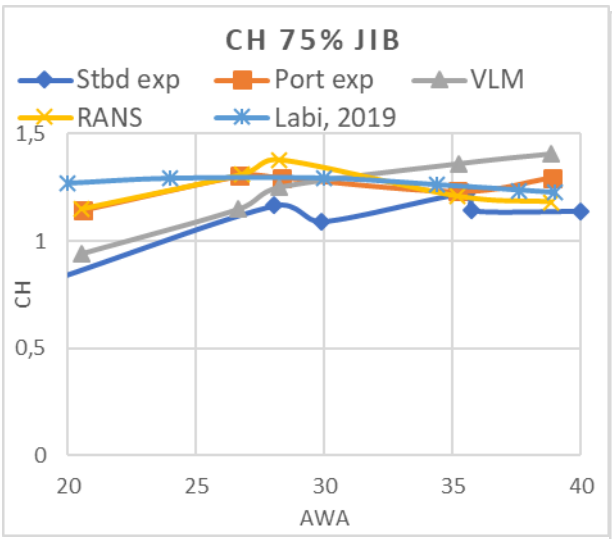
CH 75% JIB
Stbd exp
Port exp
VLM
RANS
Labi, 2019
CH
AWA

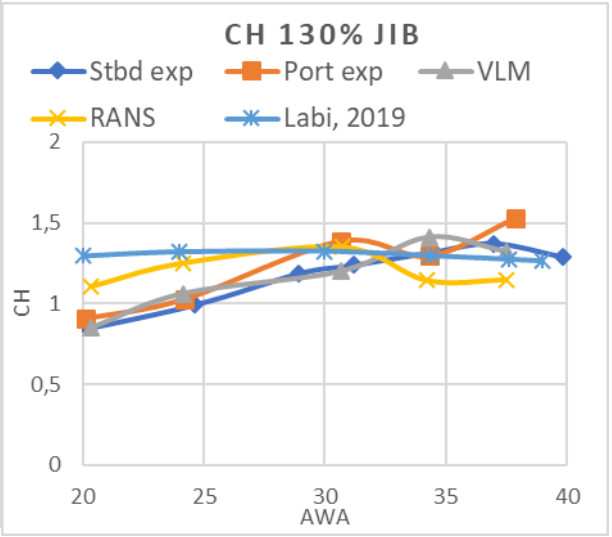
CH 130% JIB
Stbd exp
Port exp
VLM
RANS
Labi, 2019
CH
AWA

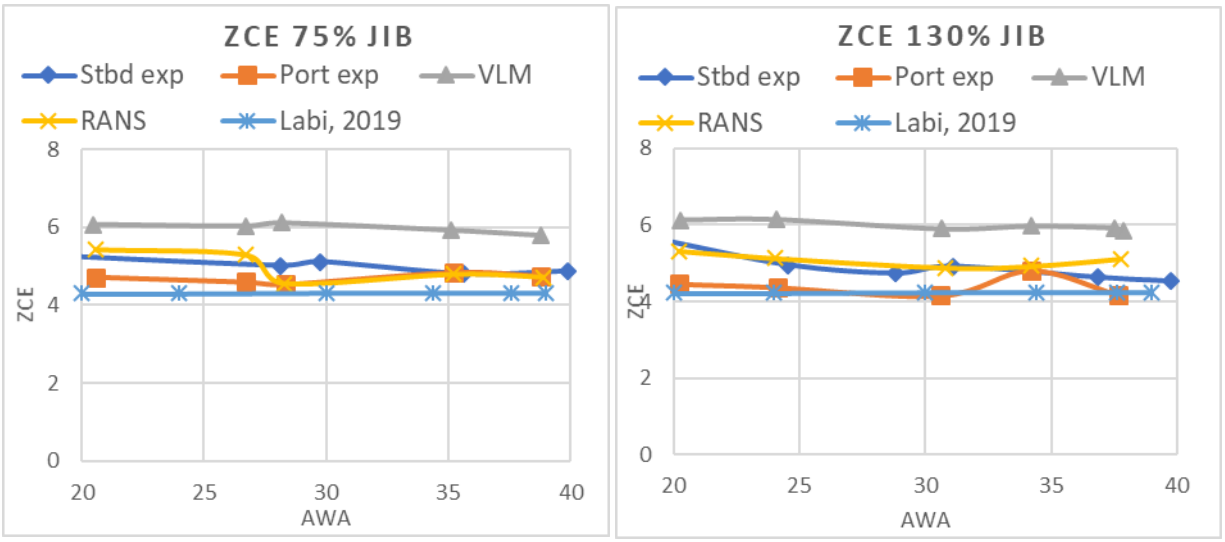

Figure 13 - Model comparation with experimental results and numerical solutions for *Fujin* yacht with two different jib sails

Observing the previous figure, it is possible to notice that the difference between the present model to the experimental and numerical results is not big, and is similar to the difference between the experimental and numerical results itself. Despite generating optimistic results, with a slightly higher values of *Cl*, *CR* and *CH* and lower numbers of *Cd*, the model should be balanced by the fact that the height of the centre of effort (*Zce*) is generally smaller than the other methods. Giving these observations and results, the aerodynamic model is validated.

5. HYDRODYNAMIC MODEL

Three of the already presented references, Böhm (Bohm, 2014), Graf (Graf and Böhm, 2005) and Offshore Racing Congress (ORC, 2017), also have the interest of describing the hydrodynamic forces on sailing yachts. Böhm (Bohm, 2014) uses a commercial CFD solver based on the RANS method, being an extremely complex and time-consuming solution, accurate but costly and not desired at all for a preliminary design toll.

Graf (Graf and Böhm, 2005) applies a simpler method, using the linear wing theory in combination with empirical corrections of non-linear phenomena to describe the hydrodynamic forces. This is an interesting approach to post process towing tank results but is not useful for this master thesis. The Offshore Racing Congress (ORC, 2017) uses the very known concept of dividing the drag in two parts, viscous and residual, also separates the hull (or canoe) forces from the appendages (rudder and keel mainly), without forgetting the consequences due to hell, induced drag, immersed transom and added resistance in waves.

For preliminary design and VPP application of this kind, the best method to describe the hydrodynamic loads in a sailing yacht is the Delft Systematic Yacht Hull Series (DSYHS), which has been developed since the 1970's and had a recent general update with more modern hull shapes in the late 1990's.

Keuning (Keuning and Sonnenberg, 1998) says:

"*the DSYHS is probably the largest systematic series with such a high degree of consistency in both the model shapes and measurement techniques, procedures and analysis*."

And he is not the only one to trust in this series, which is largely used in the yacht industry and is already coupled with many commercial VPP software.

5.1. Delft Systematic Yacht Hull Series

Keuning (Keuning and Sonnenberg, 1998) explains that the DSYHS does the analysis of the bare hull separated from appendages in order to permit the development of new appendages, which may be tested or modelled and then included to a DSYHS analysis. Also, this series includes vessel's trim, leeway and heel, to compute ship resistance and side force.

To summarize, based on Keuning (Keuning and Sonnenberg, 1998) once again, the DSYHS is a polynomial regression from experimental data. In total, over 50 models were tested as bared hulls, from speeds varying from Froude number 0.1 until 0.6, in 3 different conditions, upright, upright with trim and heeling 20 degrees, so the impact of trim and heel could be computed. In the towing tank tests, three degrees of freedom were considered: heave, roll and pitch.

Later, the same author but in a different document (Katgert and Keuning, 2008), presents new results. The goal of this newer publication was to show that sailing yacht's hull have changed with time, allowing higher speeds, and demanding more tests, increasing to 56 the number of tested models in the DSYHS. This last and new version, called the Series 7, also changes the range of speed tested, going up to Froud number equal to 0.75.

In a newer publication, Keuning (Keuning and Katgert, 2010) shows how the heel changes the water line length, wetted area and other vessel's parameter that have impact on the ship resistance, side force and yaw moment. In another text, Keuning (Keuning and Verweft, 2009) presents update results for the impact of keel and ruder on the yacht's side force. He considers both appendages as hydrofoils, calculating the lift coefficient with the formulation developed by Whicker and Fehlnew (Whicker and Fehlner, 1958), where foil are not extended to the free surface, being completely submerged. The effect called 'end plate' is used to

consider the interaction of the hull over the keel, and the 'lift carry over' effect to include the influence of keel and rudder on the hull, this last effect being more significant.

Keuning (Keuning and Verweft, 2009) presents the Delfts Various Keel Series (DVKS), a series similar to the DSYHS in terms of method, but now for different keels, tested on few hull models. The DVKS has been updated along the decades to include modern keel shapes. He also describes effects on appendages lift due to: vessel heel, foil proximity to the free surface, and asymmetry on the hull due to heel. These last effects are important and should be discussed for the case of hydrofoils, which interacts with the hull, the flow around it, and the free surface, which is very close to the hydrofoil and may have free surface piercing effect for Dali-Moustache and Chistera foils.

The following table presents the Delft Systematic Yacht Hull Series range of application according to Keuning (Keuning and Sonnenberg, 1998), it is important to keep these limitations as a reference because any parameter not being respected may induce to an error in the prediction of the hydrodynamic forces.

		Low range	High range
Length - Beam Ratio	Lwl/Bwl	2.73	5.00
Beam - Draft Ratio	Lwl/Tc	2.46	19.38
Length - Displacement Ratio	$Lwl/\nabla c^{\frac{1}{3}}$	4.34	8.50
Longitudinal Centre of Buoyancy	LCB	-8.20%	0.00%
Longitudinal Centre of Flotation	LCF	-9.50%	-1.80%
Prismatic Coefficient	Cp	0.52	0.60
Midship Area Coefficient	Cm	0.65	0.78
Loading Factor	$Aw/\nabla c^{\frac{1}{3}}$	3.78	12.67

Table 9 - Range of hull parameters tested in the DSYHS (Keuning and Sonnenberg, 1998)

Where *Lwl* stands for hull length over the water line, *Bwl* the hull beam at water plane, *Tc* the canoe draft, ∇c the canoe volumetric displacement and *Aw* the hull water plan area.

5.2. Canoe Upright Resistance at Calm Water

Initially, the viscous resistance is calculated in Newtons as:

$$Rfh = \frac{1}{2} * \rho_{water} * V^2 * Sc * Cf \tag{73}$$

Where ρ_{water} is the water density in kg per cubic meter, V is the vessel speed in meters per second, Sc is the wetted area of the hull at rest in square meters, and Cf is the friction coefficient, calculated with the following equation:

$$Cf = \frac{0.075}{(\log(Rn) - 2)^2} \tag{74}$$

Where Rn is the Reynolds number:

$$Rn = \frac{V * 0.7 * Lwl}{\nu} \tag{75}$$

And ν is the kinematic viscosity of the fluid, in this case water. Keuning (Keuning and Sonnenberg, 1998) also provides a formulation to find the wetted area of the hull at rest using the midship area coefficient (Cm).

$$Sc = \left(1.97 + 0.171 * \frac{Bwl}{Tc}\right) * \left(\frac{0.65}{Cm}\right)^{\frac{1}{2}} * (\nabla c * Lwl)^{\frac{1}{2}} \tag{76}$$

The residuary resistance is estimated using the equation presented by (Katgert and Keuning, 2008):

$$\begin{aligned} Rrh = \nabla c * \rho * g \Bigg\{ & a_0 \\ & + \Bigg(a_1 * \frac{LCB_{fpp}}{Lwl} + a_2 * Cp + a_3 * \frac{\nabla c^{\frac{2}{3}}}{Aw} + a_4 * \frac{Bwl}{Lwl} + a_5 * \frac{LCB_{fpp}}{LCF_{fpp}} + a_6 \\ & * \frac{Bwl}{Tc} + a_7 * Cm \Bigg) * \frac{\nabla c^{\frac{1}{3}}}{Aw} \Bigg\} \end{aligned} \tag{77}$$

Where g is the gravity acceleration in meters per square seconds, LCB_{fpp} is the longitudinal centre of buoyancy from the forward perpendicular in meters, and LCF_{fpp} is the longitudinal centre of flotation from the forward perpendicular in meter as well. The coefficients from a_0 to a_8 are a function of Froude number, that may be interpolated from the points presented in the following table.

Fn	0.15	0.2	0.25	0.3	0.35	0.4	0.45	0.5	0.55	0.6
a0	-0.0005	-0.0003	-0.0002	-0.0009	-0.0026	-0.0064	-0.0218	-0.0388	-0.0347	-0.0361
a1	0.0023	0.0059	-0.0156	0.0016	-0.0567	-0.4034	-0.5261	-0.5986	-0.4764	0.0037
a2	-0.0086	-0.0064	0.0031	0.0337	0.0446	-0.125	-0.2945	-0.3038	-0.2361	-0.296
a3	-0.0015	0.007	-0.0021	-0.0285	-0.1091	0.0273	0.2485	0.6033	0.8726	0.9661
a4	0.0061	0.0014	-0.007	-0.0367	-0.0707	-0.1341	-0.2428	-0.043	0.4219	0.6123
a5	0.001	0.0013	0.0148	0.0218	0.0914	0.3578	0.6293	0.8332	0.899	0.7534
a6	0.0001	0.0005	0.001	0.0015	0.0021	0.0045	0.0081	0.0106	0.0096	0.01
a7	0.0052	-0.002	-0.0043	-0.0172	-0.0078	0.1115	0.2086	0.1336	-0.2272	-0.3352

Table 10 - Coefficients for polynomial equation for upright residuary resistance of bare hull (Katgert and Keuning, 2008)

To calculate the Froude number, the following equation is used:

$$Fn = \frac{V}{\sqrt{Lwl * g}} \tag{74}$$

5.3. Change in Resistance Due to Heel

To include the effects of heel in the resistance estimation it is necessary to calculate the new wetted area of the hull, which, according to Keuning (Keuning and Sonnenberg, 1998), is:

$$Sc\varphi = Sc_{(\varphi=0)}\left\{1 + \frac{1}{100} * \left(s_0 + s_1 * \frac{Bwl}{Tc} + s_2 * \left(\frac{Bwl}{Tc}\right)^2 + s_3 * Cm\right)\right\} \tag{79}$$

The coefficients from s_0 to s_3 are a function of the heel angle, and are calculated interpolating the points from the next table.

ϕ	5	10	15	20	25	30	35
S_0	-4.112	-4.522	-3.291	1.85	6.51	12.334	14.648
S_1	0.054	-0.132	-0.389	-1.2	-2.305	-3.911	-5.182
S_2	-0.027	-0.077	-0.118	-0.109	-0.066	0.024	0.102
S_3	6.329	8.738	8.949	5.364	3.443	1.767	3.497

Table 11 - Coefficients for polynomial equation of canoe wetted surface under heel (Keuning and Sonnenberg, 1998)

Where φ is the yacht hell angle in degrees.

The new viscous resistance ($Rfh\varphi$) is calculated with the same equation 73, but with the new value of wetted surface.

To estimate the change in residuary resistance, the following equation is used:

$$\Delta Rrh_{\varphi} = \Delta Rrh_{\varphi=20} * 6 * \varphi^{1.7} \tag{80}$$

Where the change in residuary resistance at 20º of heel is calculated as follows.

$$\Delta Rrh_{\varphi=20} = \nabla c * \rho * g \left\{ u_0 + u_1 * \frac{Lwl}{Bwl} + u_2 * \frac{Bwl}{Tc} + u_3 * \left(\frac{Bwl}{Tc}\right)^2 + u_4 * LCB + u_5 * LCB^2 \right\} \quad (81)$$

The coefficients between u_0 and u_5 are a function of Froude number, and are provided by the following table:

Fn	0.25	0.3	0.35	0.4	0.45	0.5	0.55
u_0	-0.0268	0.6628	1.6433	-0.8659	-3.2715	-0.1976	1.5873
u_1	-0.0014	-0.0632	-0.2144	-0.0354	0.1372	-0.148	-0.3749
u_2	-0.0057	-0.0699	-0.164	0.2226	0.5547	-0.6593	-0.7105
u_3	0.0016	0.0069	0.0199	0.0188	0.0268	0.1862	0.2146
u_4	-0.007	0.0459	-0.054	-0.58	-1.0064	-0.7489	-0.4818
u_5	-0.0017	-0.0004	-0.0268	-0.1133	-0.2026	-0.1648	-0.1174

Table 12 - Coefficients for polynomial equation of change in resistance of bare hull heeled 20º (Keuning and Sonnenberg, 1998)

5.4. Appendages Resistance

The appendages are divided into three components: keel, rudder and bulb. For all of them, the following equation is used to estimate the viscous resistance:

$$Rv_{appendage} = Rf_{appendage} * (1 + k_{apendage}) \quad (82)$$

Where *Rf* is calculated with the same equation 73, but with the appendage dimensions instead of the yacht's. The form coefficient *1+k* is calculated similarly for the keel and rudder:

$$1 + k_{appendage} = 1 + 2 * \frac{t_{appendage}}{c_{appendage}} + 60 * \left(\frac{t_{appendage}}{c_{appendage}}\right)^4 \quad (83)$$

Where *t* is the appendage thickness and *c* is its chord. For the bulb, the following equation is used to estimate the form coefficient:

$$1 + k_{bulb} = 1 + 1.5 * \left(\frac{t_{bulb}}{c_{bulb}}\right)^{\frac{3}{2}} + 7 * \left(\frac{t_{bulb}}{c_{bulb}}\right)^3 \quad (84)$$

The residuary resistance is estimated for the keel only, with the equation:

$$Rrk = \nabla k * \rho * g \left\{ A_0 + A_1 * \frac{T}{Bwl} + A_2 * \frac{Tc + Zcbk}{\nabla k^{\frac{1}{3}}} + A_3 * \frac{\nabla c}{\nabla k} \right\} \quad (85)$$

Where ∇k is the keel volumetric displacement, *T* is the yacht's draft and *Zcbk* is the vertical position of the centre of buoyancy of keel measured from the water free surface in meters.

The necessary coefficients are a function of Froude number, and are interpolated from the following table:

Fn	0.2	0.25	0.3	0.35	0.4	0.45	0.5	0.55	0.6
A_0	-0.00104	-0.0055	-0.0111	-0.00713	-0.03581	-0.0047	0.00553	0.04822	0.01021
A_1	0.00172	0.00597	0.01421	0.02632	0.08649	0.11592	0.07371	0.0066	0.14173
A_2	0.00117	0.0039	0.00069	-0.00232	0.00999	-0.00064	0.05991	0.07048	0.06409
A_3	-0.00008	-0.00009	0.00021	0.00039	0.00017	0.00035	-0.00114	-0.00035	-0.00192

Table 13 - Coefficients for polynomial residuary resistance equation on the keel (Keuning and Sonnenberg, 1998)

The change in resistance due to heel is estimated as:

$$\Delta Rrk\varphi = Ch * Fn^2 * \varphi * \nabla k * \rho * g \tag{86}$$

Where *Ch* is:

$$Ch = H_1 * \frac{Tc}{T} + H_2 * \frac{Bwl}{Tc} + H_3 * \frac{Bwl}{T} + H_4 * \frac{Lwl}{\nabla k^{\frac{1}{3}}} \tag{87}$$

And:

H_1	-3.5837
H_2	-0.0518
H_3	0.5958
H_4	0.2055

Table 14 - Coefficient of polynomial equation for the variation of resistance in appendages due to heel (Keuning and Sonnenberg, 1998)

5.5. Side Force Production

The force (*Fh*) in Newton is perpendicular to the boats keel, and is estimated as:

$$Fh = \frac{\beta * \frac{1}{2} * \rho * V^2 * Sc}{\cos(\varphi)} \left\{ b_1 * \frac{T^2}{Sc} + b_2 * \left(\frac{T^2}{Sc}\right)^2 + b_3 * \frac{Tc}{T} + b_4 * Tc * \frac{T}{Sc} \right\} \tag{88}$$

Where β is the yacht's leeway angle in radians, and the coefficients are a function of the heel angle, interpolated from the table:

φ	0	10	20	30
b_1	2.025	1.989	1.98	1.762
b_2	9.551	6.729	0.633	-4.957
b3	0.631	0.494	0.194	-0.087
b_4	-6.575	-4.745	-0.792	2.766

Table 15 - Coefficients for polynomial equation to determine the side force (Keuning and Sonnenberg, 1998)

The actual side force (*SF*), which is horizontal, is equal to the product of *Fh* and the cosines of the heel angle.

With such data it is possible to calculate the induced resistance:

$$Ri = \frac{Fh^2}{\pi * Te^2 * \frac{1}{2} * \rho * V^2} \tag{89}$$

Where the effective span (*Te*) is equal to:

$$Te = T * \left(A_1 * \frac{Tc}{T} + A_2 * \left(\frac{Tc}{T}\right)^2 + A_3 * \frac{Bwl}{Tc} + A_4 * TR \right) (B_0 + B_1 * Fn) \tag{90}$$

Where *TR* is the ratio between the keel chord at its tip and root. The necessary coefficients are a function of the heel angle, provided in the following table:

φ	0	10	20	30
A_1	3.7455	4.4892	3.9592	3.4891
A_2	-3.6246	-4.8454	-3.9804	-2.9577
A_3	0.0589	0.0294	0.0283	0.025
A_4	-0.0296	-0.0176	-0.0075	-0.0272
B_0	1.2306	1.4231	1.545	1.4744
B_1	-0.7256	-1.2971	-1.5622	-1.3499

Table 16 - Coefficients to estimate the effective span (Keuning and Sonnenberg, 1998)

Finally, all resistances may be added to find the total resistance:

$$Rt = Ri + Rfh\varphi + \Delta Rrh\varphi + \Delta Rrk\varphi + Rrh + Rv_{keel} + Rv_{rudder} + Rv_{bulb} + Rrk \tag{91}$$

5.6. Experimental Hydrodynamic Validation

To check the implemented code and validate the hydrodynamic model, some results were generated to compare numerical data with towing tank values. The experimental results were generated by Technology University of Delft (Delft, 2018), and the model compared is the Sysser 62 because of its large data base and also it is one of the most modern models tested, which main dimensions are presented in the following table.

Parameter	Unit	Value
Hull		
Water line length	[m]	2.08
Beam	[m]	0.505714
Draft	[m]	0.107417
Total draft of hull with keel	[m]	0.326417
Displacement	[m]	0.043959
Volume of displacement of canoe body	[m^3]	0.041339
Longitudinal Centre of Buoyancy	[%]	-4.48
Longitudinal Centre of Flotation	[%]	-6.88
Prismatic Coefficient	[-]	0.541545
Midship Area Coefficient	[-]	0.676269
Water level area	[m^2]	0.715434
Longitudinal position centre of buoyancy to forward perpendicular	[m]	1.13
Longitudinal position centre of flotation to forward perpendicular	[m]	1.18
Keel		
Keel span	[m]	0.219
Keel average chord	[m]	0.338
Keel chord at tip	[m]	0.262
Keel chord at root	[m]	0.414
Keel thickness	[m]	0.0507
Keel area	[m^2]	0.1539
Vertical position of centre of buoyancy of keel from its root	[m]	0.09336
Volume of displacement of keel	[m^3]	0.00262
Keel sweep back angle	[o]	45
Rudder		
Rudder span	[m]	0.096
Rudder average chord	[m]	0.11
Rudder thickness	[m]	0.0132
Rudder area	[m^2]	0.055
Rudder sweep back angle	[o]	5.4

Table 17 - Sysser 62 dimensions and parameters

The validation was done in 4 steps, initially the hull was tested upright, with no leeway and no appendages. Subsequently appendages were added, then the model was yawed and finally heeled. The resistance in Newton was compared for different model speeds, and the side force was computed just for the two last cases, where the leeway angle was different to zero. The following figure presents the Delft and implemented model results.

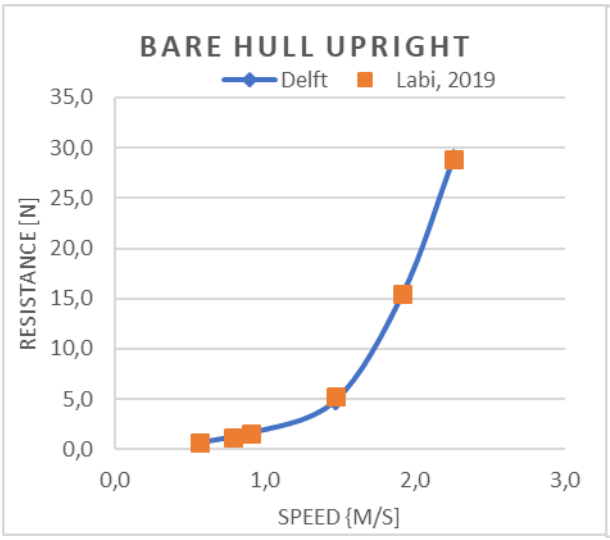
BARE HULL UPRIGHT
Delft
Labi, 2019
RESISTANCE [N]
35,0
30,0
25,0
20,0
15,0
10,0
5,0
0,0
0,0
1,0
2,0
3,0
SPEED {M/S]

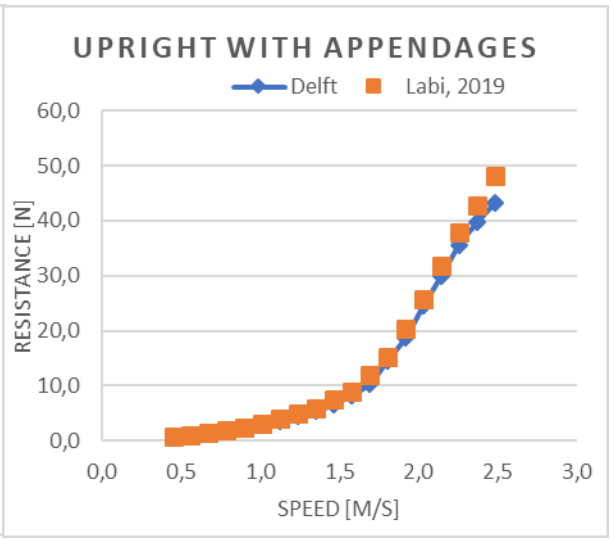
UPRIGHT WITH APPENDAGES
Delft
Labi, 2019
RESISTANCE [N]
60,0
50,0
40,0
30,0
20,0
10,0
0,0
0,0
0,5
1,0
1,5
2,0
2,5
3,0
SPEED [M/S]

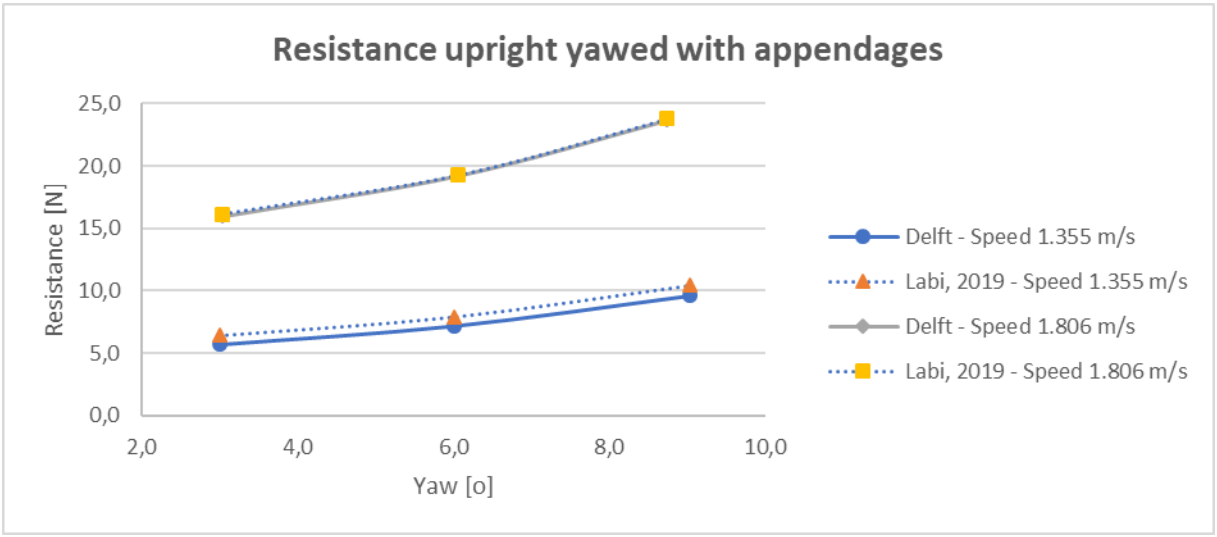
Resistance upright yawed with appendages
Resistance [N]
25,0
20,0
15,0
10,0
5,0
0,0
2,0
4,0
6,0
8,0
10,0
Yaw [o]
Delft - Speed 1.355 m/s
Labi, 2019 - Speed 1.355 m/s
Delft - Speed 1.806 m/s
Labi, 2019 - Speed 1.806 m/s

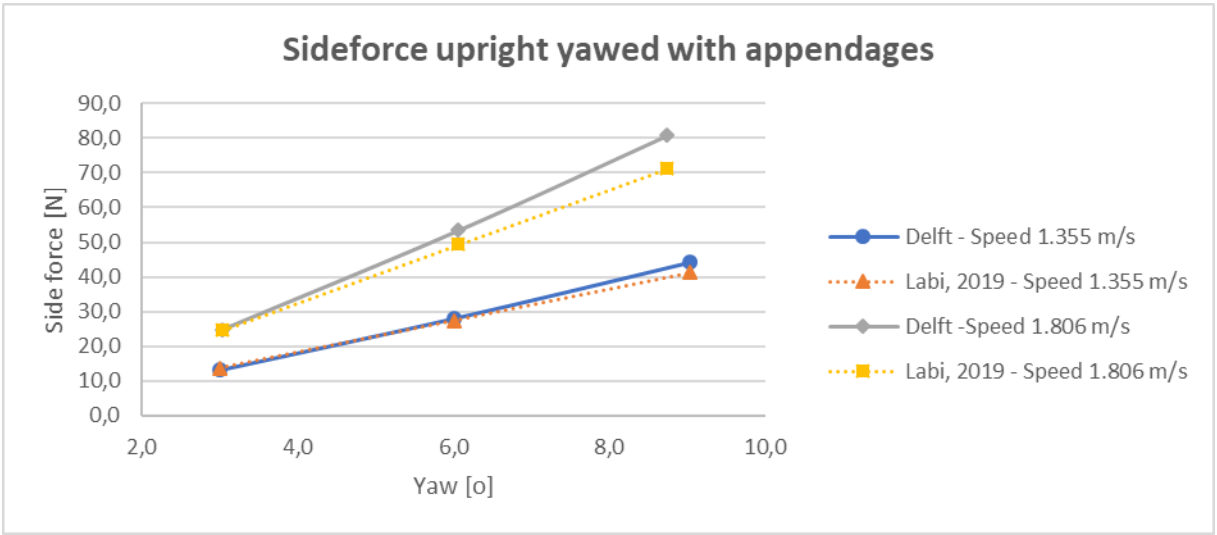
Sideforce upright yawed with appendages
Side force [N]
90,0
80,0
70,0
60,0
50,0
40,0
30,0
20,0
10,0
0,0
2,0
4,0
6,0
8,0
10,0
Yaw [o]
Delft - Speed 1.355 m/s
Labi, 2019 - Speed 1.355 m/s
Delft -Speed 1.806 m/s
Labi, 2019 - Speed 1.806 m/s

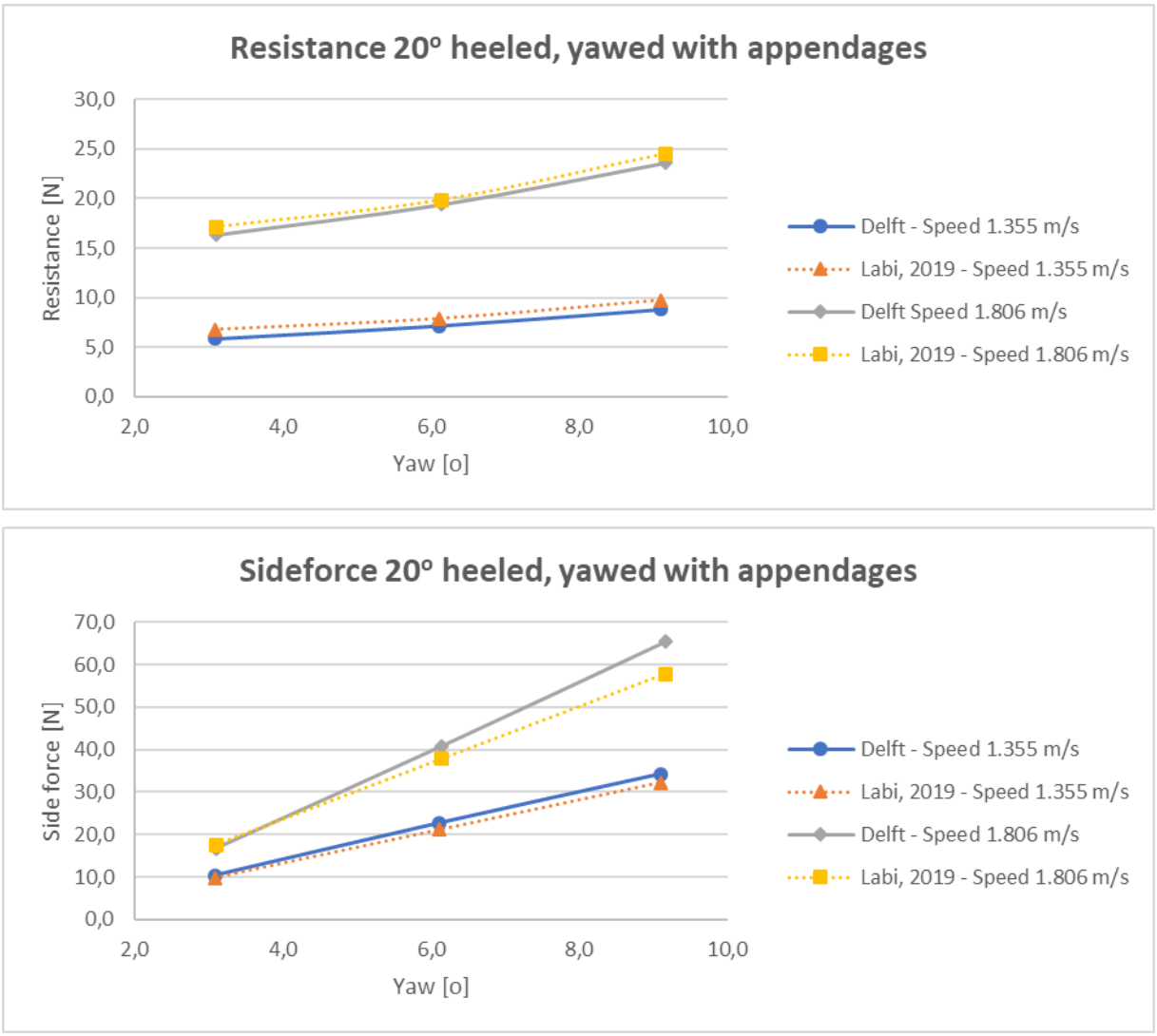

Figure 14 - Model validation comparing with Delft results

Observing the previous figure, it is possible to notice that there is a good agreement between the experimental results and the ones found with the developed code, especially regarding the resistance. There is a light disagreement regarding the side force at high leeway angle, above 6 degrees, which means, in case the final VPP finds solutions with leeway angles of this magnitude, the results should be questioned.

6. FOILS MODEL

The foils model is based in the classic wing theory:

$$L = Cl * \frac{1}{2} * \rho * S * V^2 \tag{92}$$

$$D = Cd * \frac{1}{2} * \rho * S * V^2 \tag{93}$$

Where *L* is the lift force, perpendicular to flow and in Newton, *D* is the drag, also in Newton but parallel to flow, *Cl* and *Cd* are the lift and drag coefficients and *S* is the foil's or wing's area in meter square. To include the effects of free surface proximity, the Glauert biplane theory is used, which is presented by Daskovsky (Daskovsky, 2000). In his work the foil domain is discretized, what is not done in the present work for simplification reasons.

The biplane theory calculates new values of *Cl* and *Cd* depending on the distance of the foil from the free surface (*h*) and its aspect ratio (*AR*), which is the ratio between foil span and chord (*c*).

The new drag coefficient is calculated as:

$$Cd = Cd_0 + (1 + \sigma) * \frac{{Cl_0}^2}{\pi * AR} \tag{94}$$

Where Cd_0 and Cl_0 are the coefficients for an infinite wing, and σ is:

$$\sigma = \frac{1}{1 + 12 * h/c} \tag{95}$$

The new lift coefficient is calculated with the following equation:

$$Cl = Cl_0 * K \tag{96}$$

Where:

$$K = \frac{16 * \left(\frac{h}{c}\right)^2 + 1}{16 * \left(\frac{h}{c}\right)^2 + 2} \tag{97}$$

Subsequently, for each foil an individual formulation was done depending on its geometry.

6.1. Dynamic Stability System (DSS)

The following figure represents a hull heeled (ϕ), seeing from behind and cut at midship by a vertical plan. Some important parameters are also presented as the foil lift force (*L*), righting moment arm (*RMA*), the depth of the foil's centre of effort (*h*) and the angle the foil has with the horizontal when the yacht is upright (α).

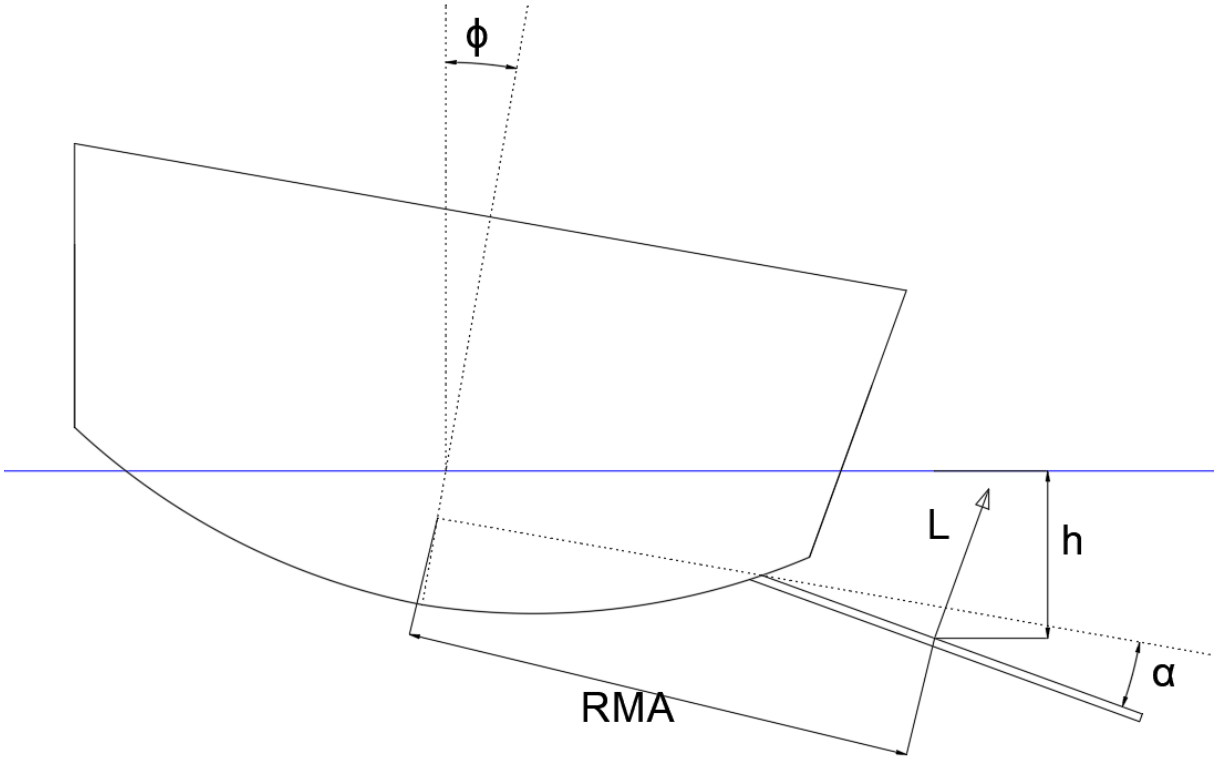

Figure 15 - Hull with DSS foil (author's drawing)

Initially the distance from the free surface to the centre of effort of the foil must be calculated:

$$h_{DSS} = \frac{Bwl}{2} * \sin(\varphi) + \frac{Span}{2} * \sin(\varphi + \alpha) + h_0 * \cos(\varphi) \tag{98}$$

Where h_0 is the initial distance of the foil from the free surface. Then the righting moment arm may be found:

$$RMA_{DSS} = \frac{Bwl}{2} + \frac{Span}{2} * \cos(\alpha) \tag{99}$$

At this point it is possible to estimate the lift and drag from equations 92 and 93, correcting the lift and drag coefficients with equations 94 and 96. Finally the lift force may be decomposed in order to have a righting moment (*RM*) and a side force (*SF*) component, calculated as:

$$RM_{DSS} = RMA_{DSS} * L * \cos(\alpha) \tag{100}$$

$$SF_{DSS} = L * \sin(\alpha + \varphi) \tag{101}$$

6.1.1 Experimental Correction

In the Solent University towing tank (more details regarding the facility and the model manufacture are presented in APPENDIX A2), a model was tested with and without a DSS foil, with constant trim, heave and heel, so the difference between similar test conditions

indicated the real lift and drag of the foil. The foil is a NACA 63-412 profile and was tested with an angle of attack of 8 degrees. Comparing experimental and numerical results, it was possible to define an efficiency coefficient (*eff*) to correct the theoretical forces to have similar results to the ones found experimentally, doing so, a more realistic model is created, including some effects not predicted, as foil-hull interaction, tip vortex and foil water piercing. The main model's dimensions are presented in the following table.

Parameter	Unit	Value
Hull		
Length	[m]	1.522
Water line length	[m]	1.435
Beam	[m]	0.506
Water line beam	[m]	0.343
Draft	[m]	0.107
Total draft of hull with keel	[m]	0.326
Displacement	[kg]	11.5
1+k hull	[-]	1.086
Keel		
1+k keel	[-]	1.252
Wetted surface keel	[m²]	0.04
Keel average chord	[m]	0.0675
Bulb		
1+k bulb	[-]	1.217
Wetted surface bulb	[m²]	0.023
Bulb length	[m]	0.27
Foil		
1+k DSS	[-]	1.252
Wetted surface DSS	[m²]	0.0204
DSS average chord	[m]	0.07
DSS span	[m]	0.234
Foil distance from free surface	[m]	0.00
Foil angle with the horizontal	[o]	0.00
Foil angle of attack	[o]	8.00
Cl	[-]	1.1502
Cd	[-]	0.0146

Table 18 – Towing tank mode dimensions

Using a scale factor of 10 and applying the ITTC 1978 method, it was possible to compare the foil test result with the theoretical model before and after being corrected by the efficiency coefficient. In the following figure the drag and side force are compared for different ship speeds and heel angle.

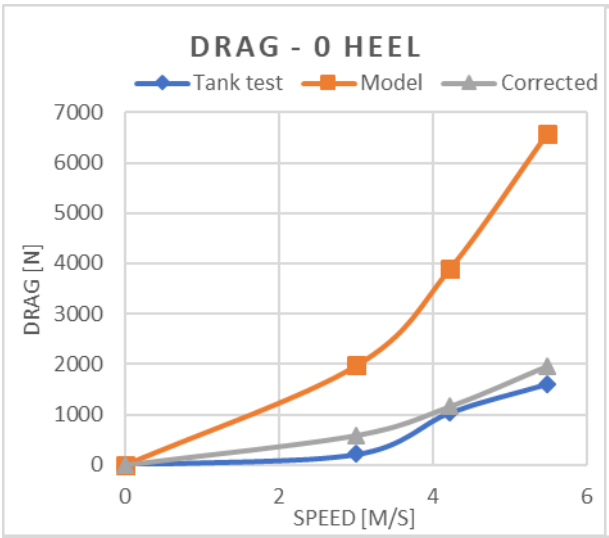
DRAG - 0 HEEL
Tank test
Model
Corrected
DRAG [N]
SPEED [M/S]

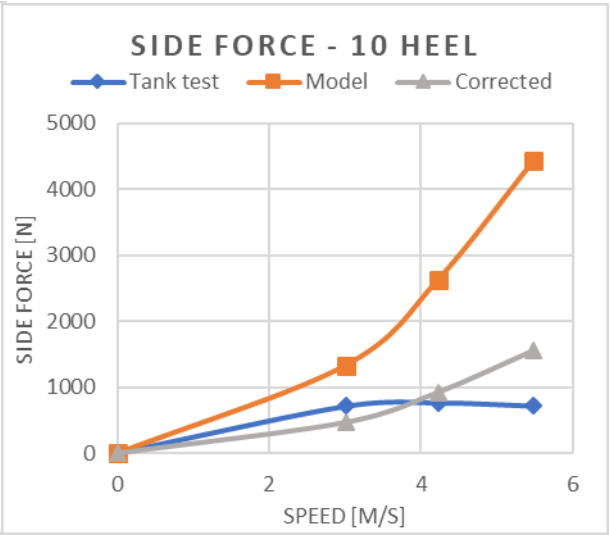
SIDE FORCE - 10 HEEL
Tank test
Model
Corrected
SIDE FORCE [N]
SPEED [M/S]

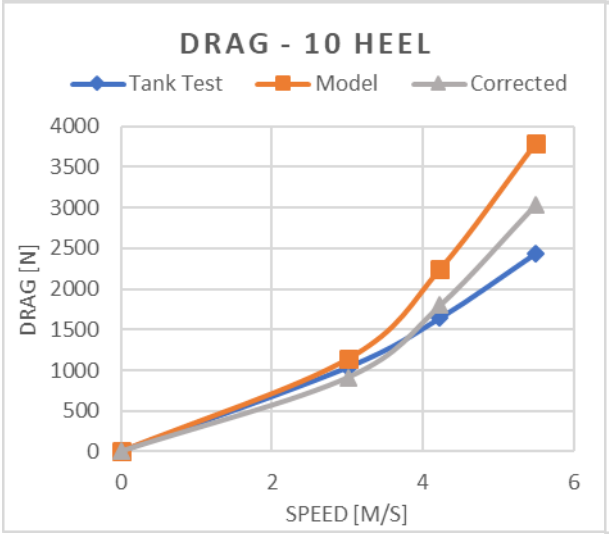
DRAG - 10 HEEL
Tank Test
Model
Corrected
DRAG [N]
SPEED [M/S]

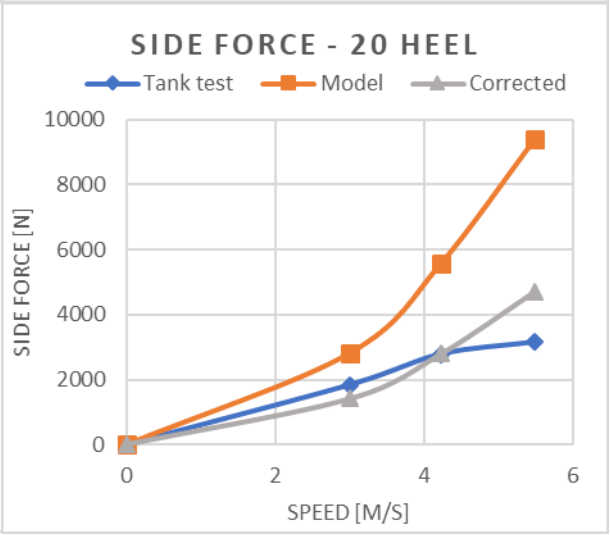
SIDE FORCE - 20 HEEL
Tank test
Model
Corrected
SIDE FORCE [N]
SPEED [M/S]

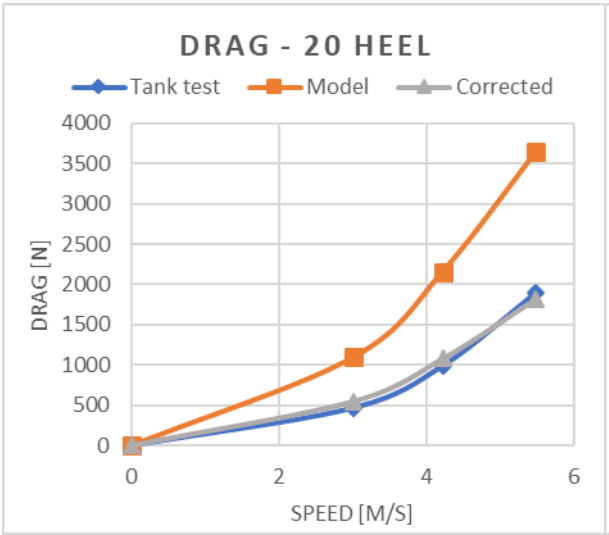
DRAG - 20 HEEL
Tank test
Model
Corrected
DRAG [N]
SPEED [M/S]

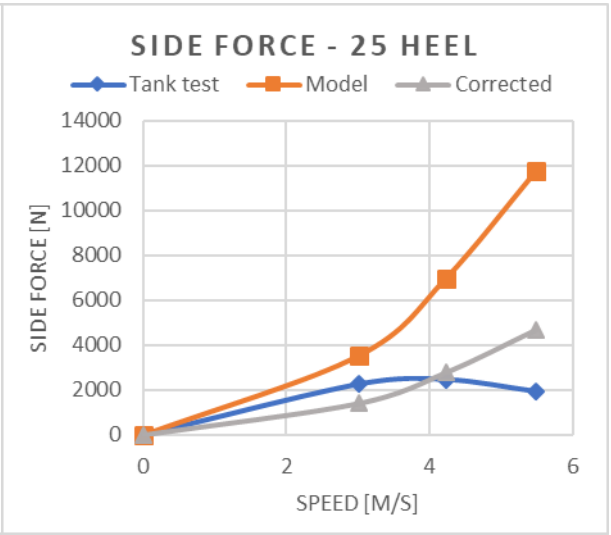
SIDE FORCE - 25 HEEL
Tank test
Model
Corrected
SIDE FORCE [N]
SPEED [M/S]

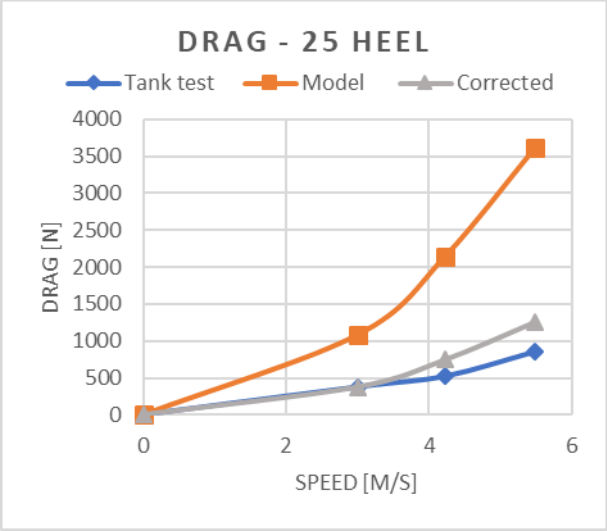

Figure 16 - DSS foil comparation between tank results, model calculation and model correction

The following table presents the efficiency coefficient for drag and side force, as an average efficiency, which will be used in the final model in order to not favour one component more than the other.

φ	eff drag	eff side force	average
0	0.3	[-]	0.3
10	0.8	0.35	0.575
20	0.5	0.5	0.5
25	0.35	0.4	0.375
30	0.25	0.25	0.25

Table 19 - Efficiency correction coefficient for DSS

6.2. Dali Moustache (DM)

The Dali Moustache foil is similar to the DSS foil, but it has a second foil profile in its end, for this reason it is divided in two parts, called 1 and 2, being the 1 modelled as the DSS foil, just presented previously. The following figure presents a vessel with a DM foil, but indicates dimensions and forces concerning the foil's part 2 only.

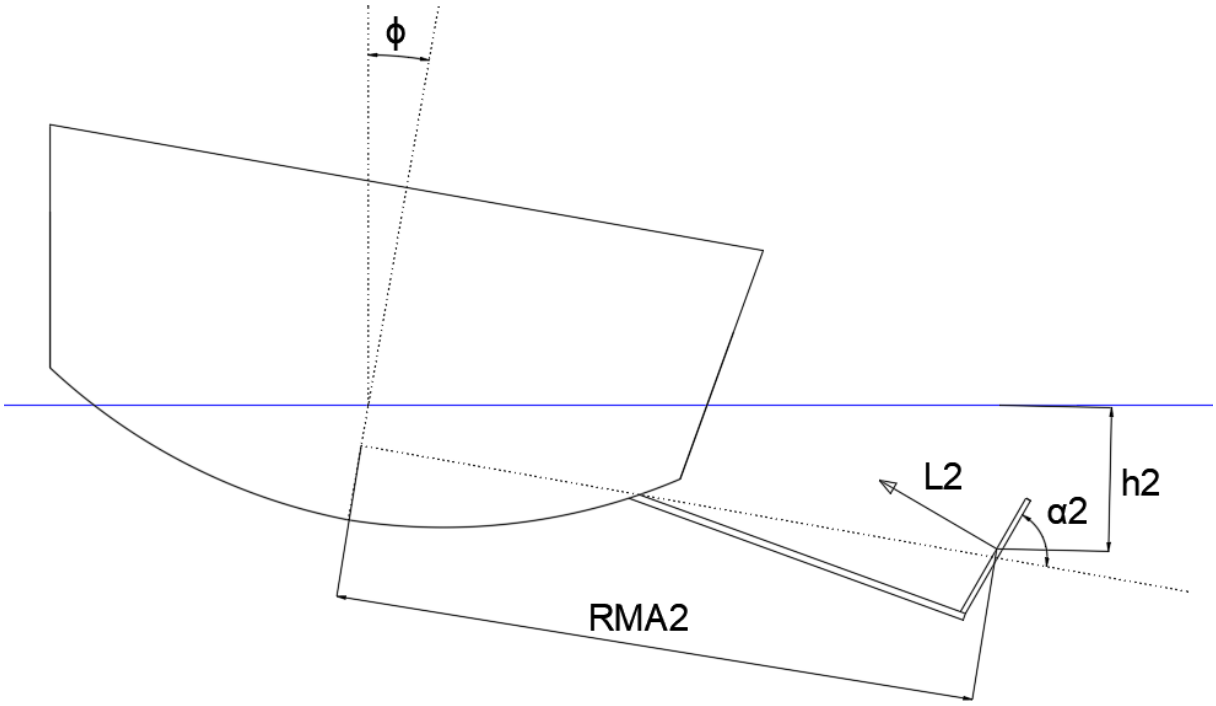

Figure 17 - Hull with Dali Moustache foil (author's drawing)

Similar to what was done for the DSS, it is necessary to define the depth and righting moment arm of the second part of the foil.

$$h_{DM2} = \frac{Bwl}{2} * \sin(\varphi) + Span_1 * \sin(\varphi + \alpha_1) + h_0 * \cos(\varphi) - \frac{Span_2}{2} * \sin(\alpha_2 - \varphi) \quad (102)$$

$$RMA_{DM2} = \frac{Bwl}{2} + Span_1 * \cos(\alpha_1) + \frac{Span_2}{2} * \cos(\alpha_2) \quad (103)$$

For the DM foil, in some situations the part 2 may exit the water, for this reason it is important to also know how far its top is from the free surface:

$$h_x = \frac{Bwl}{2} * \sin(\varphi) + Span_1 * \sin(\varphi + \alpha_1) + h_0 * \cos(\varphi) - Span_2 * \sin(\alpha_2 - \varphi) \quad (104)$$

And, if h_x is below zero, it means the foil is exiting the water, and then a new span must be calculated for the second part in order to consider in the model only what is actually inside the water:

$$Span_2^{'} = Span_2 + \frac{h_x}{\cos(90 - \alpha_2 - \varphi)} \quad (105)$$

Finally, the lift and drag may be calculated as presented previously and the righting moment and side force may be calculated for the second part:

$$RM_{DM2} = RMA_{DM2} * L_2 * \cos(\alpha_2) \quad (106)$$

$$SF_{DM2} = -L_2 * \sin(\alpha_2 - \varphi) \quad (107)$$

At this point it is important to say that the side force of the second part is negative because it acts in the opposite direction of the side force generated by the first part (or the DSS). To compute the final drag, side force and righting moment, the values found for both parts should be added.

6.2.1. Experimental correction

Similarly to what was done for the DSS, the DM was also tested in the same model and towing tank as the previous example (more details regarding the facility and the model manufacture are presented in APPENDIX A2). The following table presents the foil dimensions, once the hull, keel and bulb are the same.

Parameter	Unit	Value
Foil		
1+k DM	[-]	1.2524416
Wetted surface DM	[m²]	0.0371
DM average chord 1	[m]	0.07
DM average chord 2	[m]	0.064
DM span 1	[m]	0.154
DM span 2	[m]	0.142
Foil distance from free surface	[m]	0.025
Foil angle with the horizontal 1	[o]	54
Foil angle with the horizontal 2	[o]	67
Foil angle of attack 1	[o]	8.00
Foil angle of attack 2	[o]	0.00
Cl 1	[-]	1.1502
Cd 1	[-]	0.0146
Cl 2	[-]	0.3423
Cd 2	[-]	0.0057

Table 20 - Dali Moustache foil main dimensions for tank test at model scale

Repeating the same processes described previously for the DSS, it is possible to compare the tank results at full scale with the foil's modelled data and its corrections for different heel angles and speeds, as presented in the following figure.

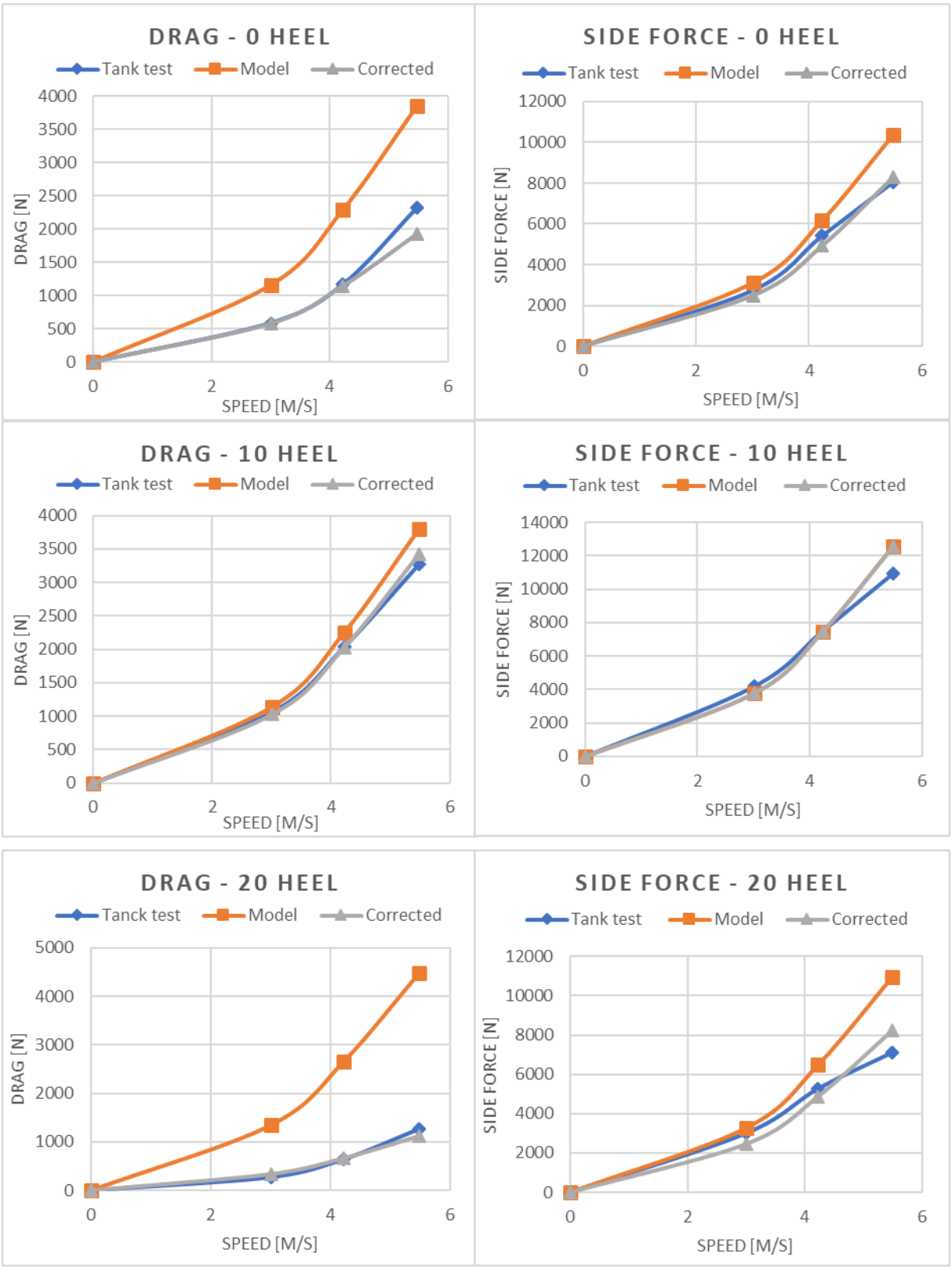
DRAG - 0 HEEL
Tank test
Model
Corrected
DRAG [N]
SPEED [M/S]
SIDE FORCE - 0 HEEL
Tank test
Model
Corrected
SIDE FORCE [N]
SPEED [M/S]
DRAG - 10 HEEL
Tank test
Model
Corrected
DRAG [N]
SPEED [M/S]
SIDE FORCE - 10 HEEL
Tank test
Model
Corrected
SIDE FORCE [N]
SPEED [M/S]
DRAG - 20 HEEL
Tanck test
Model
Corrected
DRAG [N]
SPEED [M/S]
SIDE FORCE - 20 HEEL
Tank test
Model
Corrected
SIDE FORCE [N]
SPEED [M/S]

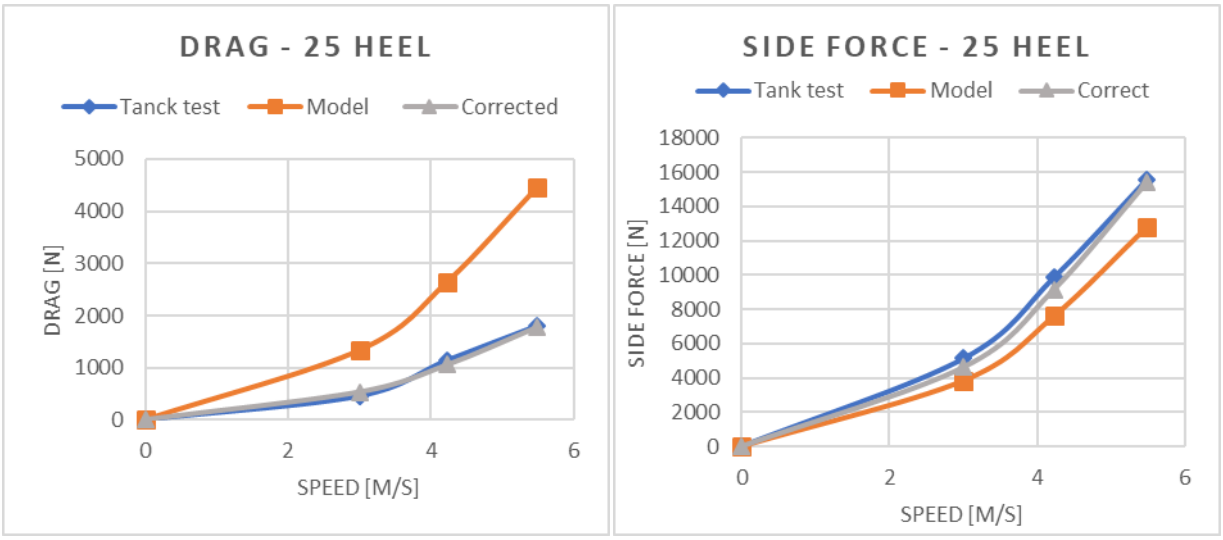

Figure 18 - DM foil comparation between tank results, model calculation and model correction

The next table presents the correction coefficients for drag and side force, as the average, which is the one actually used, as explained previously.

φ	eff drag	eff side force	average
0	0.5	0.8	0.65
10	0.9	1	0.95
20	0.25	0.75	0.5
25	0.4	1.2	0.8
30	0.6	1.2	0.9

Table 21- Efficiency correction coefficient for DM

6.3. Figaro Foil (FF)

Similar to what was done for the two previous foils, a drawing was done to present the Figaro foil and its characteristics.

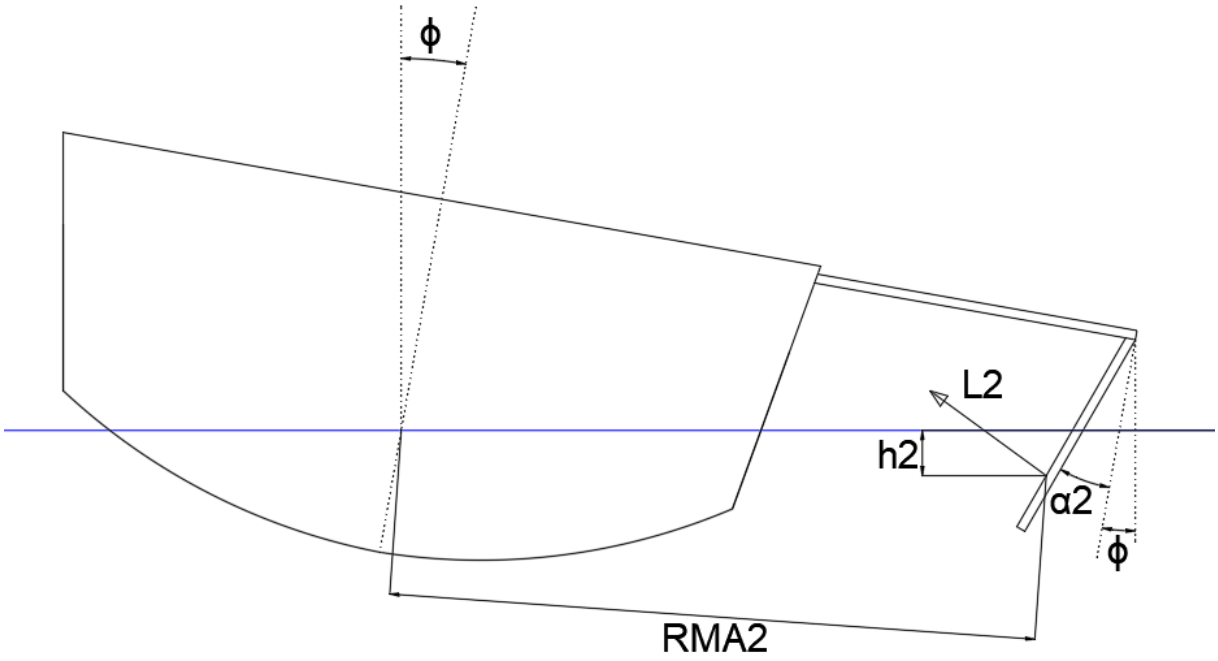

Figure 19 - Hull with Figaro foil (author's drawing)

The Figaro foil, different from the previous ones, has a wetted surface that depends on the yacht's heel angle. From the model used in the towing tank, the following function was found to predict the wetted area at full scale.

$$WS_{FF} = 0.0658 * \varphi + 0.3589 \tag{108}$$

Assuming that the foil is also divided in two parts, and that the second part is not fully inside the water, it is necessary to calculate a span of the foil's wetted part:

$$Span_2^{'} = \frac{WS_{ff}}{chord} \tag{109}$$

At this point it is possible to estimate the depth of the centre of effort and the righting moment arm:

$$h_{FF2} = \frac{Span^{'}{}_2}{2} * \cos(\varphi + \alpha_2) \tag{110}$$

$$RMA_{FF2} = \frac{B}{2} + Span_1 + \left(\frac{Span'_2}{2} - Span_2\right) * \sin(\alpha_2) \tag{111}$$

Finally, the drag and lift may be calculated, which yields to the estimations of righting moment and side force (which is negative for the same reason applied for the DM foil).

$$RM_{FF} = RMA_{FF2} * L * \sin(\alpha_2) \tag{112}$$

$$SF_{FF} = -L * \cos(\alpha_2 + \varphi) \tag{113}$$

6.3.1. Experimental correction

Following the same logic used for the two previous foils, towing tank test were done. The Figaro foil model scale dimensions are presented in the following table.

Parameter	Unit	Value
Foil		
1+k FF	[-]	1.2524416
FF average chord 1	[m]	0.07
FF average chord 2	[m]	0.047
FF span 1	[m]	0.174
FF span 2	[m]	0.61
Foil angle with the horizontal 2	[o]	36
Foil angle of attack 2	[o]	0.00
Cl 2	[-]	0.3423
Cd 2	[-]	0.0057

Table 22 - Figaro foil main dimensions for tank test at model scale

Likewise, the results of the tank at full scale, the model calculation and its correction are presented for comparation.

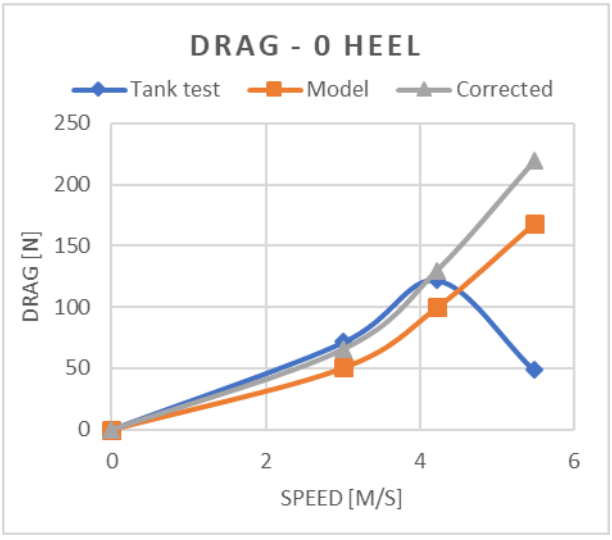

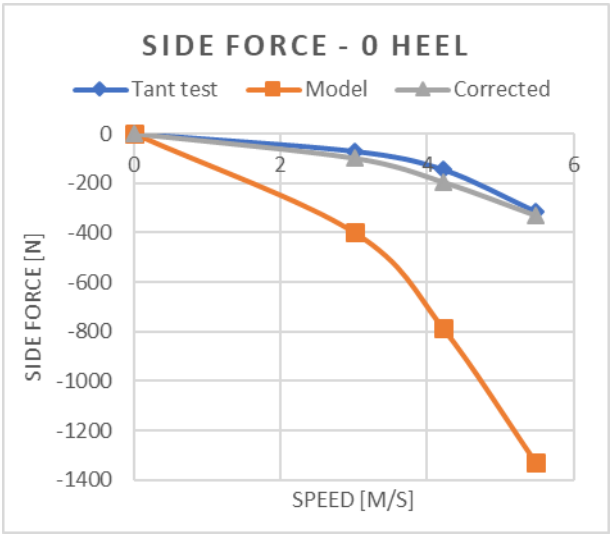

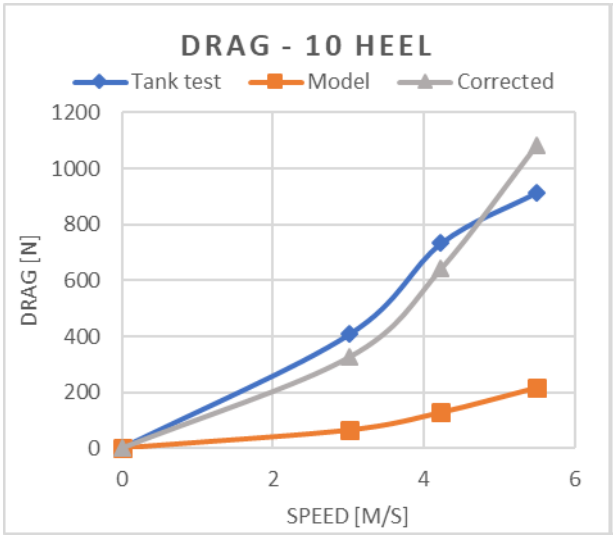

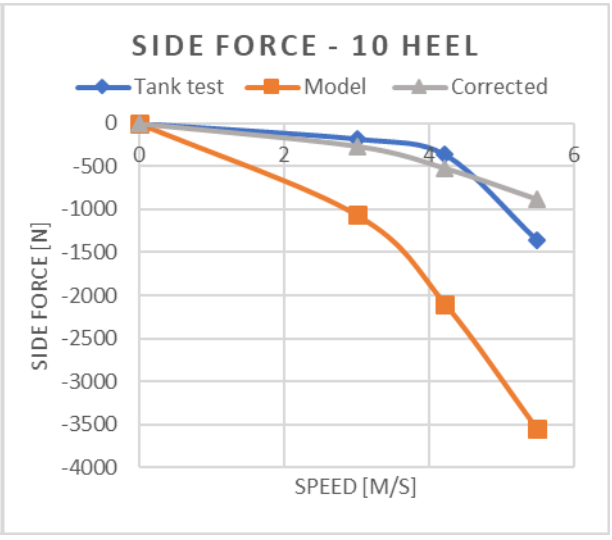

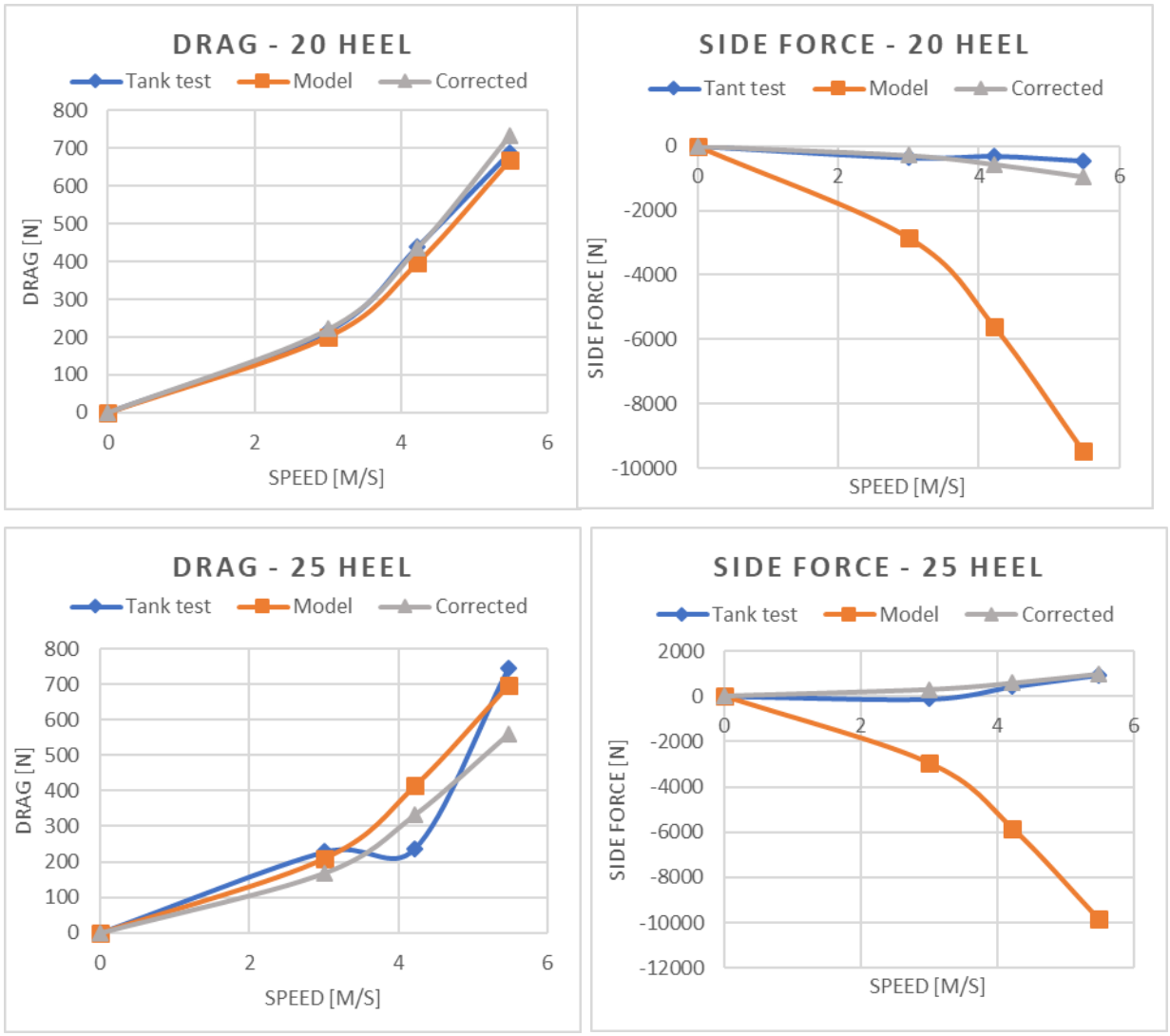

Figure 20 - Figaro foil comparation between tank results, model calculation and model correction

Notice that the side force at 25 degrees of heel is positive for tank results, which indicates that the foil is actually providing force in a non-suitable direction, which should be avoided during sailing, so it is interesting to de power the sails to have smaller heel angles. The following table presents the correction factor for drag and side force, as the average.

φ	eff drag	eff side force	average
0	1.3	0.25	0.775
10	5.0	0.25	2.625
20	1.1	0.1	0.6
25	0.8	-0.1	0.35
30	0.8	-0.1	0.35

Table 23 - Efficiency correction coefficient for Figaro

The results highlights that for 10 degrees of heel the average efficiency is higher than one, given the fact that the efficiency drag is equal to 5, which is too far from the others and suggests a very particular interaction between the foil and bow waves, or any other physical

phenomenal. For this reason and to maintain a certain coherence with the other values founded, in the code itself the efficiency coefficient is not higher than 1.

7. VELOCITY PREDICTION PROGRAM STRUCTURE

The three models presented previously, aerodynamic, hydrodynamic and foil, are coded as functions, that are used by the VPP, which works sending the necessary data for the functions to run and reads its output, compare it and define new parameters that are used in the functions again until forces and momentum balance are found. The following diagram represents the structure of the VPP.

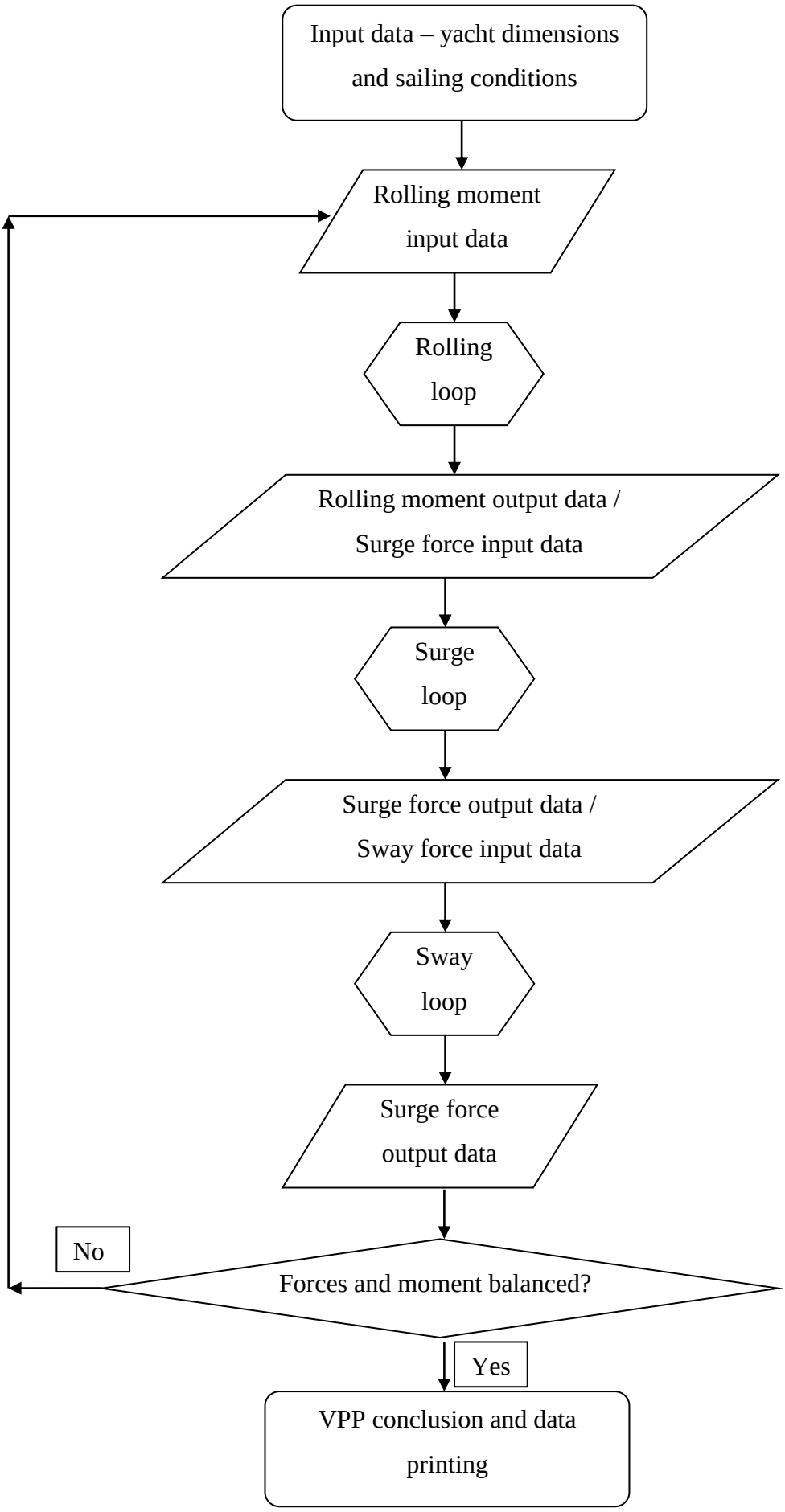
Input data – yacht dimensions and sailing conditions
Rolling moment input data
Rolling loop
Rolling moment output data / Surge force input data
Surge loop
Surge force output data / Sway force input data
Sway loop
Surge force output data
No
Forces and moment balanced?
Yes
VPP conclusion and data printing

Observing the diagram, it is possible to notice there is three loops, Rolling moment, Surge and Sway, it yields to a three degrees of freedom VPP. Due to the limitations in the aerodynamic and hydrodynamic model, it would be actually impossible to include the missing degrees, Heave, Pitch and Yaw.

In the following paragraphs, each loop is presented in more details.

7.1. Rolling Moment Loop

The loop starts by calculating the righting moment:

$$RM = RMV + RGz + RM_{crew} + RM_{foil} \tag{114}$$

Where RM_{foil} is the righting moment generated by the foil, as presented previously. *RMV* is a dynamic righting moment, suggested by ORC documentation (ORC, 2017) and calculated as:

$$RMV = \frac{5.955 * 10^{-5}}{3} * \nabla * LSM * \left(1 - 0.625\frac{B}{\sqrt{AMS}} - 2.1\right) * \frac{V}{Lwl} * \varphi \tag{115}$$

Where *LSM* is the length of the second moment of inertia in meters, φ is the heel in radian and *AMS* is the hull maximum section area in meters, calculated with the following equation:

$$AMS = Cm * B * Tc \tag{116}$$

RGz is the hydrostatic righting moment:

$$RGz = Gz * \nabla * \rho_{water} * g \tag{117}$$

Where *Gz* is the hydrostatic righting moment arm, which is a function of the hull shape and its heel angle. The developed code does not calculate the different values of *Gz*, which must be included as input data. RM_{crew} is the righting moment generated by the crew weight:

$$RM_{crew} = W_{crew} * g * Arm_{crew} * \cos(\varphi) \tag{118}$$

Where W_{crew} is the crew weight and Arm_{crew} is the crew weight righting moment arm, which varies between -0.5**B* and 0.5**B*.

The heeling moment is calculated with the following equation:

$$HM = HMA + Fh * RM4 \tag{119}$$

Where *RM4* is the vertical hydrodynamic centre of pressure, equal to 0.43 times the yacht draft.

While there is a difference between the righting and heeling moment, the code loops until a balance is found. If the righting moment is higher than the heeling moment the heel angle should decrease as the sail reef and flat, the crew should also move to the centre of the boat in

order to decrease the lever arm of its weight. If the heeling moment is higher that the righting moment, the opposite must happen.

Once all these parameters are corrected, the three functions are called by the loop to update the moments and forces, and a new analysis of rolling moment is done until balance is found.

7.2. Surge Loop

Similar to what is done for the rolling moment, in surge, a balance between the aerodynamic driving force and the hydrodynamic drag (generated by hull, appendages and foil) must be found. If the aerodynamic thrust is higher than the drag, the yacht speed must increase, otherwise if the drag is more important, then the velocity should decrease. Again, the loop calls the three functions with updated input values and a new balance is verified.

7.3. Sway Loop

This last loop balances the aerodynamic and hydrodynamic side force (understanding that the foil side force is also a hydrodynamic force). If the aerodynamic side force is higher than the hydrodynamic one, the leeway angle should increase, otherwise decrease. Similar to the previous loops, the three functions are called with updated input values and the loop continues until a balance in sway is found.

7.4. VPP Validation

To verify that the code is well written and correct, the developed VPP results were compared with 2 commercial software, WinVPP and MaxSurfVPP. The yacht used as a reference is the full-scale version of the model tested in the towing tank, presented previously. Its main dimensions are presented in the following table.

Parameter	Symbol	Unit	Value
Hull			
Yacht length	*L*	[m]	15,22
Beam	*B*	[m]	4,72
Total draft of hull with keel	*T*	[m]	3,6
Canoe draft	*Tc*	[m]	0,6
Freeboard Forward	*Ff*	[m]	1,52
Freeboard Aft	*Fa*	[m]	1,52
Water line length	*Lwl*	[m]	14,35
Beam at water line	*Bwl*	[m]	3,43

Volumetric displacement	∇	[m³]	11,22
Volumetric displacement of canoe body	∇c	[m³]	10,66
Longitudinal Centre of Buoyancy	*LCB*	[%]	-7,45
Longitudinal Centre of Flotation	*LCF*	[%]	-6,86
Longitudinal position centre of buoyancy to forward perpendicular	LCB_{fpp}	[m]	7,77
Longitudinal position centre of flotation to forward perpendicular	LCF_{fpp}	[m]	8,35
Prismatic Coefficient	*Cp*	[-]	0,54
Midship Area Coefficient	*Cm*	[-]	0,71
Water level area	*Sc*	[m²]	38,66
Keel			
Keel span	s_{keel}	[m]	2,85
Keel average chord	c_{keel}	[m]	0,675
keel chord at tip	$c_{keel\ tip}$	[m]	0,6
keel chord at root	$c_{keel\ root}$	[m]	0,75
Keel thickness	t_{keel}	[m]	0,081
Keel area	A_{keel}	[m²]	3,94
Keel vertical position of centre of buoyancy	*Zcbk*	[m]	1,14
Volumetric keel displacement	∇k	[m³]	0,104
Rudder			
Rudder span	s_{rudder}	[m]	1,6
Rudder average chord	c_{rudder}	[m]	0,35
Rudder Thickness	t_{rudder}	[m]	0,042
Rudder area	A_{rudder}	[m²]	1,16
Bulb			
Bulb chord	c_{bulb}	[m]	2,7
Bulb thickness	t_{bulb}	[m]	0,3915
Bulb wet surface area	S_{bulb}	[m²]	2,26
Rig			
Vertical distance between rig base and water level	*HBI*	[m]	1,55
Rigging height from deck	*I*	[m]	20,25
Deck boom distance	*BAS*	[m]	2,1
Mast width	*MW*	[m]	0,2
Distance from mast to bow	*J*	[m]	5,94
Main sail			
Main span	*P*	[m]	19,88
Top main horizontal length	*HBI*	[m]	2,1
7/8 P main horizontal length	*MGT*	[m]	2,74
3/4 P main horizontal length	*MGU*	[m]	3,38
1/2 P main horizontal length	*MGM*	[m]	4,65
1/4 P main horizontal length	*MGL*	[m]	5,93
Main foot	*E*	[m]	7,19
Genoa			
Genoa luff	*JL*	[m]	20,25

Top genoa transversal length	*JH*	[m]	0,1
7/8 JL genoa transversal length	*JGT*	[m]	0,8167
3/4 JL genoa transversal length	*JGU*	[m]	1,63
1/2 JL genoa transversal length	*JGM*	[m]	3,27
1/4 JL genoa transversal length	*JGL*	[m]	4,9
Genoa transversal at clew	*LPG*	[m]	6,18
Height of genoa hoist	*IG*	[m]	20,25
Asymmetric Spinnaker			
Spinnaker area	$S_{spinnaker}$	[m²]	240,63
Hight above the deck of spinnaker halyard	*ISP*	[m]	26,65
Tack point asymmetric spinnaker	*SPL*	[m]	5,94

Table 24 - VPP test yacht main dimensions

Another input of the VPP is the table that relates the heel angle with the hydrostatic righting moment arm *Gz*, presented in the following table.

ϕ	0.00	7.46	12.76	17.82	23.61	31.09	38.09	45.35	54.3
Gz	0.00	0.239	0.403	0.544	0.675	0.802	0.903	0.980	1.02

Table 25 - *Gz* values as a function of heel angle

The VPPs were tested at two different wind speeds, 8 and 16 knots, going up and down wind. The following figure presents the different yacht's predicted speed with the three software for several wind angle.

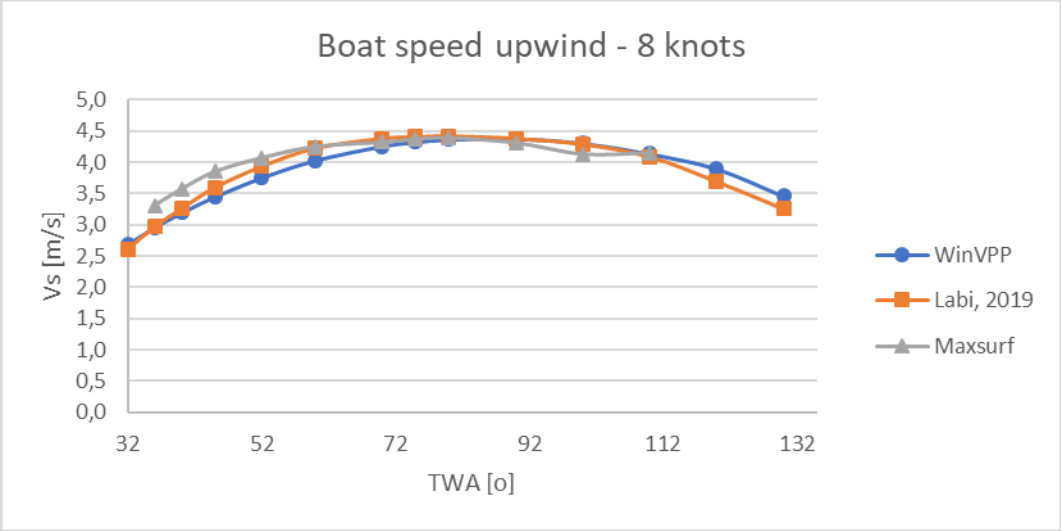

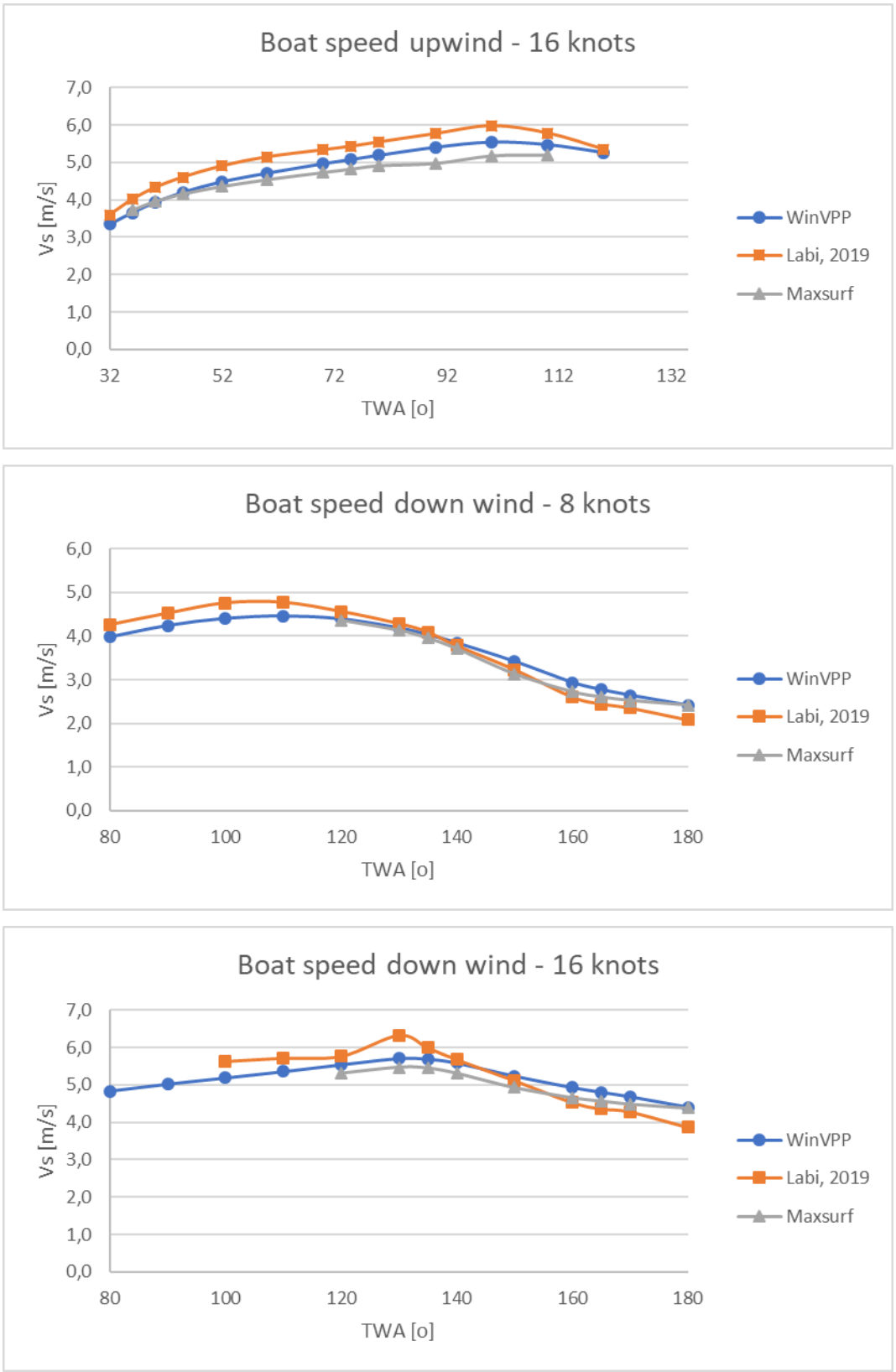

Figure 21 - VPP validation, comparing results with two commercial software

Observing the previous figure and its graphics, it is possible to notice that the difference between the 3 software is small, what validates the developed VPP.

8. VPP RESULTS WITH FOILS

The same boat presented in Table 24 was tested with the three different foils, which have the same shape as the ones used in the towing tank, but at full scale, with dimensions presented in the following table.

Parameter	unit	DSS	DM	FF
Chord 1	[m]	0.7	0.7	0.7
Span 1	[m]	2.34	1.54	1.74
Chord 2	[m]	-	0.64	0.47
Span 2	[m]	-	1.42	1.61
h0	[m]	0.0	0.25	-
α1	[o]	0.0	54	-
α2	[o]	-	67	36
Angle of attack 1	[o]	8	8	-
Angle of attack 2	[o]	-	0.0	0.0

Table 26 - Foils main dimensions at full scale

The following figure presents the boat speed and heel angle for different wind directions and intensity, for up wind sailing (main sail with jib) and down wind (main sail with spinnaker).

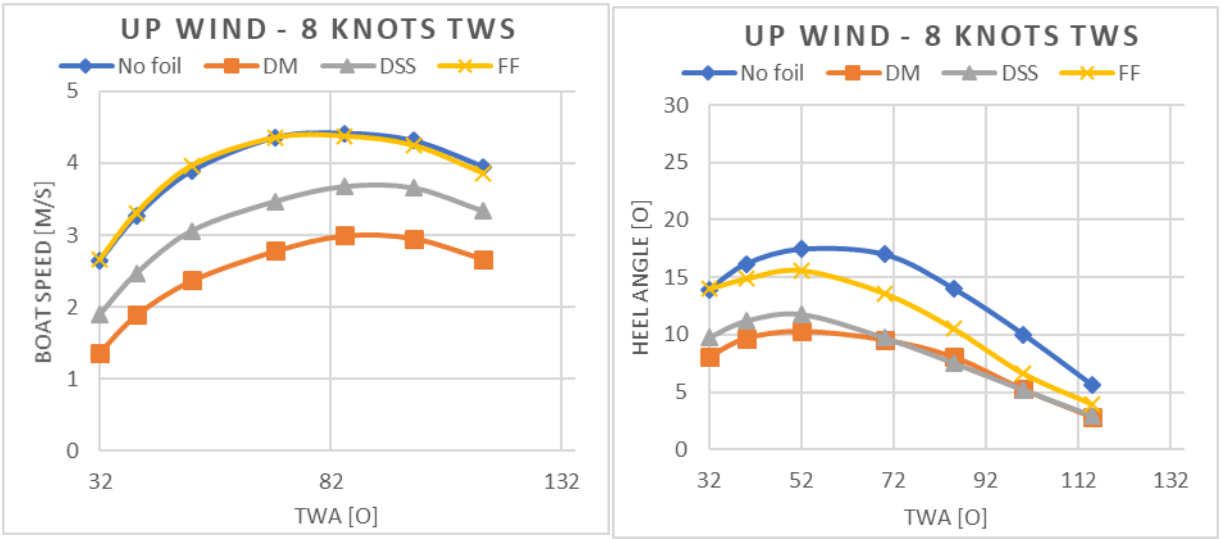

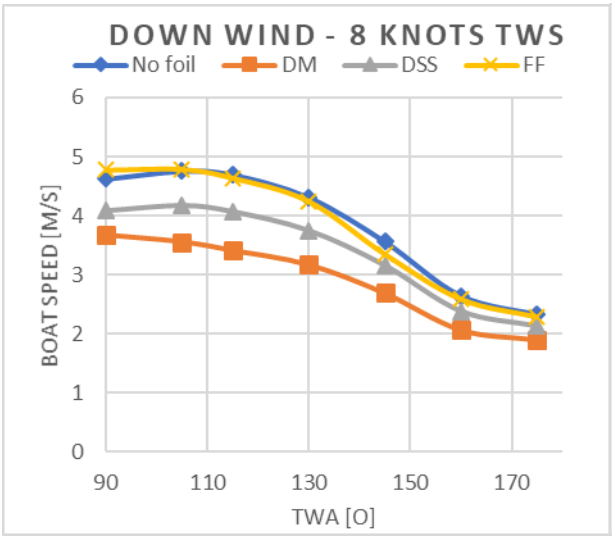
DOWN WIND - 8 KNOTS TWS
No foil
DM
DSS
FF
BOAT SPEED [M/S]
0
1
2
3
4
5
6
90
110
130
150
170
TWA [O]

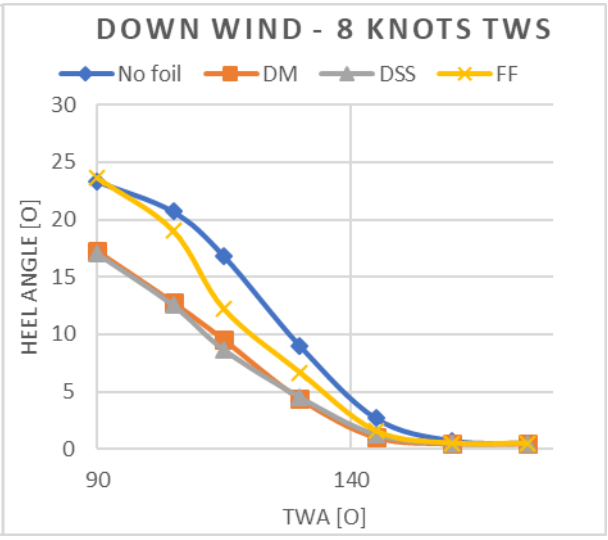
DOWN WIND - 8 KNOTS TWS
No foil
DM
DSS
FF
HEEL ANGLE [O]
0
5
10
15
20
25
30
90
140
TWA [O]

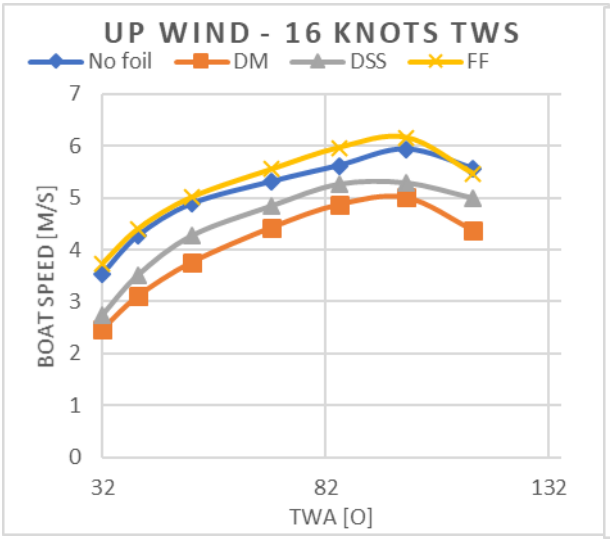
UP WIND - 16 KNOTS TWS
No foil
DM
DSS
FF
BOAT SPEED [M/S]
0
1
2
3
4
5
6
7
32
82
132
TWA [O]

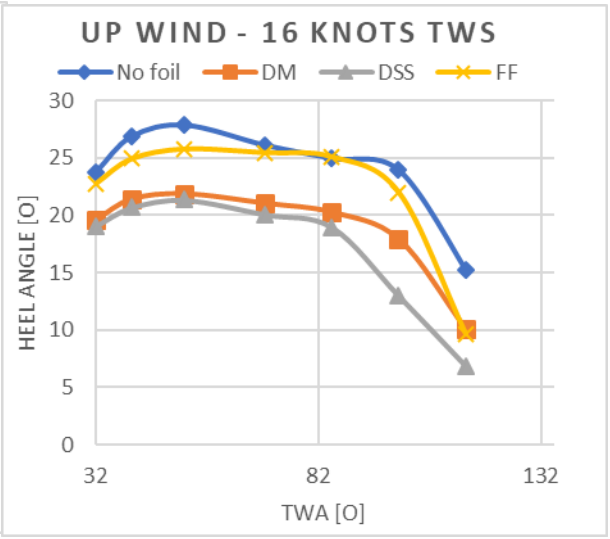
UP WIND - 16 KNOTS TWS
No foil
DM
DSS
FF
HEEL ANGLE [O]
0
5
10
15
20
25
30
32
82
132
TWA [O]

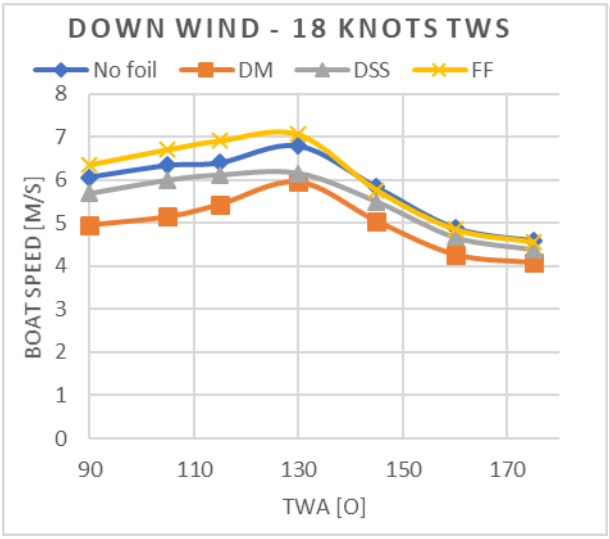
DOWN WIND - 18 KNOTS TWS
No foil
DM
DSS
FF
BOAT SPEED [M/S]
0
1
2
3
4
5
6
7
8
90
110
130
150
170
TWA [O]

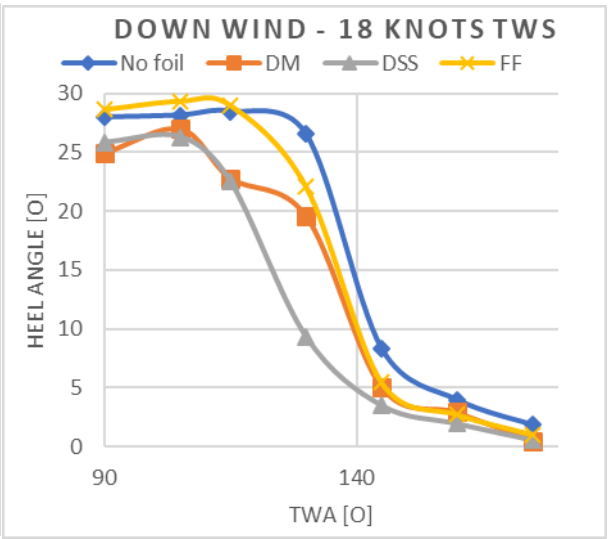
DOWN WIND - 18 KNOTS TWS
No foil
DM
DSS
FF
HEEL ANGLE [O]
0
5
10
15
20
25
30
90
140
TWA [O]

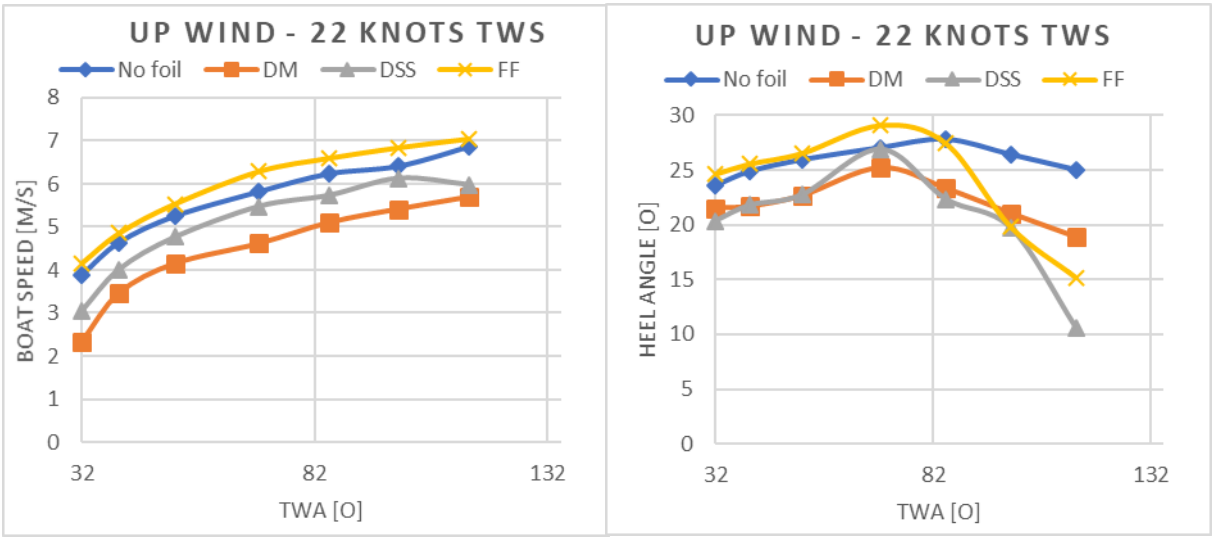

Figure 22 - VPP results comparing the three different foils and the hull with no foil at different wind conditions sailing up and down wind

Initially, it is important to say that the hydrodynamic model is limited to Froude numbers up to 0.6, which means the maximum boat speed the VPP may reach for the present boat in 7.12 knots, for this reason the maximum TWS up wind is 22 knots and down wind is 18 knots.

These results indicate that actually the only foil that provides an increment in boat speed is the Figaro solution, with a light improvement, while the DSS and specially the Dali Moustache present worst results.

Observing the geometry of the foils and the results, it was possible to notice that the DSS and DM generate a very important side force in the same direction of the aerodynamic side force, which must be balanced by the hydrodynamic side force, yielding the solution to high leeway angles, what also generates more residual drag, slowing the yacht down, explaining the low boat speed results. As a possible optimization to overcome this effect at least partially is to decrease the angle of α_1 in order to decrease the side force component when the hull is heeled.

Because the model is limited in terms of boat speed and then wind speed, it was not possible to generate results where the benefits of foiling righting moment would allow the vessel to sail with significant more sails power, what could yield to a yacht with better performance at strong breeze if compared to the craft with no foil. Observing the previous figure, it is possible to notice that the DSS and DM present smaller heel angle, what is comfortable for the crew and is interesting for cruising vessels.

8.1. Foils Optimization

To optimize the performance of all three foils, some changes may be done:

- Increase the righting moment lever arm by increasing the foil span for its first part.
- Once the span is increased, the chord of foils part 1 may be reduced, what reduces the drag.
- Reduce the angle α_1 for the DSS and DM to decrease the side force and increases the righting moment when the hull is heeled.
- The angle of attack may be reduced to decrease the foil drag.

To show graphically how these optimizations impact in the yacht speed, some simulations were performed for the yacht sailing upwind, at 16 knots of wind speed and 52º of TWA. The first analysis was done for the DSS foil, increasing its aspect ratio (division between foil span and chord):

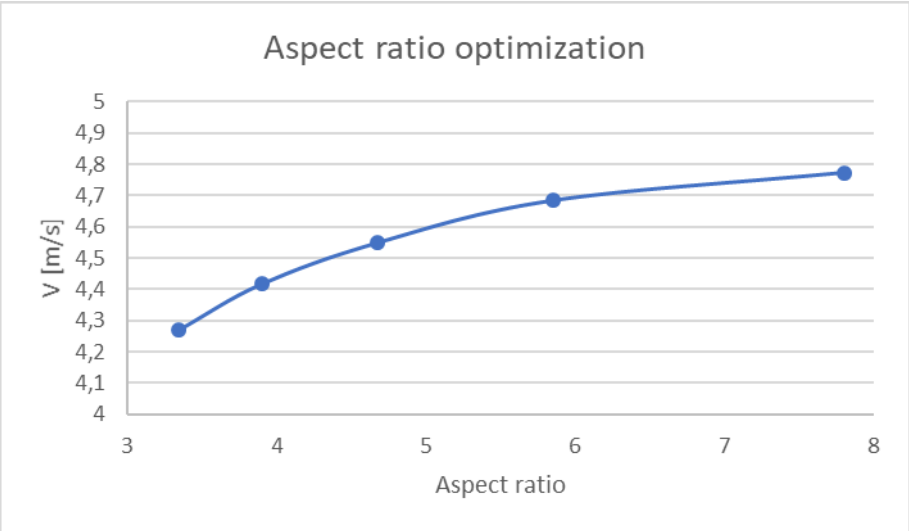

Figure 23 - Aspect ratio optimization

Regarding the angle of attack, the DSS foil was simulated in the same sailing conditions, and the following figures shows how a decrement in such angle provides higher boat speed.

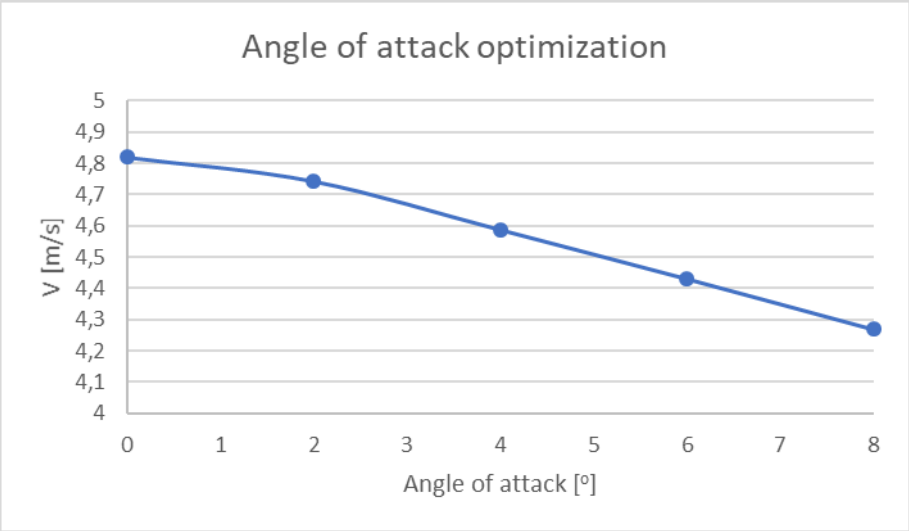

Figure 24- Angle of attack optimization

The Dali Moustache foil was tested with different angles of α1 at the same wind condition as previously, and according to Figure 25, its decrement generates improvements in the yachts speed.

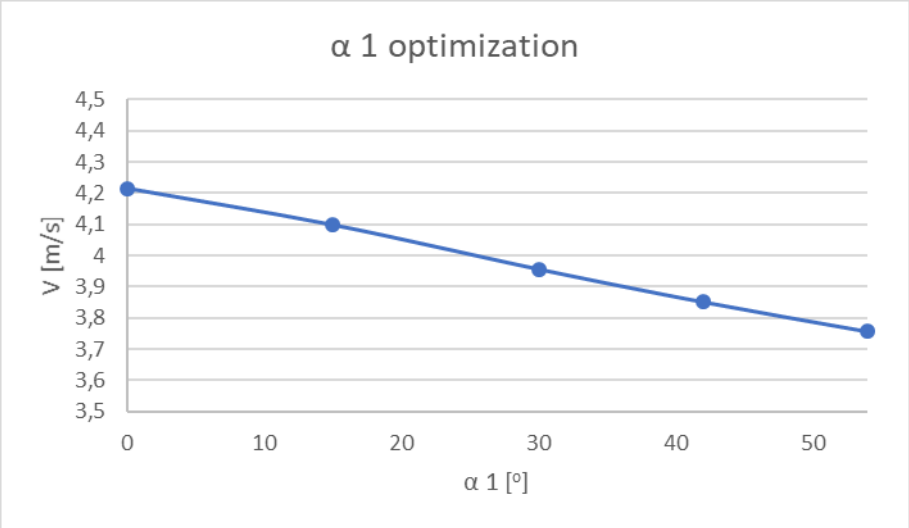

Figure 25 – α1 optimization

After some tests, a preliminary optimization was found, respecting construction limitations to be realistic. The new foils dimensions are presented in the following table.

Parameter	unit	DSS	DM	FF
Chord 1	[m]	0.3	0.3	0.3
Span 1	[m]	3.2	3.2	3.2
Chord 2	[m]	-	0.64	0.47
Span 2	[m]	-	1.42	1.61
h0	[m]	0.25	0.25	-
α1	[o]	-15.0	0.0	-
α2	[o]	-	80	20
Angle of attack 1	[o]	0.0	0.0	-
Angle of attack 2	[o]	-	0.0	0.0

Table 27 - Foils dimensions after optimization

The same cases presented in Figure 20 are shown again, but now for the optimized foils.

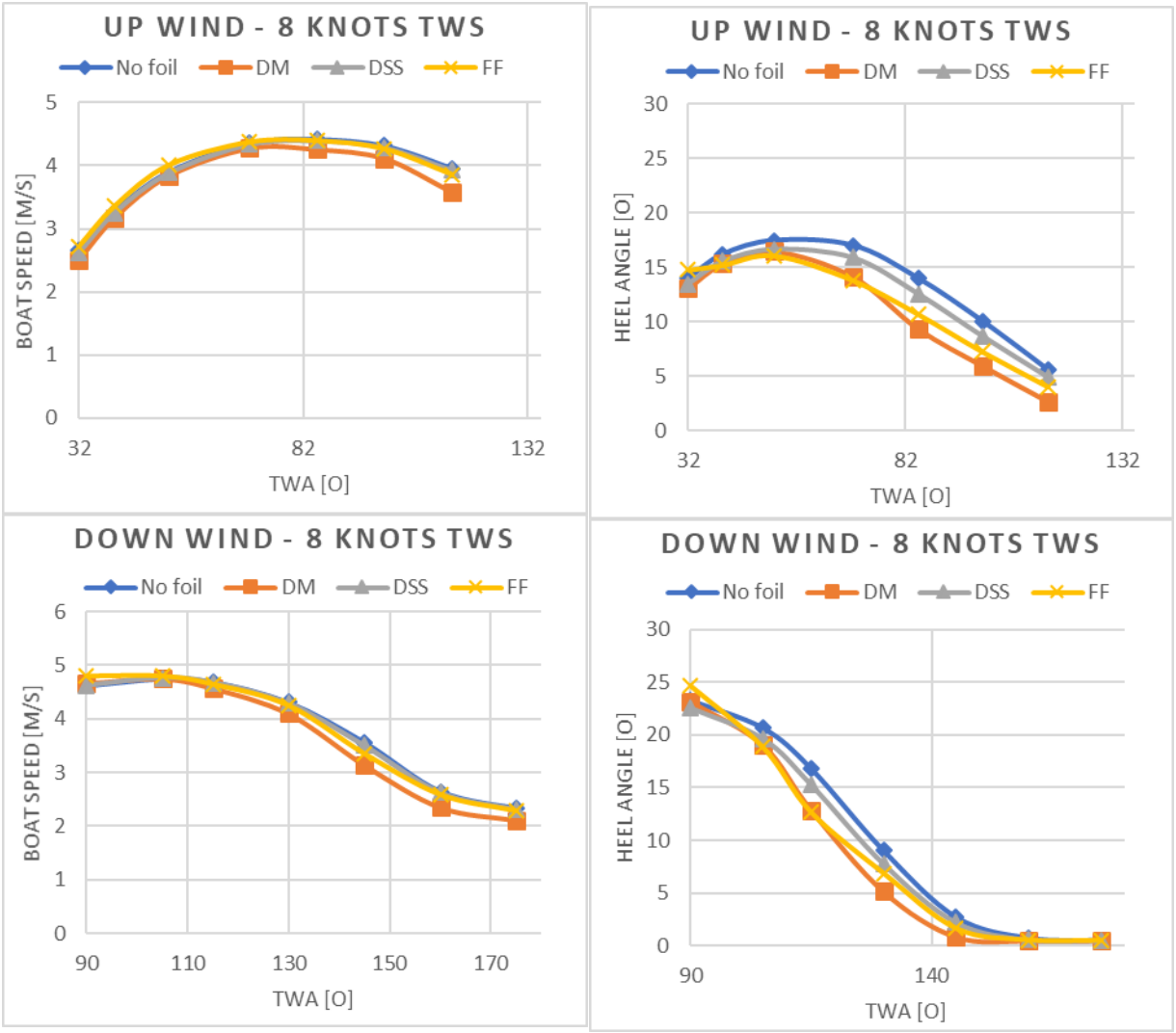

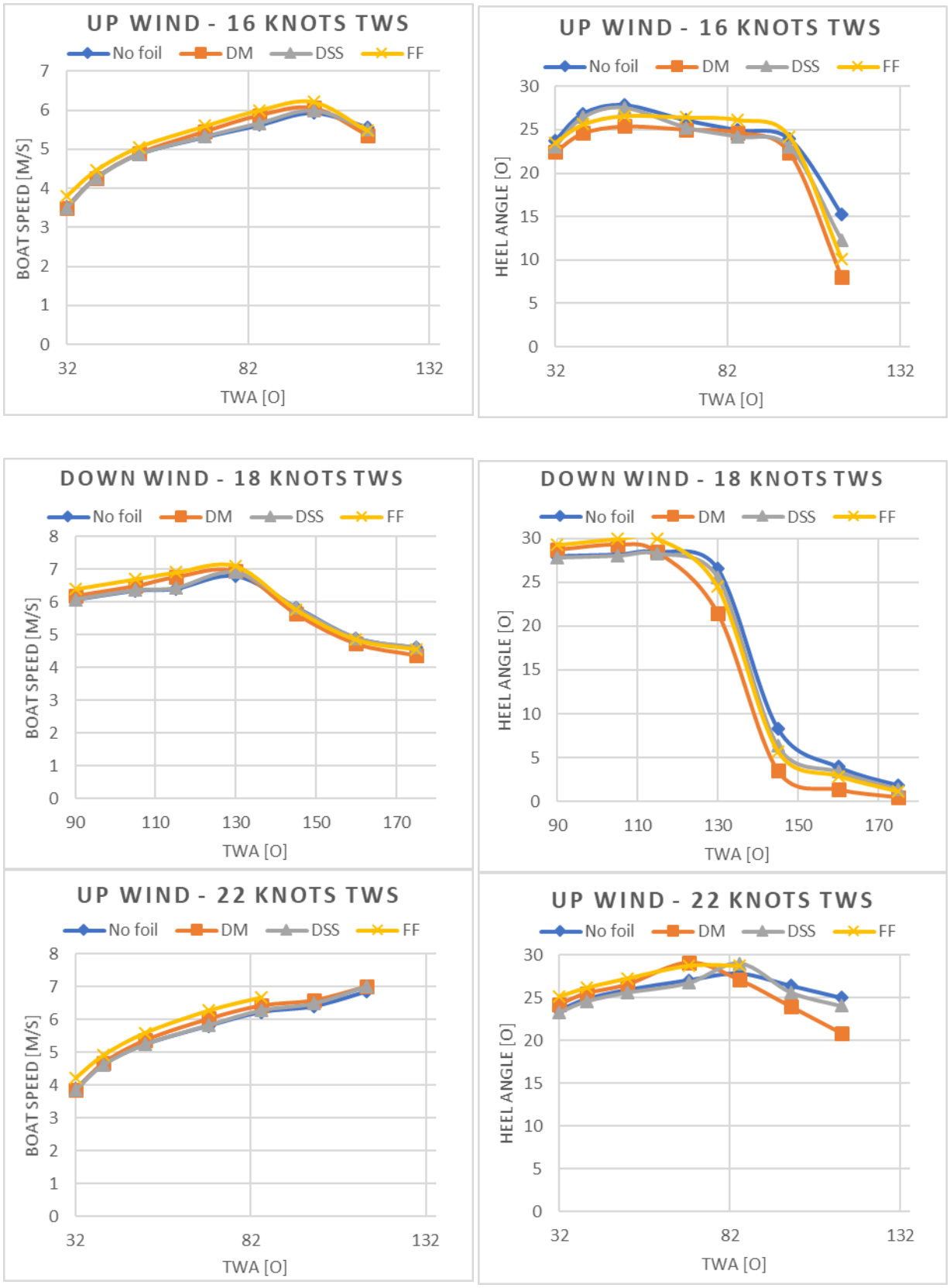

Figure 26 - VPP results comparing the three different foils optimized and the hull with no foil at different wind conditions sailing up and down wind

The new results show that the optimization increased the boat speed, but still no solution presents results significantly better than the ones found for the boat with no foil. One possible

reason why the VPP is uncapable to find better results for the foiling boat is because the model developed neglects an important degree of freedom, heave. Both the hydrodynamic as the aerodynamic models do not calculate vertical forces, and one of the advantages of having foils in modern yacht is that it partially lifts the boat out of the water, reducing the craft's displacements and subsequently its drag.

Another conclusion that may be observed is that the developed VPP allows the user to optimize the yacht project, by easily varying some parameters and being able to visualize which parameters increase the performance and which increase the comfort, but unfortunately this tool is useful for preliminary design only, and for a more precise velocity estimation a more sophisticated methodology should be used: CFD or experimental testing.

Generally, VPP results and yacht performance are plotted in polar plot. The following figure present the polar plot of the 4 different configurations: no foil, DSS, DM and FF after optimization. The results in blue regard up wind conditions, while green lines indicate down wind results.

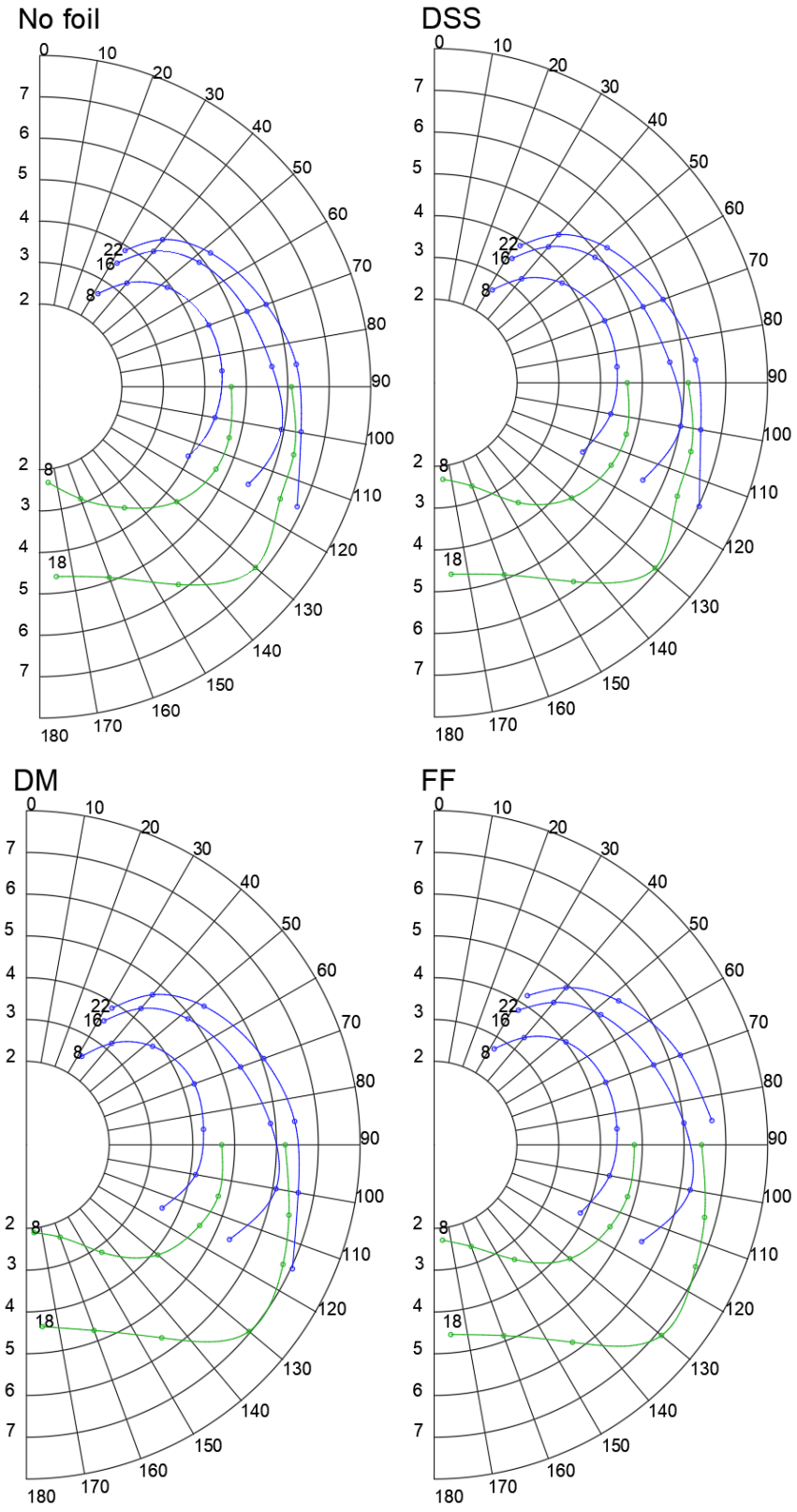

Figure 27 - Polar plot for the 4 different configuratons: no foil, DSS, DM and FF

To better visualise the improvement the optimization provided, the following polar plot compares the up-wind boat velocity at 16 knots of true wind speed and the down wind velocity at 18 knots of TWS. The results previous to the optimization are in dotted lines while the after optimization results are in a continuous line

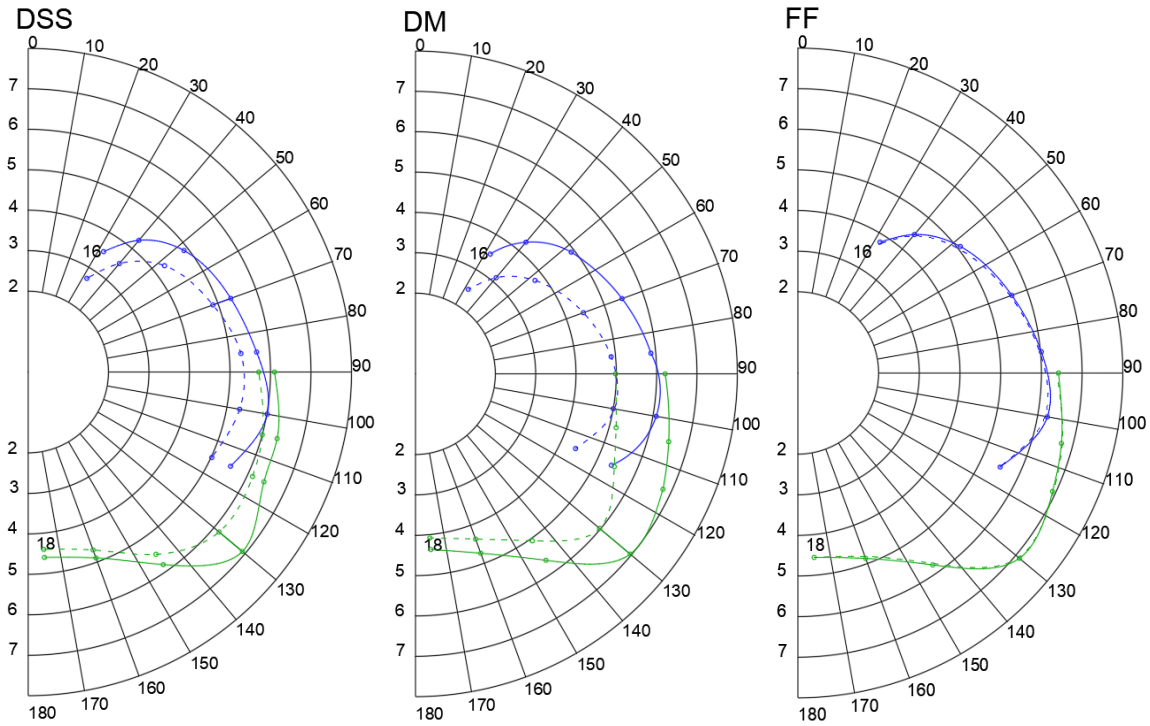

Figure 28 - Polar plot comparing the boat speed before and after the foils were optimized

9. CONCLUSION

9.1. VPP

The developed VPP combines three different models: aerodynamic based on the ORC method, hydrodynamic based on the DSYHS and a foil model based on the bi-plane theory and corrected by experimental data. The two first models, aerodynamic and hydrodynamic, were compared to experimental results and showed a good agreement, proving to be solid methods for VPPs with no more than 3 degrees of freedom. The foil model was not validated with experimental results due to a lack of published data on the subject, but the experimental corrections performed increased the robustness of the model.

The VPP was also compared to two commercial VPPs (that do not include hydrofoils in their models) and the difference between results are small, showing that the developed one makes a good interaction between the aerodynamic and hydrodynamic models, finding a correct load balance which yields to a correct velocity prediction.

Three degrees of freedom are balanced in the developed VPP, roll, surge and sway, but does not consider a balance in pitch, yaw and heave. To include such forces, it would be necessary to have more sophisticated fluid dynamic models, furthermore the use of a CFD program

would be suitable, what in another hand would increase significantly the computational cost of the VPP, what is not the interest in the present work, which has as objective the development of a preliminary design tool.

Regarding the foil model, the bi-plane theory used cannot include some effect as the foil and hull interaction, tip vortex and water piercing. For this reason the experimental correction was done, but to have a more precise result it would be important to have a better look at the interaction between the foil and the bow's waves, in the sense that the longitudinal position of the foil may have significant impact in the drag, once the foil may increase the bow's wave height (what increases the drag), or the opposite, decreasing the resistance and increasing the yacht performance.

9.2. Results

Observing the VPP results that compare the three foils with the yacht with no foil, it is possible to notice that the benefits that the foil generates in righting moment are not necessarily enough to overcome the increase in drag. The foils showed to decrease the boat speed, but also showed a decrease in heel angle, what is interesting for cruiser yachts, where the crew comfort may be more important that the craft's velocity.

The Figaro foil is the only device that generates significant side force in the same direction of the hydrodynamic side force, what is extremely interesting to decrease the leeway angle and as a consequence to reduce the induced resistance. The DSS and DM generate a more significant righting moment, decreasing the heel angle, but in another hand the side force generated has an opposite direction to the hydrodynamic one, which is not convenient. Comparing the DSS and the DM, the last one has a second part that balances the side force and increases the righting moment and lift, what makes this foil probably more interesting than the other.

To be actually capable to find a foil that provides significant better velocities than a simple yacht, the benefits in hull lift should be included in the VPP, for that, the model should include vertical loads allowing the study in heave. The benefits generated by foil lifting the yacht are related to the fact that the craft's displacement decreases, as the wetted surface, what reduces the vessel's drag and allows it to have a better performance. For heavy seas, a yacht lifted by a foil may also present better seakeeping properties once its interaction with the sea waves may be reduced.

9.3. Optimization

After an optimization prosses it was possible to notice that the developed VPP allows the understanding of which parameters in the foil design should be changed to have better results. The foil must be designed to provide the maximum lift and righting moment without generating much drag and compromising the side force, for that, a first conclusion may be done: the lever arm generated by the foil must be increased by designing foils with long span, but to not increase the drag much, the foil chord may be reduced.

Regarding the Figaro foil, because the VPP does not include heave, it is interesting to have a foil that provides not only righting moment, but side force too, so the angle its part 2 have with the free surface (α_2) must be carefully designed in order to provide significant side force when the boat is heeled.

The DSS and Dali Moustache foil have a common part that should be optimized in the same way. To generate righting moment without generating much side force, the angle it has with the water line (α_1) should be small, or even negative, to insure the foil lift is as vertical as possible when the yacht is heeling. It is also interesting to have the foil as deep as possible, to have a small interaction with the free surface.

The DM foil has an extra part that has as main benefit the generation of side force in the same direction as the hydrodynamic side force. To ensure its good application, it should be quite vertical, in order to have a significant side force component.

9.4. Future Works

This thesis showed the limitations of the DSYHS and ORC models for yachts which heave motion is an important concern. To include this and other degrees of freedom a more sophisticated model should be used, a CFD code for example, which has the drawback of increasing the solution complexity and computational cost.

With a more sophisticated VPP an analysis in heave may induce to a better understanding in the real benefits of a foil in a yacht's performance, by decreasing it displacement and drag. Another interesting study that may be done regards the yacht seakeeping, if waves are simulated and the yacht is heaved, the hull and sea interaction may be reduced, inducing to a smaller vessel response to hydrodynamic sea load, what may reduce the yacht drag and significantly increase its sea keeping comfort.

The longitudinal position of the foil may be better studied in a more complex VPP. It would be interesting to understand the interaction between the foil and the bow's waves, and a

significant optimization may be done to find a lower drag. The longitudinal position of the foil also has impact in the vessel's trim, another reason why it would be interesting to perform a more complex model.

The yaw balance could also be included in a more sophisticated VPP, allowing the understanding in the impact that the foil drag has in turning the yacht to leeward, and how big the rudder correction would have to be to ensure a yaw moment balance. With such understanding, a more detailed yacht design may be done, with a more optimized foil project.

10. REFERENCES

Aygor, T. (2017) *Analyses of Foil Configurations of IMOCA Open 60s with Towing Tank Test Results*.

Barkley, G. S. (2016) *Aero-Hydro Notes*.

Bohm, C. (2014) *A Velocity Prediction Procedure for Ssailing Yachts with a Hydrodynamic Model Bbased on Iintegrated Fully Coupled RANSE-Free-Surface Simulations*. Technology University of Delft.

Daskovsky, M. (2000) 'The hydrofoil in surface proximity, theory and experiment', *Ocean Engineering*, 27(10), pp. 1129–1159. doi: 10.1016/S0029-8018(99)00032-3.

Delft, T. U. of (2018) *No Title*, *Limited access*. Available at: http://www.dsyhs.tudelft.nl/dsyhs.php (Accessed: 8 November 2018).

Designing the IMOCA 60 (2016) *Scuttlebutt Sailing News*. Available at: https://www.sailingscuttlebutt.com/2016/11/08/history-of-the/ (Accessed: 13 September 2018).

Dewavrin, J. (2018) *Design of a Cruising Sailing Yacht with an Experimental Fluid Dynamics Investigation into Hydrofoils*.

DSS Dynamic Stability System (no date) *Dynamic Stability Systems*. Available at: https://stockmaritime.com/?modellbau/895 (Accessed: 26 June 2018).

Figaro Beneteau 3 (no date). Available at: http://www.beneteau.com/fr/figaro-beneteau-3 (Accessed: 13 September 2018).

Gohier, F. (2018) 'Experimental Iinvertigation Into Modern Hydrofoil- Assisted Monohulls : the Impact of Foils on Stability', *Journal of Sailing Technology*, pp. 1–8.

Graf, K. and Böhm, C. (2005) 'A New Velocity Prediction Method for Post-Processing of Towing Tank Test Results', *THE 17th CHESAPEAKE SAILING YACHT SYMPOSIUM*, (March).

J. -B. Souppez (2017) *Intro to Yacht Equilibrium and Aerodynamics*.

Katgert, M. and Keuning, J. A. (2008) 'A bare hull resistance prediction method derived from the results of the Delft Systematic Yacht Hull Serles extended to higher speeds', *International Conference Innovation In High Performance Sailing Yachts*, (May), pp. 29–30.

Keuning, J. A. and Katgert, M. (2010) *The influence of heel on the bare hull Resistance of a sailing yacht*.

Keuning, J. A. and Sonnenberg, U. . (1998) ‘Approximation of the Hydrody- namic Forces on a Sailing Yacht based on the “Deift Systematic Yacht Hull Séries”’, *15th International Symposium on "Yacht Design and Yacht Construction "*, (November).

Keuning, J. A. and Verweft, B. (2009) *A new method for the prediction of side force on keel and rudder of a sailing yacht based on the results of the Delft Systematic Yacht Hull Series*.

Masuyama, Y. *et al.* (2009) ‘Database of sail shapes versus sail performance and validation of numerical calculations for the upwind condition’, *Journal of Marine Science and Technology*, 14(2), pp. 137–160. doi: 10.1007/s00773-009-0056-3.

Matthew Sheahan (2015) *The foiling phenomenon - How sailing boats got up on foils to go ever-faster*. Available at: http://quant-boats.com/media/pdf/43/g0/c3/Yachting-World_foiling-phenomenon.pdf (Accessed: 13 September 2018).

ORC (2001) ‘International Measurement System’, *ORC Offshore Racing Congress*, (February). Available at: http://ocw.mit.edu/courses/mechanical-engineering/2-996-sailing-yacht-design-13-734-fall-2003/study-materials/ims_rule_book.pdf.

ORC (2017) *ORC VPP Documentation 2017*.

Perrier, P. (2017) ‘Les bateaux qui volent’, *Letter 3AFnúmero 27*.

Souppez, J.-B. R. G., Arredondo-Galeana, A. and Viola, I. M. (2019) ‘Recent Advances in Experimental Downwind Sail Aerodynamics’, *THE 23RD CHESAPEAKE SAILING YACHT SYMPOSIUM*, (March).

Welbourn, H. B. (2010) ‘MONOHULL SAILING VESSEL HAVING A LIFTING HYDROFOIL’. United States of America: United States Patent. doi: 10.1016/j.(73).

Whicker, L. F. and Fehlner, L. F. (1958) *Free-stream characteristics of a family of low-aspect-ratio, all movable control surface for application to ship design*. Maryland.

11. APPENDICES

APPENDIX A1: YACHT PARAMETERS FOR AERODYNAMIC FORMULATION

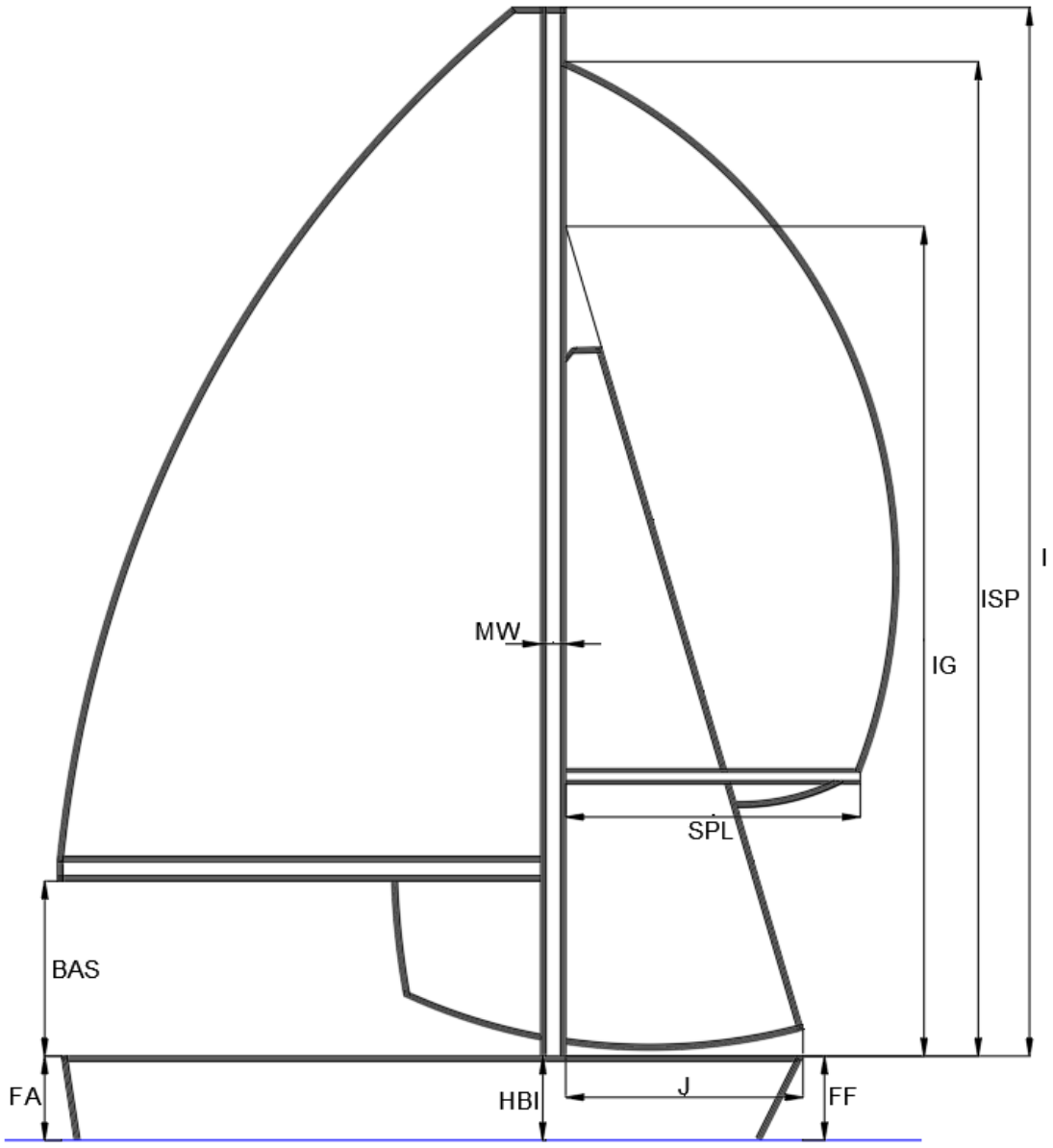

APPENDIX A2: TOWING TANK FACILITY AND MODEL MANUFACTURE

The towing tank at Solent University is 60 meters long, 3.7 meters wide and 1.8 meters deep. The carriage maximum speed is 4.6 m/s. The carriage is equipped with a computer capable to read the models forces in drag and side force in Newton, the heave in mm and the trim in degrees. The parameters to be initially defined are the model speed, heel and yaw angles. The following figure is a panoramic photo of the basin, taken by the author.

The model is fixed to the carriage by an instrument that allows the heel angle definition, the same is placed where the hull theoretically receives the aerodynamic loads, it means, where the mast is located at the full-scale craft.

The model was designed and manufactured by Juliette Dewavrin in 2017. The design was made in a 3D software and machined by a Computer Numerical Control machine in a polystyrene block, which was then covered by composite (fiberglass plus epoxy resin) to make it stronger and waterproof. The next figure is a photo taken by the author from the model installed in the carriage. It is possible to see the Dali Moustache foil installed and some weights allocated inside the model to simulate the right hull displacement.

The three hydrofoils were 3D printed in epoxy resin ABS and recovered by carbon fibre to ensure it would resist the loads. For more details about the model manufacture consult Dewavrin (Dewavrin, 2018). The following figure shows the three foils (DSS, FF and DM from top to bottom) next to a 30 cm long measuring tape to give an idea of size and shape.